NASA Contractor Report

Final Shuttle-derived Atmospheric Database: Development and Results from Thirty-two Flights

John T. Findlay
Rachel A. Jasinski

Flight Mechanics & Control, Inc.
47 East Queen's Way
Hampton, VA 23669

CONTRACT NAS9-17394
July 1990

National Aeronautics and
Space Administration

Lyndon B. Johnson Space Center
Houston, TX 77058

PREFACE

This is the third and final database developed under the subject Johnson Space Center Contract NAS9-17394 as part of FM&C's contractual obligations. The other activity involved trajectory reconstruction and instrument error analyses in support of the upcoming Aeroassist Flight Experiment (AFE) project. The atmospheric database development has been supported and encouraged by Mr. J. D. Gamble of JSC who, along with Mr. C. Cerimele, has served as the Contracting Officer's Technical Representative. Mr. Cerimele has succeeded Mr. Gamble as the Principal Investigator on the Aerodynamic Performance Extraction Experiment (APEX) for the AFE. That project has made considerable use of earlier FM&C versions of Shuttle-derived atmospheres in support of Guidance, Navigation and Control studies. Similar uses of the database are envisioned for other advanced space vehicle design activities. Moreover, the database should prove invaluable for atmospheric science investigations and model evaluations and/or development. Interested readers desiring copies of the database described in this final report should contact Mr. Gamble at (713) 283-5576 (Mail Code IA13). The final database, FINLATM, is available for Personal Computer users having the Microrim R:base software at their disposal. Equivalent spreadsheet data could also be provided.

TABLE OF CONTENTS

LIST OF TABLES

LIST OF FIGURES

LIST OF FIGURES (concluded)

ABSTRACT

The final Shuttle-derived atmospheric database developed for the National Aeronautics and Space Administration under NASA Contract NAS9-17394 to the Lyndon B. Johnson Space Center is presented herein. The relational database is comprised of data from thirty-two (32) Space Transportation System (STS) descent flights, to include the available meteorology data taken in support of each flight as well as model data based on the United States Standard 1976 and 1962 atmospheres, the NASA Marshall Space Flight Center (MSFC) Global Reference Atmospheric Model (GRAM), and the United States Air Force 1978 Reference Atmospheres (AF'78). For the most part, the available data are restricted to the middle atmosphere. In situ accelerations, sensed by the tri-redundant Inertial Measurement Unit (IMU) to an accuracy better than one milli-g, are combined with post-flight Best Estimate Trajectory (BET) information and predicted, flight-substantiated Orbiter aerodynamics to provide determinations up to altitudes of 95 km. In some instances, alternate accelerometry data with micro-g resolution were utilized to extend the database well into the thermosphere. Though somewhat limited, the ensemble of flights permit a reasonable sampling of monthly, seasonal and latitudinal variations which can be utilized for atmospheric science investigations and model evaluations and upgrades as appropriate. More significantly, the unparalleled vertical resolution in the Shuttle-derived results indicate density shears normally associated with internal gravity waves or local atmospheric instabilities. Consequently, these atmospheres can also be used as stress-atmospheres for Guidance, Navigation and Control (GN&C) system development and analysis as part of any advanced space vehicle design activities.

BACKGROUND DISCUSSIONS

Shuttle-derived density profiles and associated atmospheric implications evolved as the most interesting spin-off of the aerodynamic and aerothermodynamic research conducted during the Shuttle flight test program. As part of the overall activity, investigators throughout the Shuttle community utilized post-flight BET [1] information, in situ measurements from the Operational Instrumentation (OI), and remote sounding data to establish the aerodynamic performance and control effectiveness of the Orbiter vehicle. With few exceptions, the aerodynamic performance was virtually that predicted by the final Pre-Operational Orbiter Aerodynamic Design Data Book [2] and subsequent Flight Assessment Deltas (FAD) were published to rectify any subtle differences. [3] However, local departures were evident which could not be justified as aerodynamics per se since such phenomena were not repeatable from flight to flight. Given the accuracy and redundancy of the in situ data and the associated accuracy of the BET information, uncertainties in these data were ruled out as plausible explanations of any observed variations in the aerodynamic differences. In actuality, given the temporal and spatial limitations of the remote atmospheric soundings, coupled with the limited vertical resolution of same, the latent accuracy of the meteorology data was suspect.

In view of the aforementioned limitations in the meteorology data, it became commonplace to derive density profiles based on normal force considerations. Since the aerodynamic performance was essentially as expected, the predicted normal force coefficient, C_{N_P}, and the normal acceleration sensed by the tri-redundant IMU data, accurate to slightly better than one milli-g, could be utilized to directly compute the associated density. This was done, in part, to evaluate the available remote data from alternate sources and attempt to quantify the accuracy of the resultant aerodynamic flight determinations. Density profiles were derived that indicated local structure suggesting density shears and/or shifts ("potholes-in-the-sky") on the order of 10 to 20 percent as common occurrences, due perhaps to atmospheric overturning, Kelvin-Helmholtz instabilities, or internal gravity wave phenomena. [4] Such structure was extensively reviewed with various Shuttle investigators, to include those most familiar with conventional atmospheric measuring devices, the data reduction methodology and accuracy of same, any limitations in that type of data, and plausible atmospheric mechanisms that could effect such abrupt changes.

Though the actual cause(s) of such structure is somewhat speculative, there was little doubt as to the sharp features evident in the Shuttle profiles. The vertical resolution available in the Shuttle results (less than 100 m) is without precedent. Though neither

models nor more conventional sounding devices can replicate such structure, density derived from in situ fuselage pressure measurements from the Development Flight Instrumentation (DFI) were available on two of the earlier flights (STS-3 and STS-5) to vindicate the profiles. [5] Thus, in view of the unique profiles suggested in the Shuttle entry data, FM&C was originally enjoined under contract to the JSC to develop an atmospheric database over those altitude regions in which atmospheric phenomenon can significantly effect GN&C performance issues for aerodynamically assisted Orbital Transfer Vehicles.

The original database was published as a NASA Contractor Report (CR 4109) [6] and was based on the then available twenty-two (22) descent flights. Subsequent to that development, data based on the High Resolution Accelerometry Package (HiRAP) micro-g acceleration measurements became available. [7] FM&C appended these data at the uppermost altitudes to develop a separate database to include thermospheric heights. These latter data were available for ten (10) of the first twenty-two (22) flights as discussed in NASA CR 172043. [8] Readers might desire to review these two NASA CRs for additional background information. Included therein are discussions pertaining to the actual development required, the expected accuracy of the Shuttle-derived profiles, and correlations of the then available results versus latitude, month, and season. A more comprehensive treatise published by Gamble [9] summarized the combined results of both databases. Readers are encouraged to peruse this paper as supporting background to this report. Therein, additional discussions on the importance of such data are presented, as well as further discussions pertaining to the development required and the associated accuracy implications.

As part of this particular effort, the earlier data have been reworked (as discussed in Appendix A) and combined with an additional ten (10) flights to develop the final database reported herein. Table 1 presents a summary of the available thirty-two (32) flights. The table includes the particular STS flight designation number (or alternate designation as relevant), the date of entry, the particular landing site, an approximate local landing time, the season, and the altitude range for which data are available.

It is noted that the more recent flights are indicated with an RSOC flight designation number, primarily to eliminate redundancy in the various STS numbering systems employed. These atmospheres are based on the post-flight BETs developed under an operational contract to JSC by their current contractor, RSOC. Prior to the Shuttle stand-down, these data were generated for JSC by TRW. Alternatively, independent BETs were developed for NASA Langley Research Center (LaRC) as part of the Orbiter Experiments (OEX) research activity. Since this support has not been continued, alternate

BET information is not available for the RSOC designated flights. Certainly, there is no reason to assume that the RSOC BET data are questionable and, in fact, every reason to expect that these data are very accurate. However, any BET determination is based on statistical algorithms. Past comparisons with alternate entry profiles were commonly done to attempt to establish a more realistic assessment of the accuracy of the post-flight trajectory data. Perusal of the recommended background references will indicate to interested reviewers that limited BET accuracy is only a *potential* problem above 60 km for those flights with minimal ground-based tracking coverage available due to the entry geometry. Specifically, the flights potentially affected are those flights which descended from the high northerly latitudes as well as those descents from the more extreme southerly locations. For the ensemble of new flights, only RSOCF27, RSOCF28 and RSOCF36 might be affected as indicated in Figure 1 herein.

Based on the preceding discussions, readers should be aware of the following. Given the alternate BET data for the first 22 flights, the concept of a *datum-shift* was employed to establish an average datum which benchmarked the altitude information to best reflect any BET differences. This shift removed the well determined, statistically significant bias between the various BETs for those flights with limited geometry, changing the associated density by as much as 10 percent (when normalized versus the 1976 Standard) at 95 km. [8] Data from these flights, with the datum-shift applied as appropriate, are included in this final database. However, in the absence of alternate BET information, the RSOC BETs are utilized directly for the more recent 10 flights. Again, the RSOC data are not being questioned. It simply must be stated that the past trends were so statistically significant (see Figure 10 of Reference 9) that one could have opted to shift the datum accordingly on the three potentially affected RSOC BETs.

Before proceeding with the database development and presentation of the specific results from same, it is worthwhile to review accuracy considerations which are developed further in the appropriate references. The following discussions pertain to determinations in the middle atmosphere. Though provided to FM&C as final density profiles, similar discussions are relevant for any thermospheric determinations. These discussions are deferred to the appropriate references.

In the middle atmosphere, the derived atmospheric density is affected by BET uncertainties, acceleration measurement accuracies, and any latent errors in the predicted normal force coefficient. Significant BET uncertainties are, of course, quantified by uncertainties in both the altitude and associated velocity estimate. The former, in those few instances where necessary, were rectified by the previously discussed datum-shift and any

residual error remaining should be well within 10 percent throughout the middle atmosphere, perhaps as much as 10 percent in the mesopausal region and throughout the lower 30 km of the thermosphere.

Since the BET inertial velocity is well determined, any latent velocity errors are dominated by uncertainties in the atmospheric wind information which is derived from the remote meteorological data. A worse case scenario would indicate that uncertainties in the atmospheric winds could potentially induce a one percent density error at 75 km, possibly increasing to 3-4 percent at the lowermost altitude of 45 km. In either event, the influence of atmospheric winds throughout the altitude interval of interest is negligible.

The effect of acceleration measurement accuracies over the middle atmospheric region wherein IMU data are utilized are negligible below 88 km strictly from signal-to-noise considerations. The tri-redundant nature of these measurements provide the added confidence that no significant biases are present. Above 88 km, the density profiles are smoothed up to 95 km to extract the dominant density structure without following some of the locally induced features which may be noise related. As a point of reference, the milli-g measurement accuracy relates to approximately 10 percent of the expected signal at 95 km. Again, readers are reminded that determinations in the thermosphere were based on accelerometry with micro-g resolution though it should be understood that these data were calibrated in a flight environment that included appreciable signal due to Auxiliary Power Unit (APU) venting and Reaction Control System (RCS) jet firings.

The last item which can affect the derived density profile accuracy in the middle atmosphere are the effects of any latent aerodynamic prediction errors. As previously stated, the pre-operational predictions were essentially substantiated after the first few flights. For the purposes herein, the small over-prediction error (less than 5 percent) in the normal force coefficient has been removed as per the final FAD. Consequently, the accuracy of the rectified predicts are well within 5 percent below 75 km. Though statistically one can show that these data are accurate to within 10 percent throughout the mesopause, even these statistics are dominated by uncertainties in the available meteorology data. Thus, hueristic arguments based on repeatability of flight determinations would suggest that the predictions are even better than formal statistics might imply. It should be understood that middle-atmosphere determinations utilize aerodynamic predictions in the continuum. Thermospheric determinations are based on estimates in the free-molecular flow regime, to include transition between that regime and the continuum. The thermospheric densities provided were based on LaRC flight determined updates to both the rarefied flow coefficients and the associated bridging formula.

Even if one were to statistically combine the potential density uncertainties associated with the individual error sources previously discussed, to be sure a worse-case scenario, one would necessarily conclude that the accuracy of the Shuttle-derived results throughout the middle atmosphere is, conservatively speaking, much better than that associated with more conventional sounding devices. Coupled with the vertical sampling available (less than 100 m) and the fact that the sharp density features evident in the Shuttle results, e. g., shears and offsets, are virtually exact determinations, it is evident that the STS results provide a most unique opportunity for atmospheric extractions. Certainly, as can be seen in the various ground tracks presented herein, a typical Shuttle entry covers approximately 50^{o} of central angle as the spacecraft descends in altitude from 95 km to 45 km. Thus, some of the overall density structure observed could well be a consequence of encountering horizontal disturbances or geographically local conditions.

Table 1. STS flight summary for final atmospheric database

FLIGHT	DATE OF ENTRY	LANDING SITE	LOCAL TIME	SEASON	RANGE (KM)
STS-1	Apr 14, 1981	EAFB, CA	10:20 AM PST	Spring	45 to 95
STS-2	Nov 14, 1981		1:25 AM PST	Fall	
STS-3	Mar 30, 1982	White Sands, NM	9:05 AM MST	Spring	
STS-4	July 4, 1982	EAFB, CA	8:10 AM PST	Summer	
STS-5	Nov 16, 1982		6:30 AM PST	Fall	
STS-6	Apr 9, 1983		10:55 AM PST	Spring	45 to 160
STS-7	June 24, 1983		6:00 AM PST	Summer	45 to 140
STS-8	Sept 5, 1983		11:40 PM PST		
STS-9	Dec 8, 1983		3:45 PM PST	Fall	
STS-11 (41-B)	Feb 11, 1984	KSC, FL	7:15 AM EST	Winter	45 to 160
STS-13 (41-C)	Apr 13, 1984	EAFB, CA	5:40 AM PST	Spring	45 to 120
STS-14 (41-D)	Sept 5, 1984		5:40 AM PST	Summer	45 to 95
STS-17 (41-G)	Oct 13, 1984	KSC, FL	11:30 AM EST	Fall	45 to 91
STS-19 (51-A)	Nov 16, 1984		7:00 AM EST		45 to 95
STS-23 (51-D)	Apr 19, 1985		8:55 AM EST	Spring	
STS-24 (51-B)	May 6, 1985	EAFB, CA	8:10 AM PST		45 to 140
STS-25 (51-G)	June 24, 1985		5:15 AM PST	Summer	45 to 95
STS-26 (51-F)	Aug 6, 1985		11:45 AM PST		45 to 160
STS-27 (51-I)	Sept 3, 1985		5:15 AM PST		45 to 95
STS-30 (61-A)	Nov 6, 1985		9:45 AM PST	Fall	45 to 153
STS-31 (61-B)	Dec 3, 1985		1:35 PM PST		45 to 95
STS-32 (61-C)	Jan 18, 1986		6:00 AM PST	Winter	45 to 159
STS-26 (RSOCF26)	Oct 3, 1988		8:35 AM PST	Fall	45 to 95
STS-27 (RSOCF27)	Dec 5, 1988		3:35 PM PST		
STS-28 (RSOCF28)	Aug 13, 1989		5:35 AM PST	Summer	
STS-29 (RSOCF29)	Mar 18, 1989		6:35 AM PST	Winter	
STS-30 (RSOCF30)	May 8, 1989		11:45 AM PST	Spring	
STS-31 (RSOCF31)	Apr 29, 1990		6:00 AM PST		
STS-32 (RSOCF32)	Jan 20, 1990		1:35 AM PST	Winter	
STS-33 (RSOCF33)	Nov 27, 1989		4:30 PM PST	Fall	
STS-34 (RSOCF34)	Sept 23, 1989		8:35 AM PST		
STS-36 (RSOCF36)	Mar 4, 1990		9:10 AM PST	Winter	

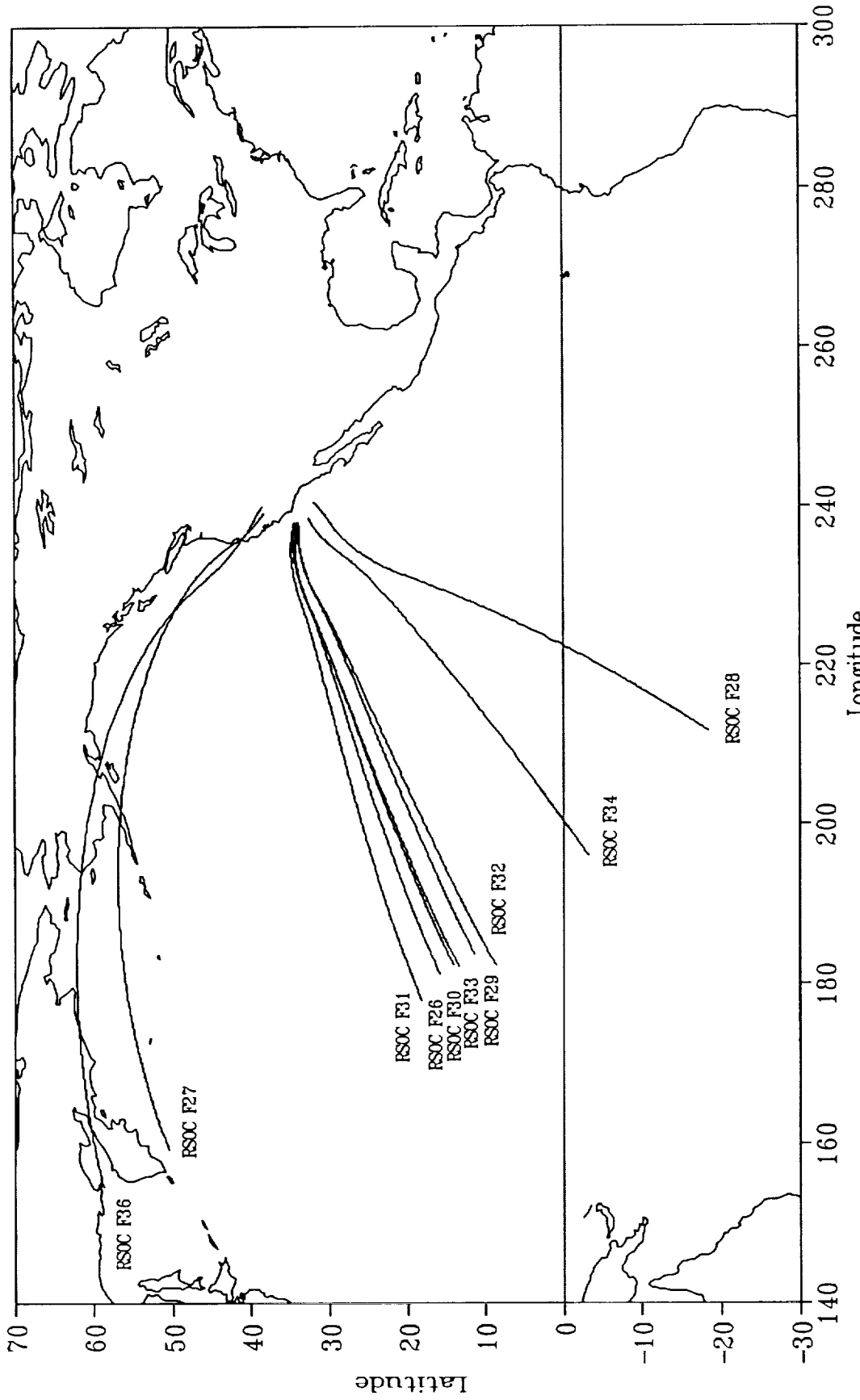

Figure 1 Ground tracks for additional STS flights.

DATABASE DEVELOPMENT

Though this section will discuss the format of the database, some reader familiarity with relational database management systems is presumed. Table 2 presents the adopted schema for the final database. Shown thereon are three relations; GENDAT, STDATMS, and FLTDAT. Attributes for the various relations are as noted. For the most part, the descriptions employed in the table should be self explanatory. Also included are the variable types as well as the units employed.

Data loaded into the GENDAT relation are essentially those summary data in Table 1 previously presented except for the numerical data, integers FLT and MONTH, which can be used for selection to correlate data across relations. The FLT integer corresponds exactly to the STS number for the first 22 flights. A value of 100 has been added to the STS number for all RSOC flights to assure a unique numbering system. The GENDAT relation contains 32 rows, one for each of the flights employed.

Data from the two generally available Standard Atmospheres, 1976 and 1962, are incorporated in the STDATMS relation. It is noted that the natural logarithm of the 1976 density and pressure are employed. Further, the 1962 density and pressure are normalized to the 1976 data. The molecular weight profile included thereon is that assumed for the 1976 standard. This relation contains 371 rows conforming to the common altitude spacing adopted. Data are loaded every 1 km between 160 km and 100 km, at 500 m intervals between 100 km and 88 km, every 100 m down to 69 km, and every 250 m between that altitude and the lowermost value of 45 km.

The relation, FLTDAT, contains the flight dependent data for the 32 flights. Included thereon are the Shuttle-derived results (the particulars of which will be discussed later), the MSFC GRAM data [10], the AF'78 information [11], and the remote measured meteorology data. Both of the models include monthly and latitudinal dependence. In addition, the GRAM provides diurnal and semi-diurnal variations, estimates of both the large and small scale density perturbations, and a spherical harmonic wind model based on geostrophic balance considerations. The GRAM also includes the Jacchia thermospheric model. By contrast, the AF'78 model is only defined up to 95 km. It is noted that the Shuttle-derived density and pressure, as well as the density and pressure from each of the models, are also normalized to the 1976 Standard.

The remote data included in the FLTDAT relation have been translated by others to conform in time and space to the Shuttle ground-track and vertical profile. These data were

either provided by LaRC[12] or extracted from the JSC BET. In the latter instance, the data are directly attributable to the generally unpublished, excellent efforts of Mr. Mel Gelman of the Climatology Branch of the National Weather Service. When alternate data were available, considerable attention was given to comparing results from both sources to try to select the most appropriate data. For the more recent 10 flights, only Gelman's data were available which, it will later be demonstrated, are excellent profiles with but one exception. Readers will note that the remote density and pressure data have also been normalized. Moreover, in the case of STS-3 and STS-5, readers are reminded that the measured data have been replaced by the aforementioned DFI derived results between altitudes of approximately 70 and 75 km. This will be evident when referring to the individual results in the attached appendix.

It can be seen that the integer, FLT, has been included in this relation as well. Again, the RSOC STS flight numbers have been increased by 100 to provide a unique search capability. Finally, the necessary trajectory data; altitude, latitude and longitude, are incorporated. Included as information is the vertical descent rate, HDOT. The FLTDAT relation consists of 10,195 rows. Within the range of flight data availability, the data have been interpolated to the same, fixed altitude increments employed by STDATMS. This was done to permit direct comparisons between the Shuttle-derived results, the meteorology data, and the various model data, both within and across flights. The increments utilized do permit some smoothing but were carefully selected to assure that the dominant density structure in the derived data was preserved. With one exception, all flights extend up to at least 95 km. A data gap on STS-17 precluded obtaining any meaningful data above 91 km. Again, some ten of the flights have been extended upwards into the thermosphere using the HiRAP data.

Though some mainframe application was necessarily required, the actual database was developed entirely on an FM&C Personal Computer (PC/AT clone) using the Microrim, Inc R:base 5000 (Version 1.01 PC-DOS) utility. The final database, FINLATM, requires approximately 1.1 megabytes of storage.

Before proceeding with the results sections, it is worthwhile to review the Shuttle-derived algorithms employed. As inferred in the background discussions, the density computation is relatively straightforward though one should realize that the interpolation required in the aerodynamic data book formulation is quite elaborate. To that extent, the principal independent variables are either the hypersonic viscous interaction parameter, V_{bar_∞}, or Mach number, M, dependent upon the flight domain; the spacecraft angle-of-attack; and the control surface configuration. Some of these parameters are directly available from the BET or can be computed from same. Configuration data include bodyflap, elevator, speed

brake, aileron and rudder deflections as recorded on the OI. The RCS jet activity is also recorded and the forces and moments due to same are extracted from the IMU data to assure that only aerodynamic effects are considered. Then the density can be obtained as follows:

$$\rho_{C_N} = (2\,m / S_{REF})\ [A_N / (V_A^{\,2}\ C_{Np})]$$

The spacecraft mass, m, is based on the final post-flight mass properties. The normal acceleration, A_N, is derived from the IMU data and the air-relative velocity, V_A, is obtained from the BET. Finally, the predicted normal force coefficient, C_{Np}, is obtained from the data book. As indicated, this predicted value has been rectified to remove the small difference between the pre-flight value and the best estimated flight performance, the latter based on the published aerodynamic consensus FAD. The constant, S_{REF}, is the reference area utilized to normalize the Orbiter aerodynamics. Computations are done at 1 second intervals and benchmarked at the BET altitude, h, prior to interpolation to the previously discussed altitude intervals. The derived density, normalized to the 1976 Standard, is loaded as attribute DD/D76 in the FLTDAT relation.

Next, the complete atmosphere can be obtained from a top-down integration of the hydrostatic equation in conjunction with the perfect gas law as follows:

$$dP = -\rho_{C_N}\ g\ dh$$

and

$$P = [R^{*}\ T\ \rho_{C_N}] / \mu$$

The pressure, P, and temperature, T, are computed using separate options as later discussed. R^{*} is the universal gas constant and the molecular weight, μ, is the same altitude dependent model utilized for the 1976 Standard which, as previously indicated, is loaded as part of the STDATMS relation.

The relation, FLTDAT, includes optional Shuttle-derived temperatures, TI and TII, and pressures, PI/P76 and PII/P76, as indicated. The optional computations refer to the initial

conditions assumed in the hydrostatic equation and the results, particularly in the thermosphere, can be very dependent upon the process utilized. Option I calculates the initial pressure by averaging the temperatures (at the uppermost altitude) from the available models and meteorology data for a specific flight. The initial pressure can then be computed from the perfect gas law using the average temperature in conjunction with the derived density for that particular flight. Option II directly computes the initial pressure as the average pressure implied from the available sources at the uppermost altitude. Again, the initial temperature can be similarly calculated.

One might refer to the preceding options as the *best* temperature and *best* pressure options, respectively. Perhaps a better estimate of either the Shuttle-derived temperature or pressure for a given flight would be the average indicated by the two separate options though, when independently averaged, the gas law might not be satisfied. Certainly, it is fair to conclude that, whenever significant differences occur in the computed temperature (or pressure) for the two options, the derived density might be suspect. Though some of the spread could result from atmospheric inconsistencies in the source data used to initialize either option, the implications are that the derived density might not be consistent with the consensus knowledge of atmospheres from the ensemble of model (or remote) data. Reference 8 addressed this apparent discrepancy and utilized the various combinations of derived pressure and temperature to attempt to quantify the accuracy threshold of the associated derived density profile. Both optional computations were (are herein) considered equally valid and information from each was (is) loaded as part of the database.

Table 2. Database schema utilized.

RELATION	ATTRIBUTE	TYPE	DEFINITION	UNITS
GENDAT	MONTH	Integer	Month of particular STS flight	N/A
	YEAR	Integer	Year of particular STS flight	
	FLT	Integer	STS flight number	
	H-UPPER	Real	Uppermost altitude of available data	km
	SEASON	Text, 6	Season of particular flight	N/A
	MONTH-A	Text, 9	Flight month in character format	
	L-SITE	Text, 9	Landing site for particular STS flight	
	LL-TIME	Text, 12	Local landing time	
STDATMS	H	Real	Altitude above Fischer ellipsoid	km
	LND76	Real	Natural log of the 1976 Standard density	kg/m
	T76	Real	1976 Standard atmospheric temperature	^{O}K
	LNP76	Real	Natural log of the 1976 Standard pressure	N/m
	MOL	Real	Molecular weight, 1976 Standard constituency	kg/kmole
	D62/D76	Real	Density ratio, 1962 to 1976 Standards	N/A
	T62	Real	1962 Standard atmospheric temperature	^{O}K
	P62/P76	Real	Pressure ratio, 1962 to 1976 Standards	N/A
FLTDAT	FLT	Integer	STS flight number (see Note 1)	N/A
	H	Real	Altitude above Fischer ellipsoid	km
	LAT	Real	Geodetic latitude	deg
	LONG	Real	Longitude	
	SIGMA-L	Real	Large scale density perturbation, GRAM	per mil
	SIGMA-S	Real	Small scale density perturbation, GRAM	
	DD/D76	Real	Density ratio, Shuttle-derived to 1976 Standard	N/A
	DGRM/D76	Real	Density ratio, GRAM to 1976 Standard	
	DAF/D76	Real	Density ratio, USAF'78 to 1976 Standard	
	DMES/D76	Real	Density ratio, measured to 1976 Standard	
	TI	Real	Shuttle-derived temperature - Option I	^{O}K
	TII	Real	Shuttle-derived temperature - Option II	
	TGRM	Real	GRAM atmospheric temperature	
	TAF	Real	USAF'78 atmospheric temperature	
	TMES	Real	Measured atmospheric temperature	
	PI/P76	Real	Shuttle-derived pressure (Option I), normalized	N/A
	PII/P76	Real	Shuttle-derived pressure (Option II), normalized	
	PGRM/P76	Real	Pressure ratio, GRAM to 1976 Standard	
	PAF/P76	Real	Pressure ratio, USAF'78 to 1976 Standard	
	PMES/P76	Real	Pressure ratio, measured to 1976 Standard	
	U-WMES	Real	North to South wind component, measured	m/sec
	V-WMES	Real	East to West wind component, measured	
	U-WGRM	Real	North to South wind component, GRAM	
	V-WGRM	Real	East to West wind component, GRAM	
	HDOT	Real	Shuttle descent rate	

(Note 1) 100 added to all RSOC designated flights to eliminate duplication.

LATEST FLIGHT RESULTS

In this section, results from the ten additional flights are presented. Density and temperature profiles and comparisons with the alternate data will be shown. Similar data for the original 22 flights are attached in Appendix A herein as earlier noted. These data, in conjunction with the more recent flights, will later be combined to demonstrate latitudinal, monthly, and seasonal effects from the total ensemble. To supplement discussions in this particular section, readers might choose to peruse some of the data in the appendix for supporting background.

Figure 2 depicts the results from the RSOCF26 designated flight, an October flight traversing the middle-latitude band into Edwards Air Force Base. The ground-track profile presented has altitude marks superimposed thereon. In view of the small font utilized, readers are advised that these benchmark points conform to every 10 km between 95 km and 45 km, respectively. This format is adopted for each of the flights presented herein. The density and temperature profiles include comparisons between the Shuttle-derived parameters, the GRAM and AF'78 models, and the remote meteorological data. The latter, indicated as "MEASURED," agrees quite well with the Shuttle-derived density profile. In this instance, the AF'78 data are also virtually in agreement with the "DERIVED" data. From Shuttle-derived considerations, these flight results represent a reasonably mundane atmosphere. Readers should note that both Shuttle-derived temperature options are plotted. Consequently, the differences in the mesopausal region are indicated by the shaded boundary.

Similar results for RSOCF27 are presented as Figure 3. As seen in the ground-track plot, this flight is one of the high latitude entry flights for which limited ground-tracking data are available for post-flight trajectory reconstruction. Whereas the flight results do exhibit lower density at northern latitudes, the effect is somewhat less than expected based on past results. Actually, one would expect that the measured results were more likely. It should be noted that, had the datum-shift been applied, the derived density would have been some 10 percent less at the uppermost altitudes. Coincidentally, the derived profile does compare favorably with the data from the two models. This has not been the situation for previous high-latitude flights. Finally, in terms of the local structure observed in the Shuttle-derived results, this would appear to be a relatively quiescent (late fall) atmosphere.

Figure 4 presents the density and temperature results for RSOCF28. Here, the measured and model data are almost in complete accord. The Shuttle-derived results indicate anything but a mundane profile. In particular, an approximate 30 percent abrupt

density shift can be observed. The implied super-adiabatic lapse rate in the derived temperature profile would indicate an unstable condition, perhaps atmospheric overturning. Similar occurrences have been observed on past flights, though generally at higher altitudes. This was previously considered to be correlated with the onset of the mesosphere. Should this be the case, the mesopausal region would extend down to approximately 77 km for this profile. Being a summer atmosphere, one would expect more turbulence to be present in the middle altitude intervals. Apart from the abrupt shift, this profile does not suggest as much turbulence as one would expect based on previous results. Some of the signal apparent above approximately 83 km should be cautiously interpreted. That signal suggests more noisy IMU data than expected, an occurrence that was observed on STS-6. Such a conclusion is mostly speculative since this was a Department of Defense (DoD) flight and much of the post-flight data generally available to make such determinations were not available on this flight. In either event, the mean profile is well described and the abrupt shift, considering the altitude at which it occurred, qualifies this as one of the more unique atmospheres encountered by Shuttle.

RSOCF29 results are presented as Figure 5. This mid-latitude March flight suggests a density structure with an apparent triangular wave superimposed about the mean. The measured data remarkably represents that implied mean. Actually, the model data compare favorably throughout as well. However, apart from the structure evident in the Shuttle-derived results, none of the profiles depart more than 10 percent from the 1976 Standard throughout the entire range. It is noted that the spread in the derived temperature profiles from the two optional computations increases within the mesopause to some 20 ^{O}K at 95 km. Though not significant, this could indicate a need for some subtle improvement in the smoothed density profile above 88 km.

Figure 6 presents the RSOCF30 results. Again, though more structure is evident in the Shuttle-derived results, the remote data are essentially a manifestation of the mean atmosphere one would expect from in situ considerations. Both models suggest a much more dense profile, particularly above 75 km. Similar comments can be made for the RSOCF31 comparisons shown as Figure 7 herein. However, in this instance the measured profile does not compare as favorably with the derived density throughout the entire altitude interval. Moreover, in this case, the GRAM density model exhibits less density over the lowermost altitudes.

Results for the RSOCF32 flight are presented in Figure 8. Here, the measured profile, apart from the small scale variations, exhibits more structure than implied in the Shuttle-derived results. Except for selected altitude regions, neither the measured nor

model atmospheres compare well with the in situ results. By contrast, the measured atmosphere for RSOCF33, as seen in Figure 9, again reflects an excellent mean atmosphere when compared with the Shuttle-derived density. This is also suggested in the RSOCF34 results shown in Figure 10 except, of course, the local density structure implied by the derived results cannot be replicated. Again, in this instance, the data from both models suggest a much higher density throughout. This is a September flight and, as will later be shown, the Shuttle-derived results herein are somewhat erratic when compared with other flights for the same period.

The RSOCF36 flight, a high latitude entry profile, exhibits the low density in the northern hemisphere that one would expect which, in this case, is a relatively smooth profile. However, as can be seen in Figure 11, this is not substantiated by the remote data. Of the ten additional flights germane to this database update, this is the only flight wherein the remote data are questionable. It should be pointed out that these data are delivered to JSC as a series of *totem-pole* atmospheres based on the various ROBIN sphere, rawindsonde, and thermistor soundings taken in support of the mission. These *totem-pole* data are interpolated versus altitude and cross-interpolated in latitude and longitude using a bi-variate process to translate the remote measurements to the Shuttle ground-track and vertical profile. Perhaps the wrong pair of *totem-poles* were utilized, or the sounding information, the source data that substantiated the more dense atmosphere, was inaccurate for unknown reasons. Again, these are purely speculative discussions. In either event, the derived data are as expected which, as shown in the next section, matches the other high-latitude data quite well. Based on past experiences, neither model would be expected to corroborate the Shuttle-derived results. Finally, one should note that the increased spread in the derived temperature data is again more pronounced for this flight.

This concludes the section on individual flight results for the additional ten flights. Again, similar results for the previous 22 flights are included in Appendix A for reader perusal. In the ensuing sections, latitudinal, monthly, and seasonal effects will be evaluated. Data from the prior flights are included therein as part of the total ensemble of Shuttle results.

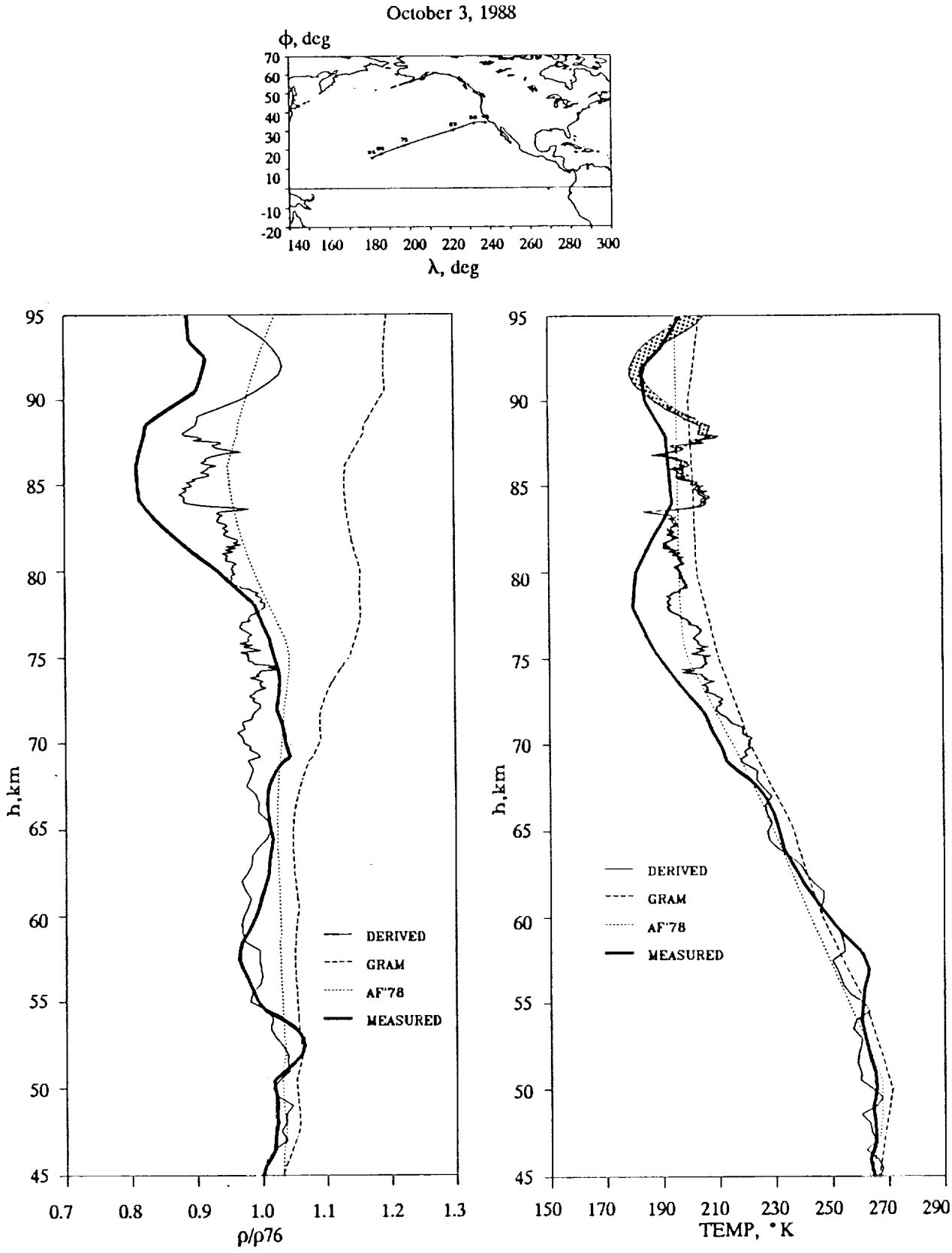

Figure 2. RSOCF26 density and temperature profile comparisons.

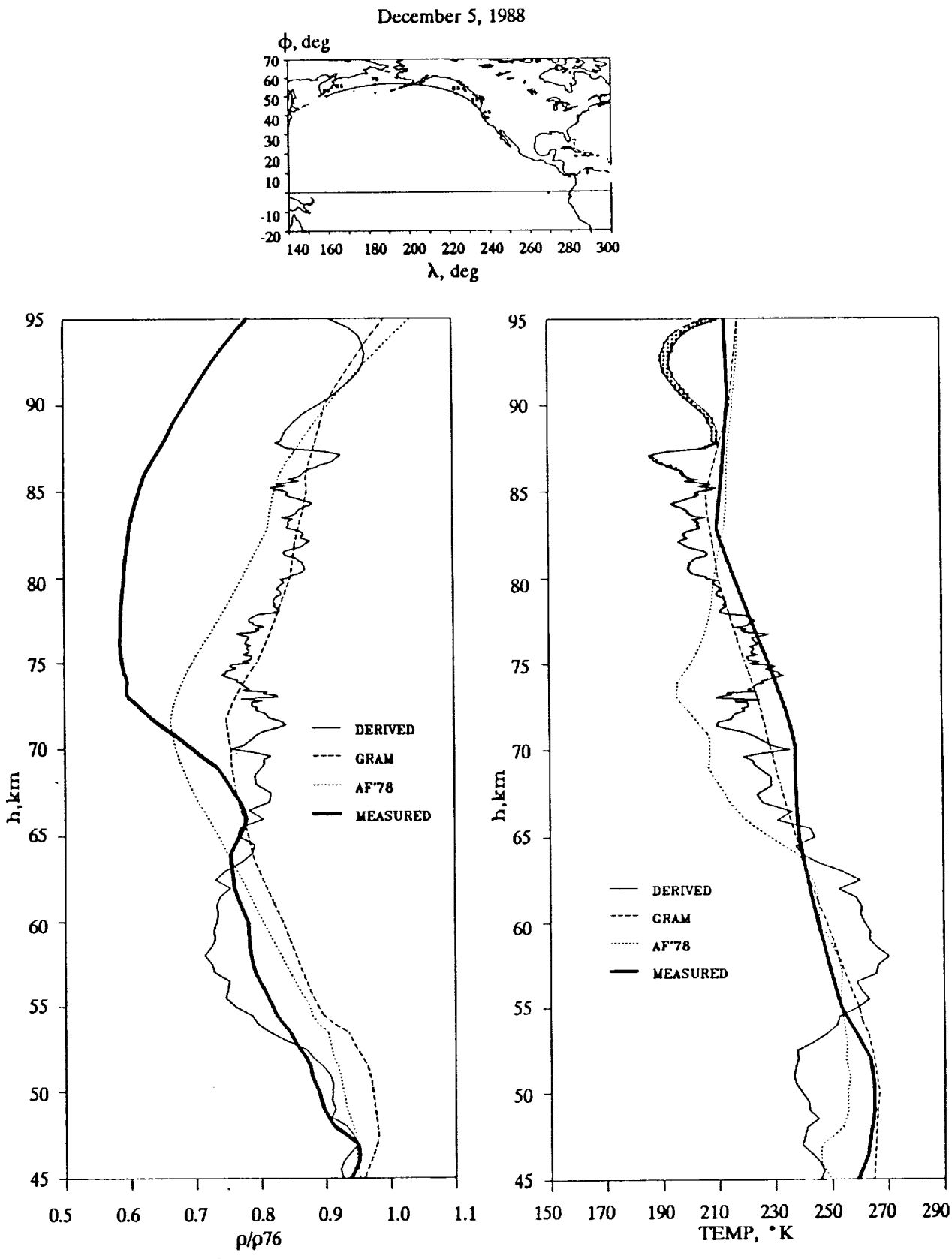

Figure 3. RSOCF27 density and temperature profile comparisons.

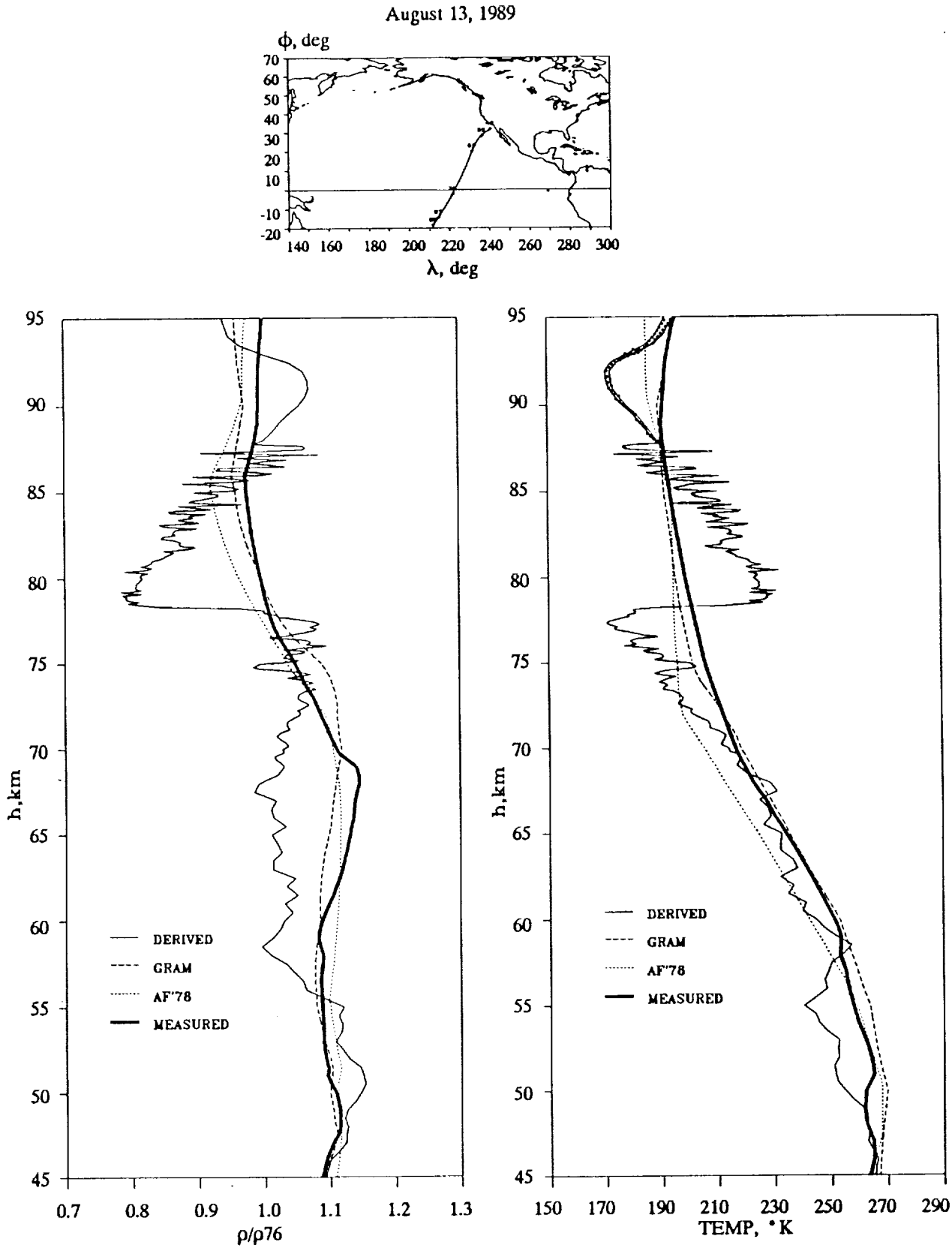

Figure 4. RSOCF28 density and temperature profile comparisons.

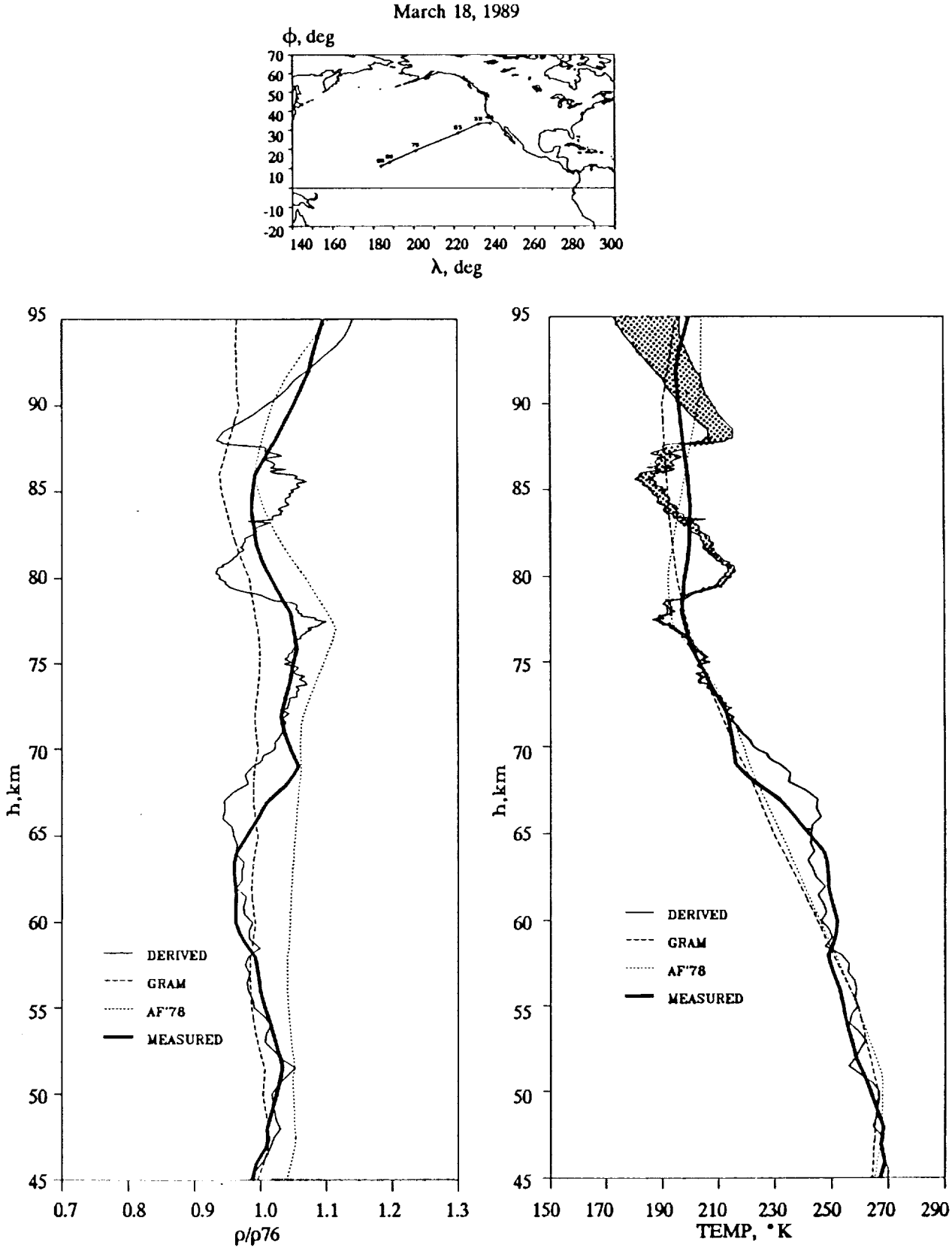

Figure 5. RSOCF29 density and temperature profile comparisons.

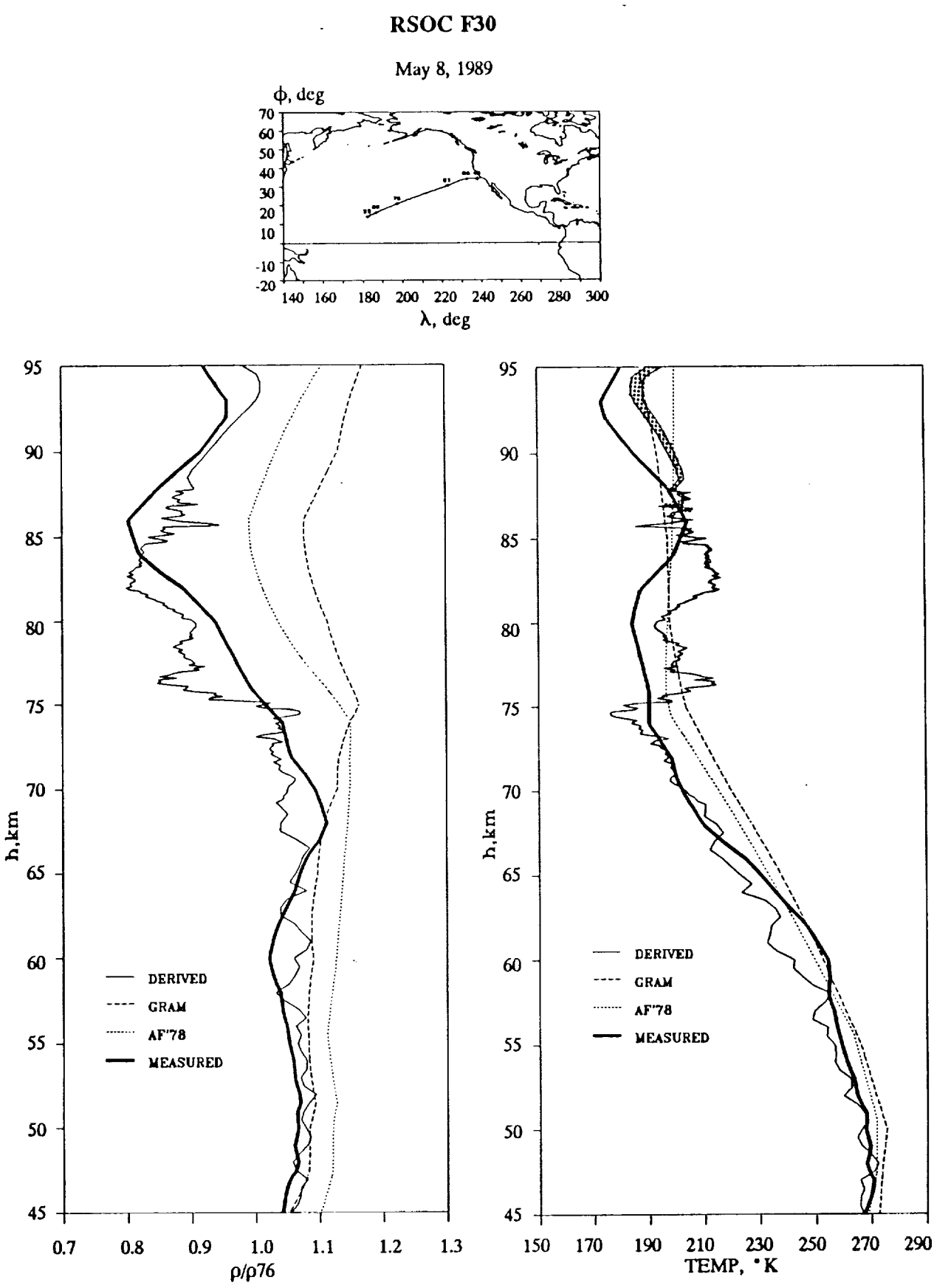

Figure 6. RSOCF30 density and temperature profile comparisons.

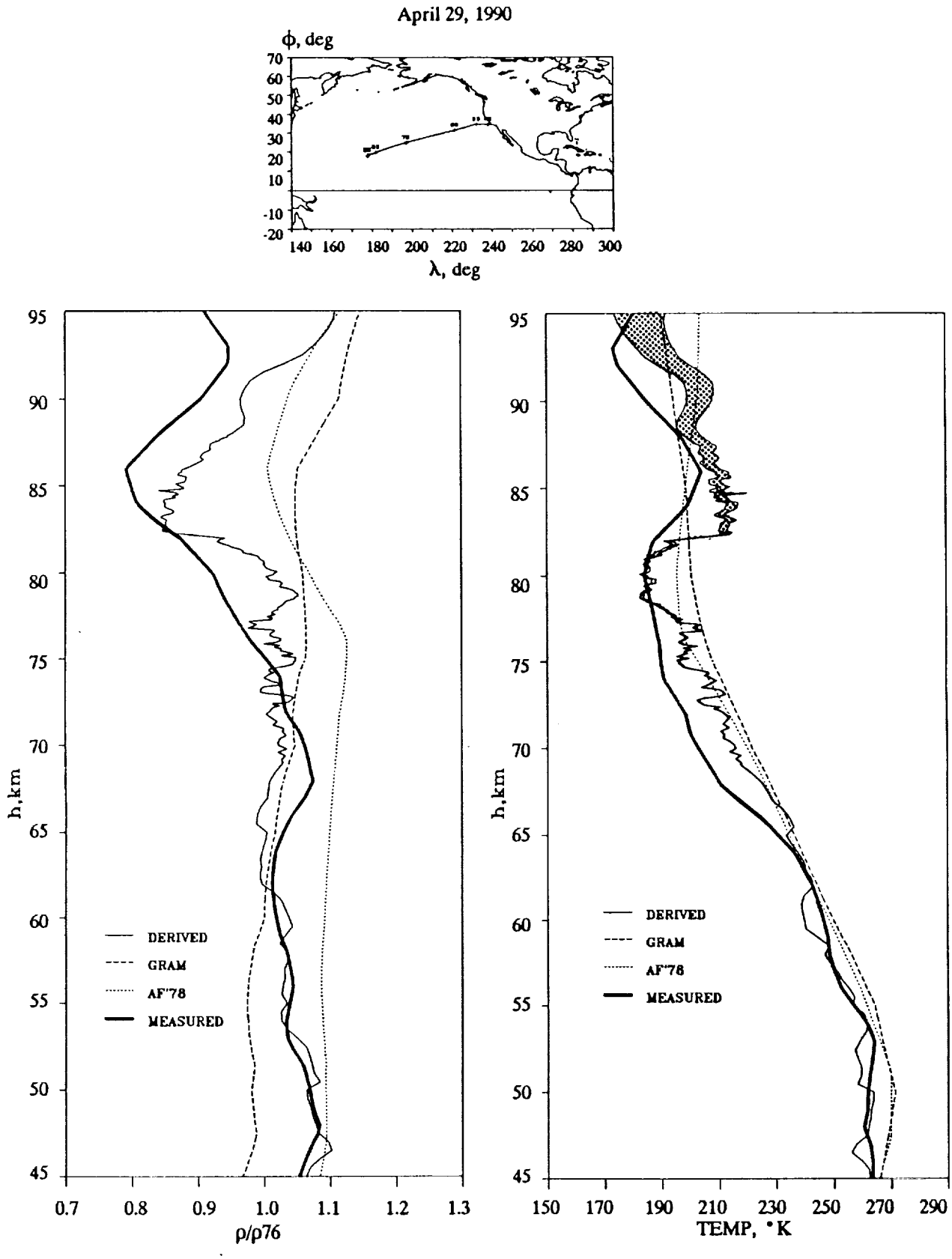

Figure 7. RSOCF31 density and temperature profile comparisons.

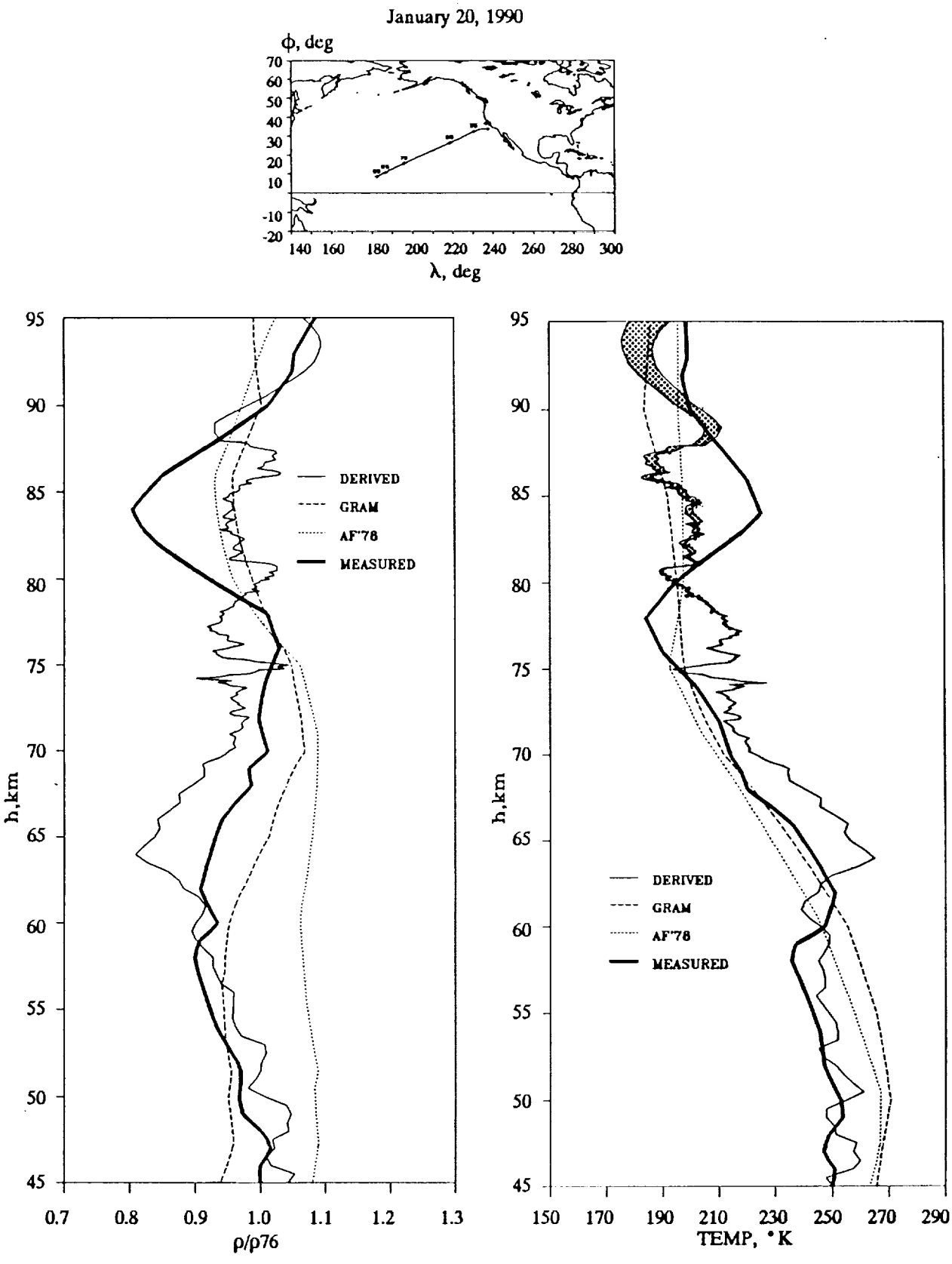

Figure 8. RSOCF32 density and temperature profile comparisons.

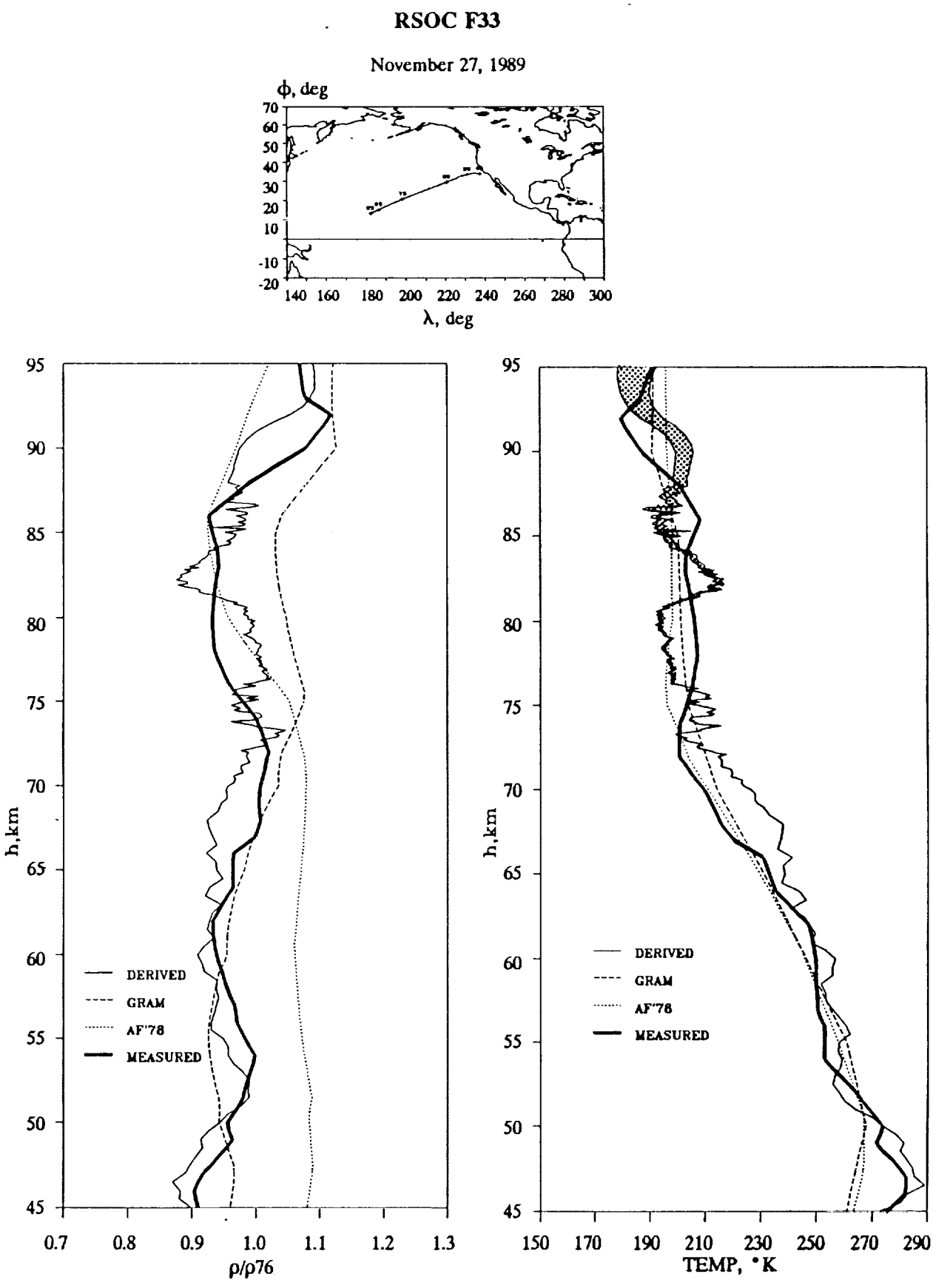

Figure 9. RSOCF33 density and temperature profile comparisons.

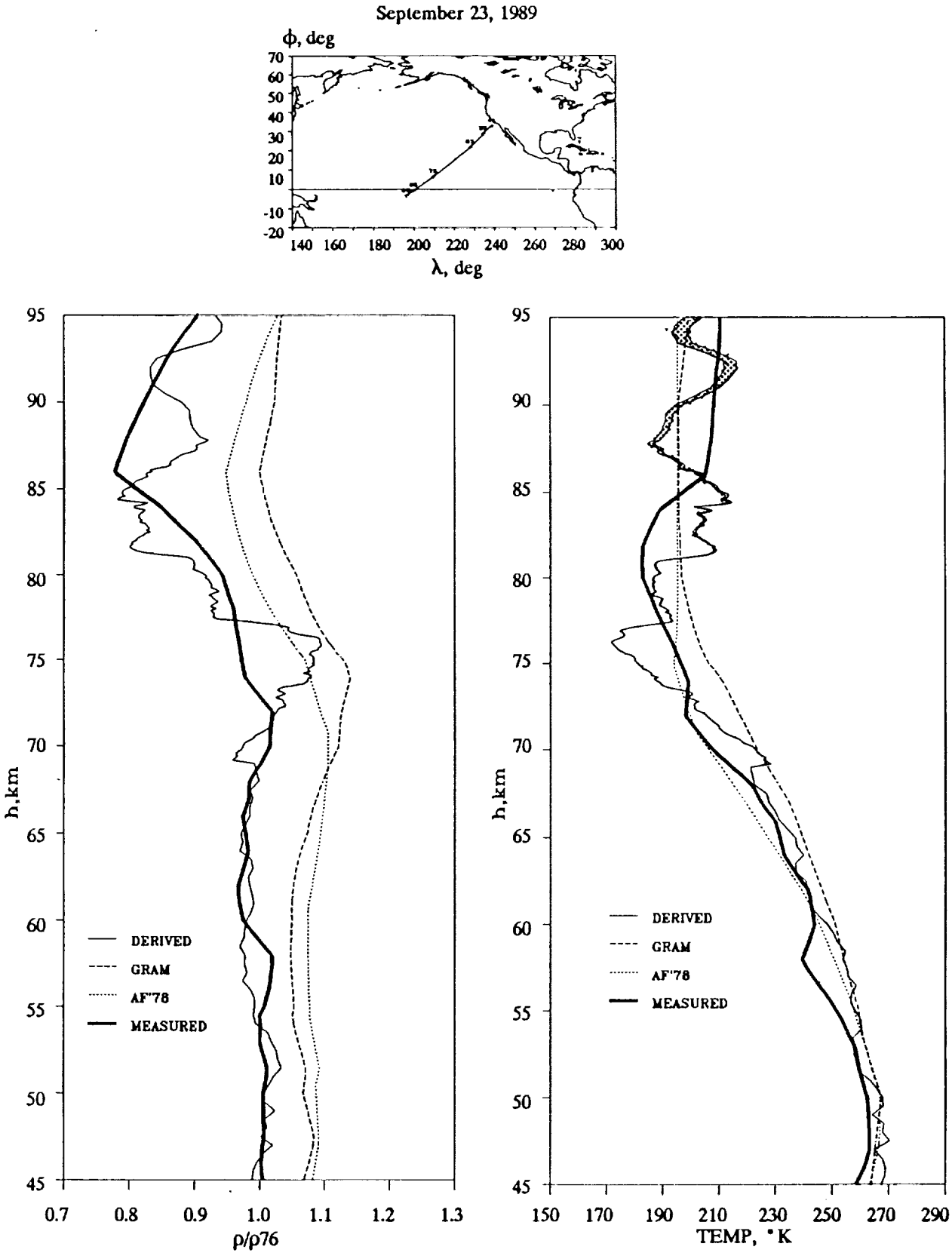

Figure 10. RSOCF34 density and temperature profile comparisons.

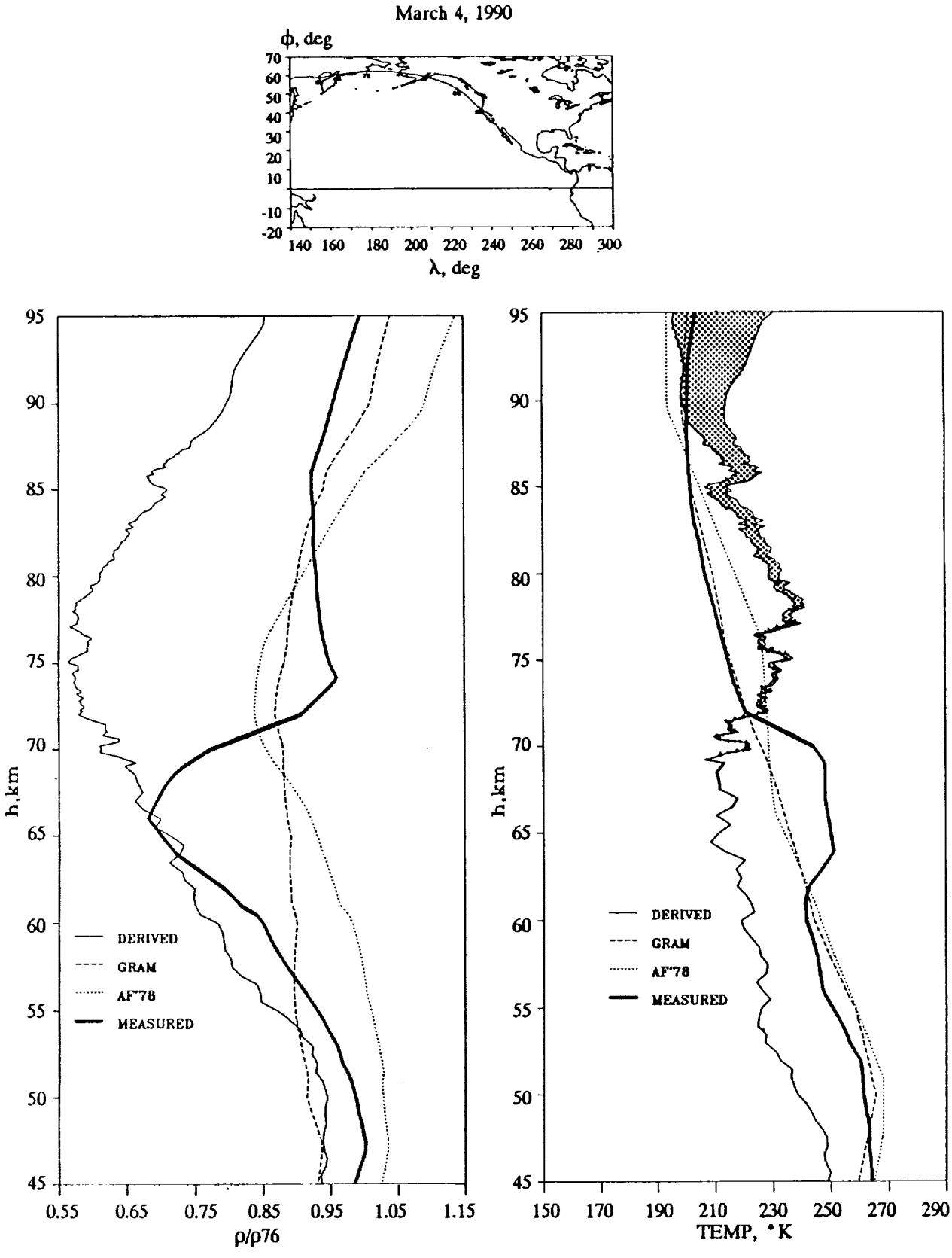

Figure 11. RSOCF36 density and temperature profile comparisons.

LATITUDINAL EFFECTS

Previous Shuttle-derived results have consistently demonstrated low density (approximately 60 percent of Standard) at the northernmost latitudes not unlike that observed by others, for example, during the Energy Budget Campaign. [13] In addition, based on the first 22 flights, it did appear that densities at the most southerly latitudes, particularly over the uppermost altitudes, were considerably lower (75 to 80 percent of Standard). Consequently, it was preliminarily reported that a density bulge existed at approximately 20^{o} N. Given the additional complement of ten flights, even recognizing that the RSOCF27 data are not quite as low as expected, the low density at the most northerly latitudes is further substantiated by the results herein. However, the additional flights and associated spread of results throughout the mesopause would tend to indicate that the determinations implied for the most southerly cases are yet to be substantiated.

Figure 12 herein shows the results for the four high-latitude entry flights. Also shown thereon, as the bold line, is the average density profile computed from same. Apart from the RSOCF27 data, the results are remarkably similar. Supporting data (see Figure 13) shows that the results of these same four flights do correlate with latitude differences though, to be sure, the implied latitudinal partials would have to be quite large and extremely non-linear, maximizing in the 50^{o} N region. Even if this were purely coincidental, the suggested average, to include the RSOCF27 results, clearly vindicates the low density determinations. It is significant that perusal of each of the separate flight results shows that none of the available models come close to matching the Shuttle high-latitude results above 65 km and, for the most part, neither do the remote data. Certainly the Shuttle results could be utilized for model upgrading.

A similar plot is presented as Figure 14 for the low-latitude entries. Again, four flights are available. The mean profile, the bold line, still indicates a lower density in the mesopause, with an average of approximately 85 percent of Standard at 95 km. Though the earlier results are not entirely refuted, the additional spread induced by the RSOCF28 flight, coupled with the results from some of the more recent mid-latitude entries, tends to diminish the determination. This is best seen in Figure 15 which shows both the northerly and southerly averages superimposed on the same graph with the average results for the remaining flights. This latter average is based on 24 entries. When one considers that there is an uncertainty which could properly be superimposed as a band about the suggested means, considerable overlap would occur between the low and mid-latitude data. Consequently, based on the ensemble of flights to date, it is premature to conclude that lower density in the southern hemisphere is the expected norm. For the remainder of this

report, these flights will be combined with the mid-latitude results to infer monthly and seasonal tendencies. Clearly, the high-latitude results must be removed from such analogies since the northerly latitude effects are so predominant.

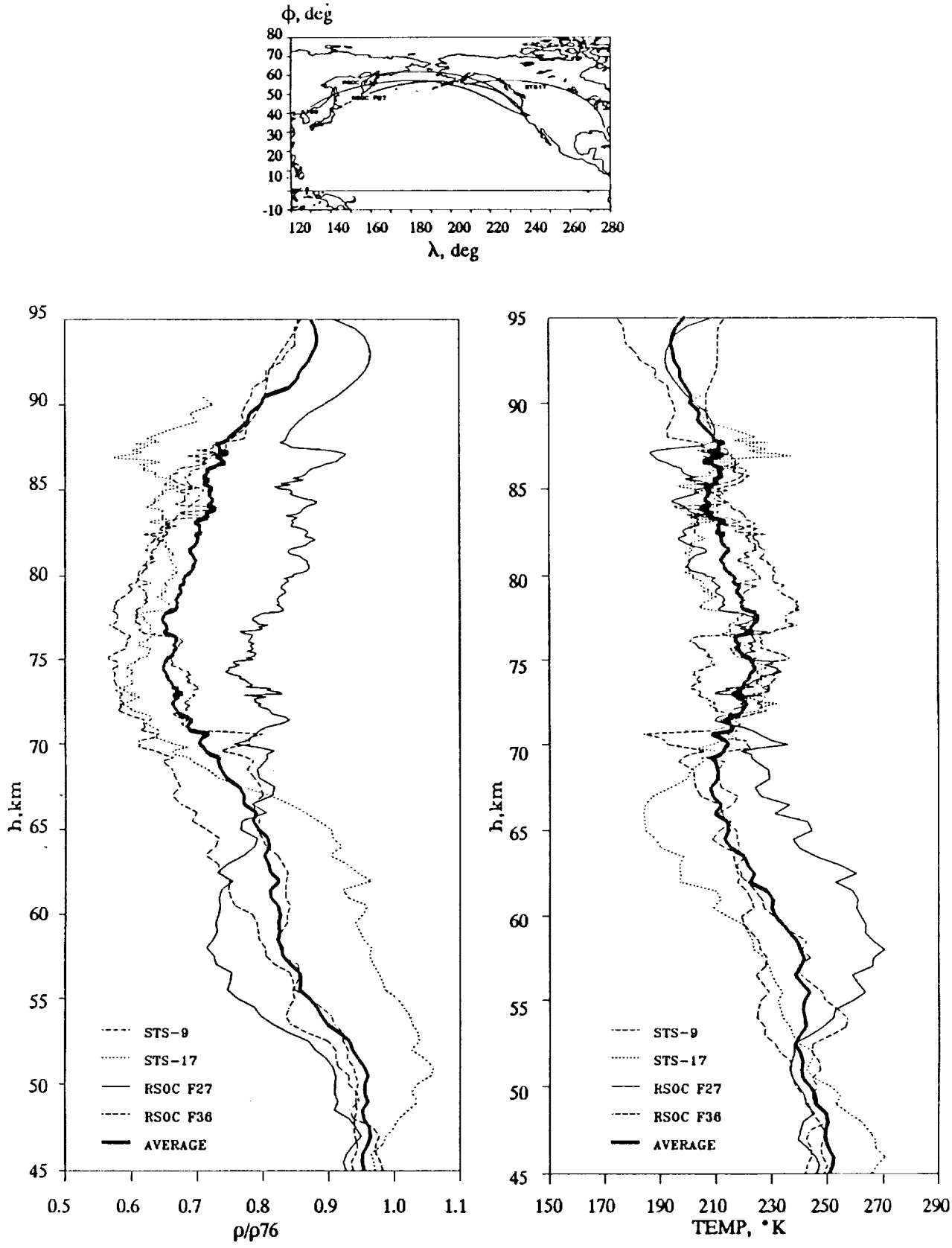

Figure 12. High-latitude density and temperature profiles.

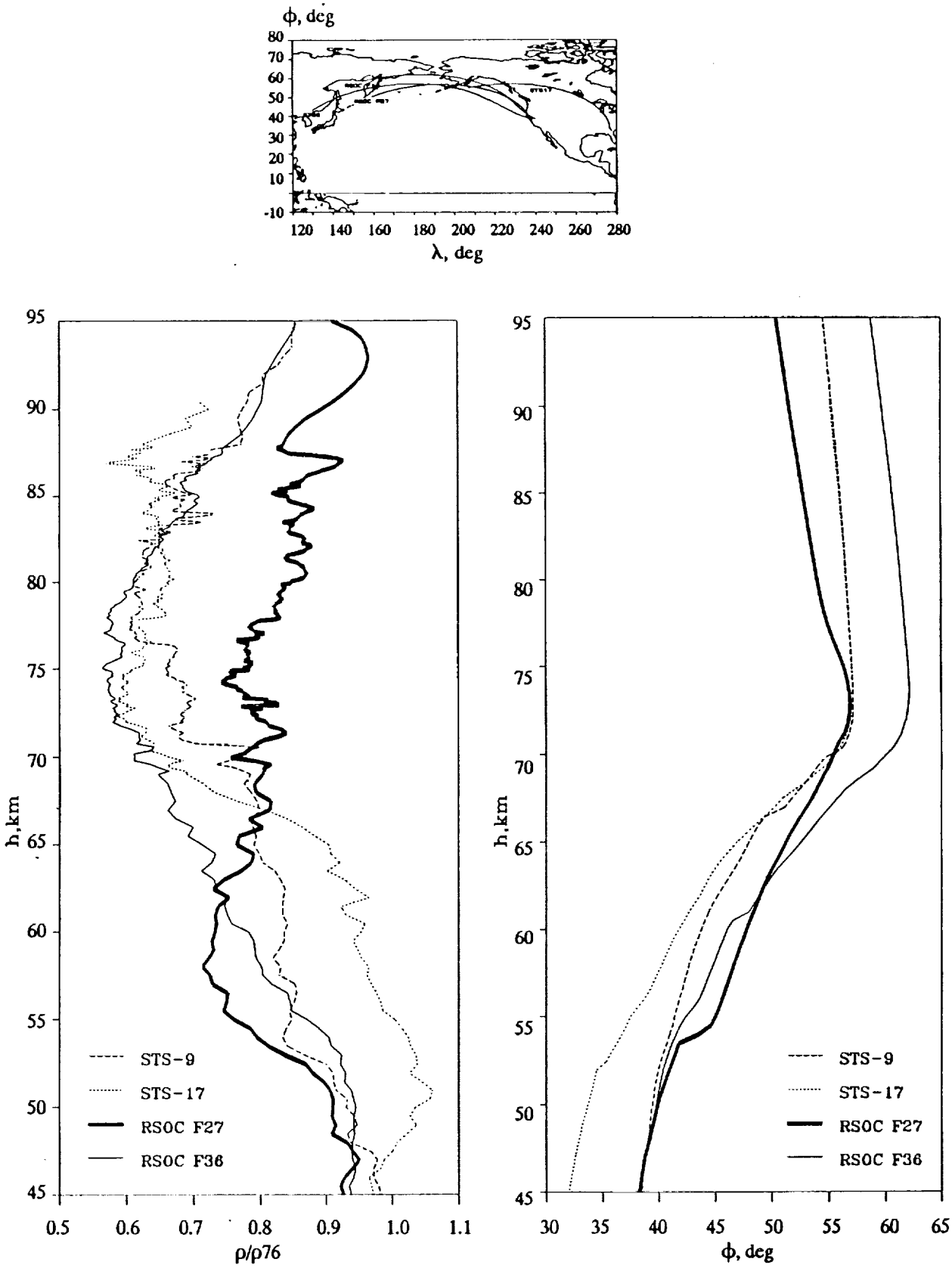

Figure 13. Density correlations at high latitudes.

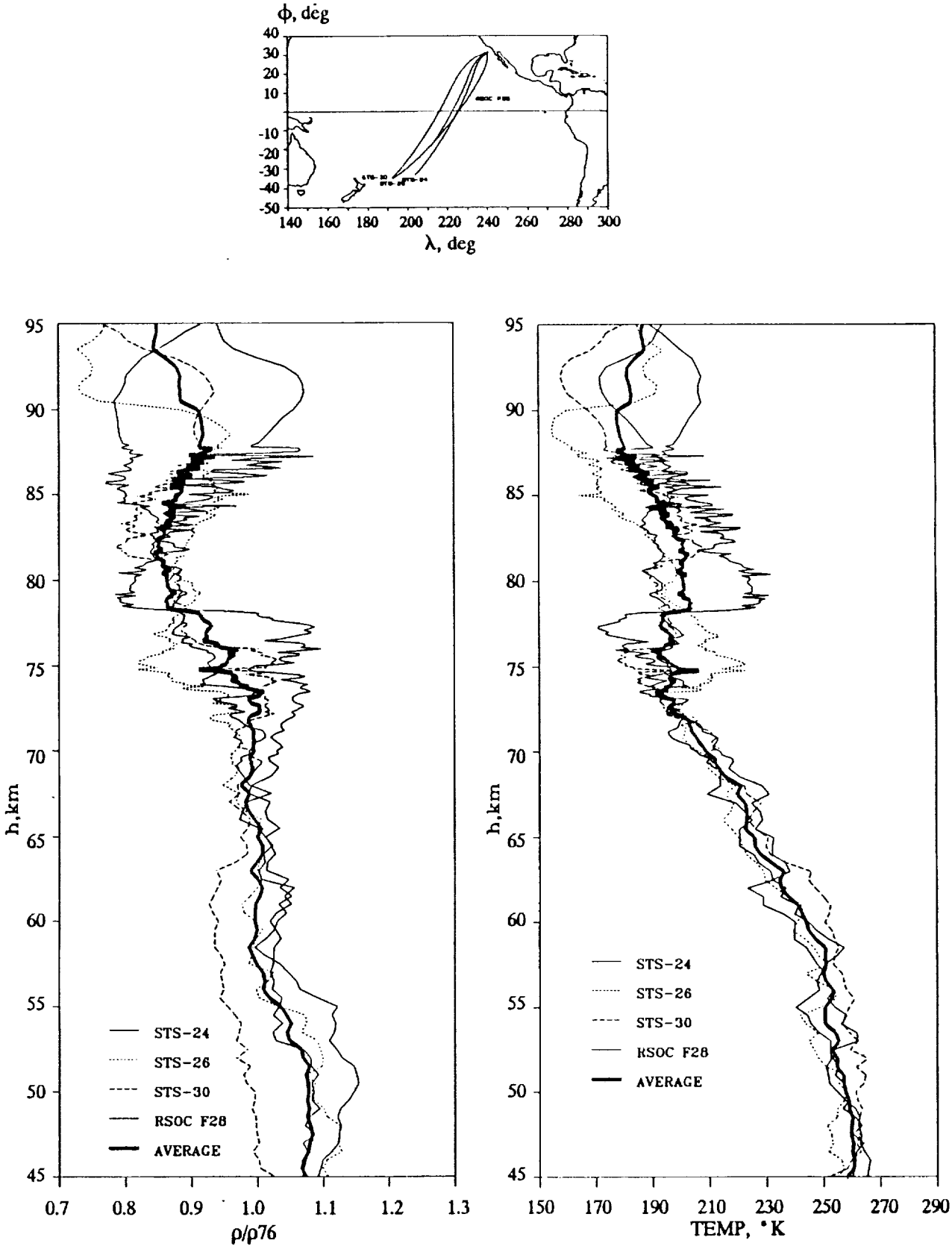

Figure 14. Low-latitude density and temperature profiles.

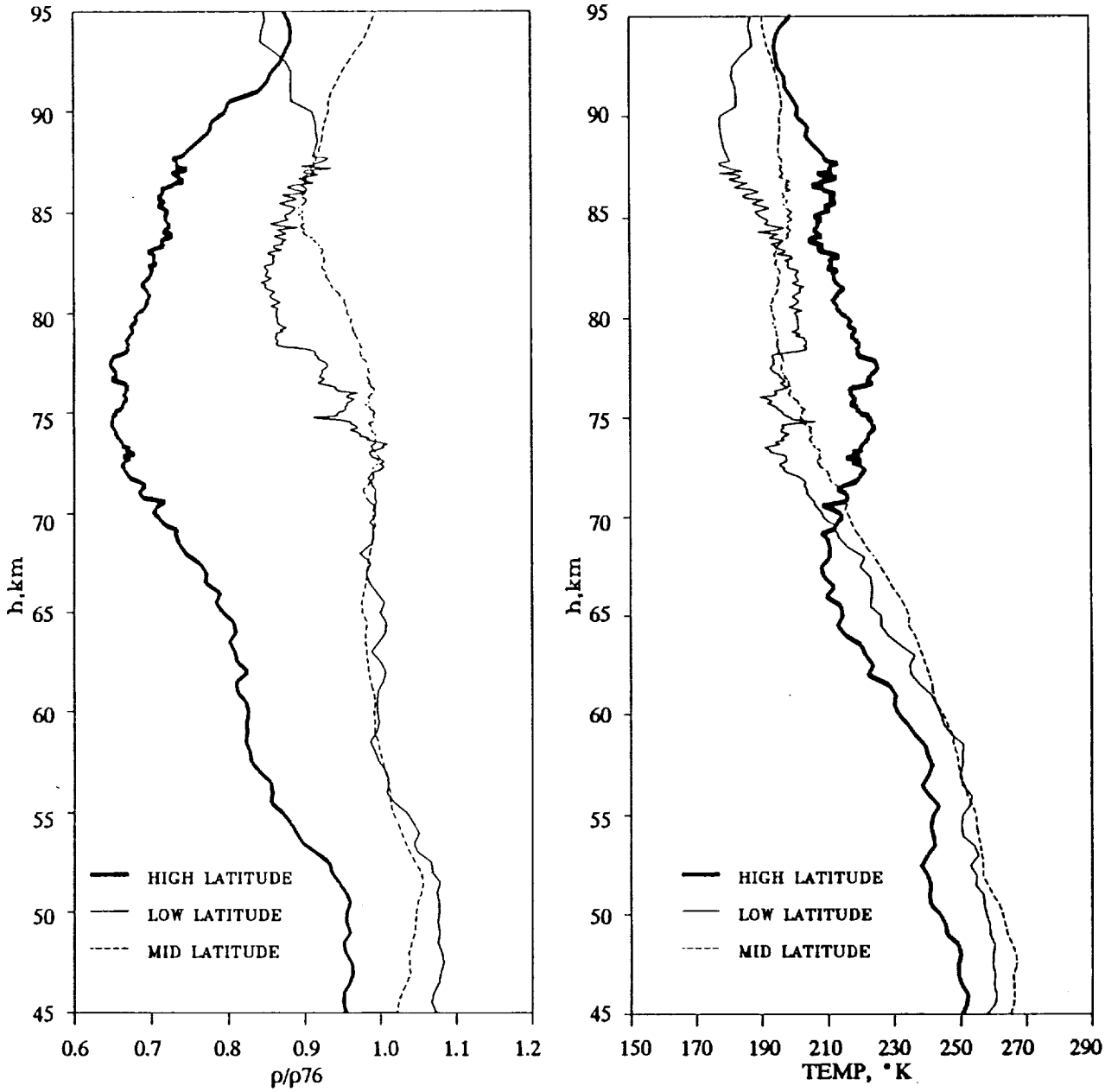

Figure 15. Average density and temperature variations with latitude.

MONTHLY AND SEASONAL SIMILARITIES

Figure 16 shows the monthly and seasonal opportunities for atmospheric determinations that are available in the total ensemble of Shuttle flights. Readers are reminded that four of these flights correspond to the high-latitude entry profiles and are not included herein. However, the low-latitude profiles will be incorporated in this section for reasons previously discussed.

Figure 17 shows the various profiles for the included 28 flights as the calendar varies from early spring (March 30) throughout late winter (March 18). The actual year of each particular flight is discounted herein. Readers scanning these data will observe certain trends in the flight results. However, monthly similarities are best seen in the included figures, Figures 18 through 25, respectively. Here, all multiple month flights are included, that is, all months with two or more flights after the high-latitude flights are removed. Figure 18 shows January results for two flights, with the computed average profile as indicated. Similarly, March results are shown as Figure 19. Though only two flights are available for each of these months, the comparisons (for March in particular) are quite good.

Five flights are available in April as seen in Figure 20. The results from each of these flights indicate virtually identical trends such that these data can be averaged with a certain degree of statistical confidence. Again, the results for May (Figure 21), June (Figure 22), and August (Figure 23) are limited to just two opportunities in each of these months. Though statistical confirmations are limited, the trends are quite similar. The two May profiles are virtually the same. Similarities also exist for June though the August results reflect the rather unique nature of the RSOCF28 flights, i. e., the abrupt density shift alluded to earlier.

September and November are two of the more abundant flight months. The September results are shown in Figure 24. Here, four flights are available. As stated previously, the RSOCF34 flight is somewhat an outlier since most of the September results have exhibited rather mundane profiles. This flight is a more southerly entry but, since the low-latitude effects were discounted previously for lack of any real determination, that must be ruled out as the basis of any discrepancy. Moreover, eventhough the flight date is essentially commensurate with the autumnal equinox, the increased variation in the density profile is not felt to be seasonal related. Despite the suggested structure from this flight, these data, in conjunction with the other three flights, still yield a reasonably solid average profile for the month. The average November profile is based on five flights as shown in Figure 25. In

this instance, similarities are quite good except that one must conclude that more density variation in the mesopause is indicative of the month.

Only three months contain flights of sufficient numbers for which some statistical confidence can be attached to the associated average profiles. These are April (5 flights), September (4 flights) and November (5 flights). The average profiles for these months are shown in Figure 26. Plotted, as the shaded boundary, are the mean profiles with the $\pm 1\,\sigma$ computed standard deviation superimposed about same. Also shown on this chart are the mean monthly atmospheres from the two models as indicated. To an extent, apart from a bias and (perhaps) a scale-factor, the AF'78 data more closely follow the trends in the derived data.

Even for such a limited number of flights, there seems to be considerable evidence that the Shuttle data could well provide a basis for mean model upgrading. For the most part, the model data exhibit a more dense atmosphere than would be suggested by the Shuttle results. Moreover, structure over the upper mesosphere and throughout the entire mesopausal region is much more apparent than that indicated by either model. Most certainly, the differences and associated spreads implied in the Shuttle results could be folded into error analyses for existing atmospheric models. However, one can only cautiously make recommendations based on the limited number of flights to date.

Lastly, it is worthwhile to show seasonal comparisons available in the Shuttle flights of record. Keeping in mind that the high-latitude entries are not included in this analysis, the remaining 28 flights still permit multiple seasonal opportunities. Spring profiles for eight flights are shown in Figure 27. Also superimposed is the mean spring profile. Summer data are given in Figure 28. Again, data from eight flights are shown, to include the average summer profile. Data from seven fall flights are shown in Figure 29 and the four winter flights are presented as Figure 30. Again, the average seasonal profiles are shown on these two figures. Figure 31 presents the composite average profiles obtained for the four seasons. Some trending is noticeable below 75 km. However, were these data plotted as a statistical band some overlap would occur. Consequently, the inferred seasonal determinations might be somewhat overstated as a result of this presentation. Again, a larger ensemble of flights would be required. Given more ample data, monthly effects could be quantified for each calendar month. Then, seasonal effects would be better determined.

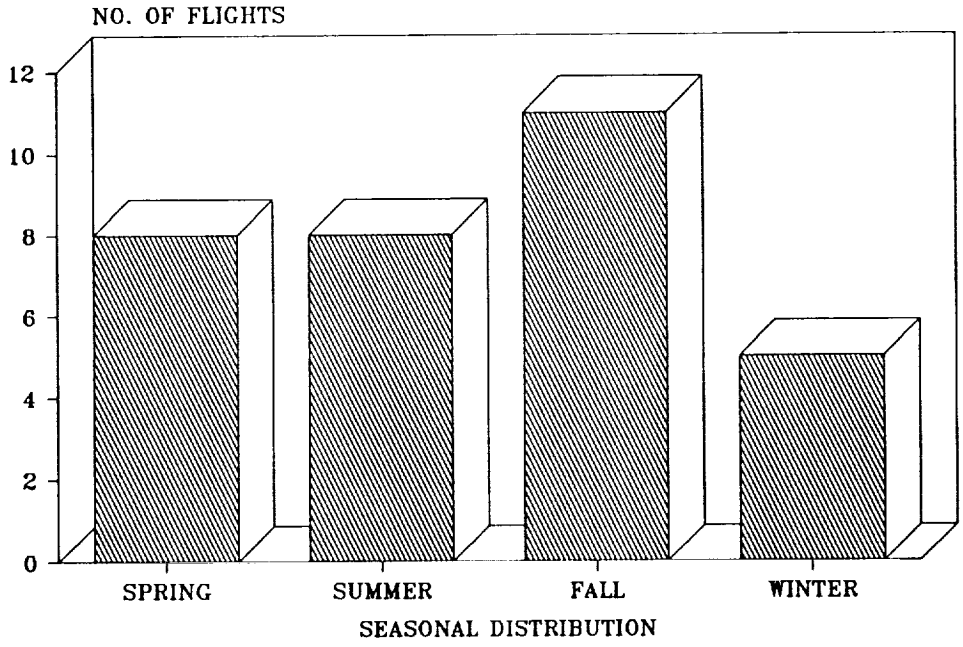

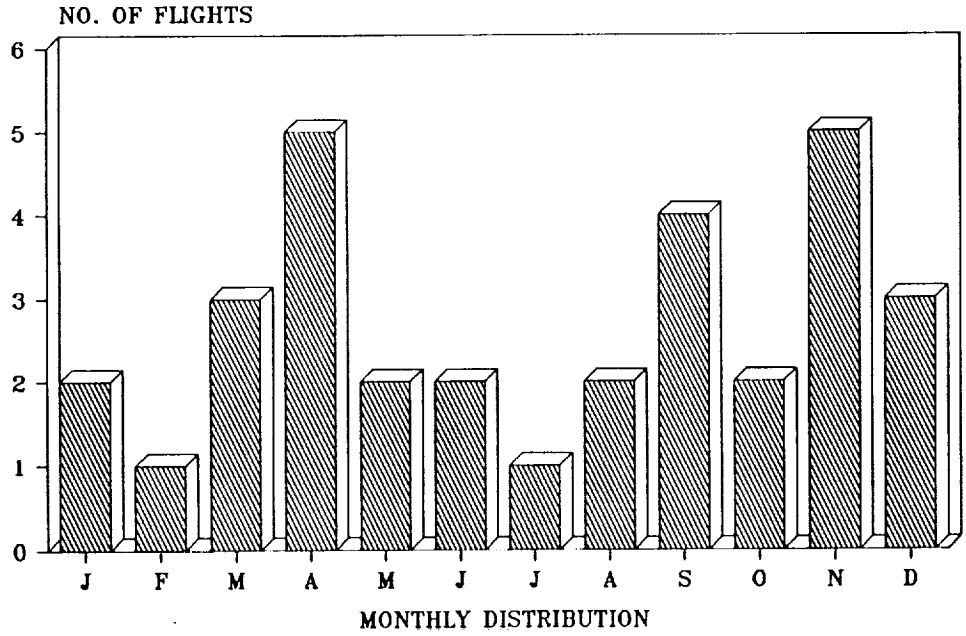

Figure 16. Seasonal and monthly coverages in the Shuttle flights.

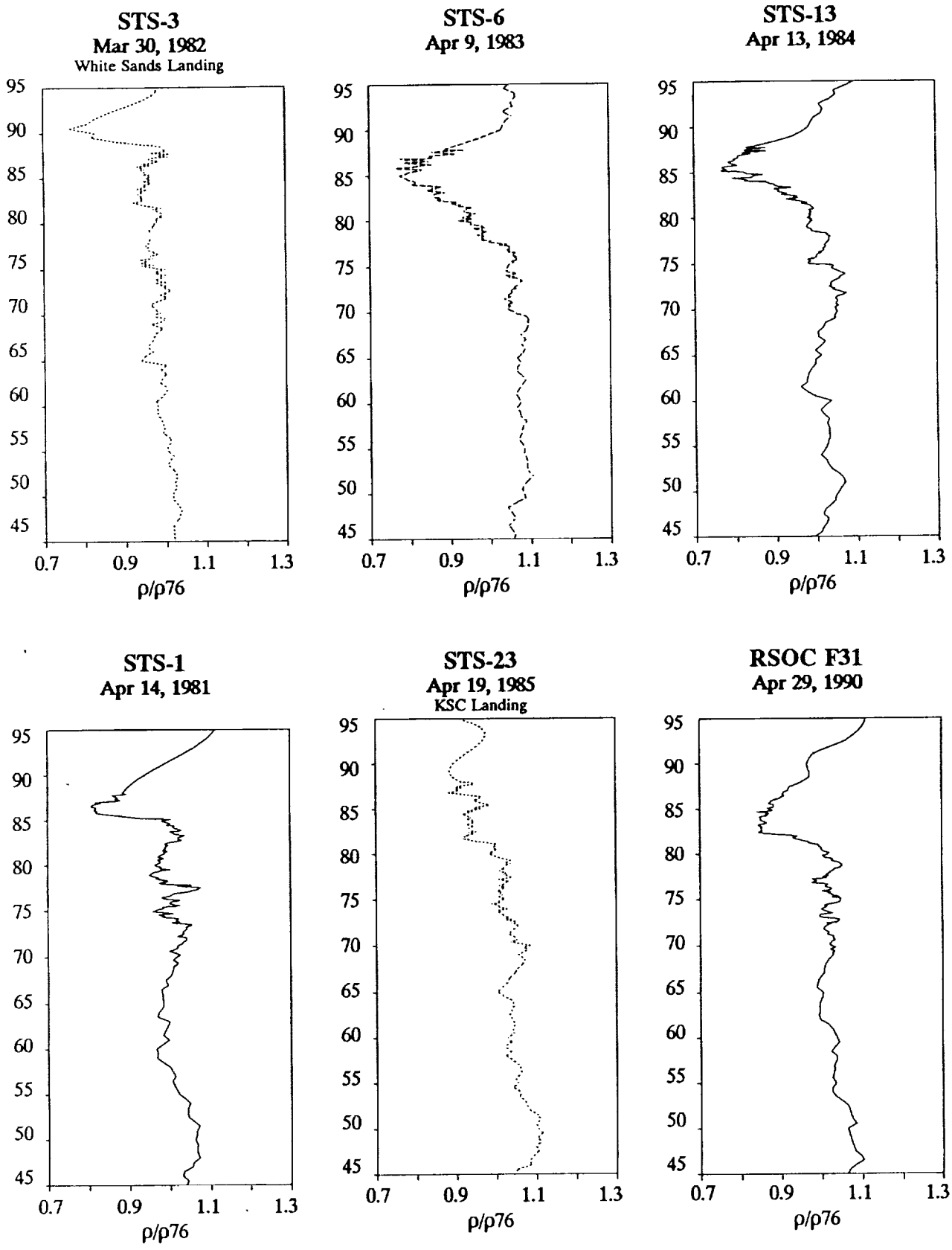

Figure 17. Middle and low-latitude derived density composite.

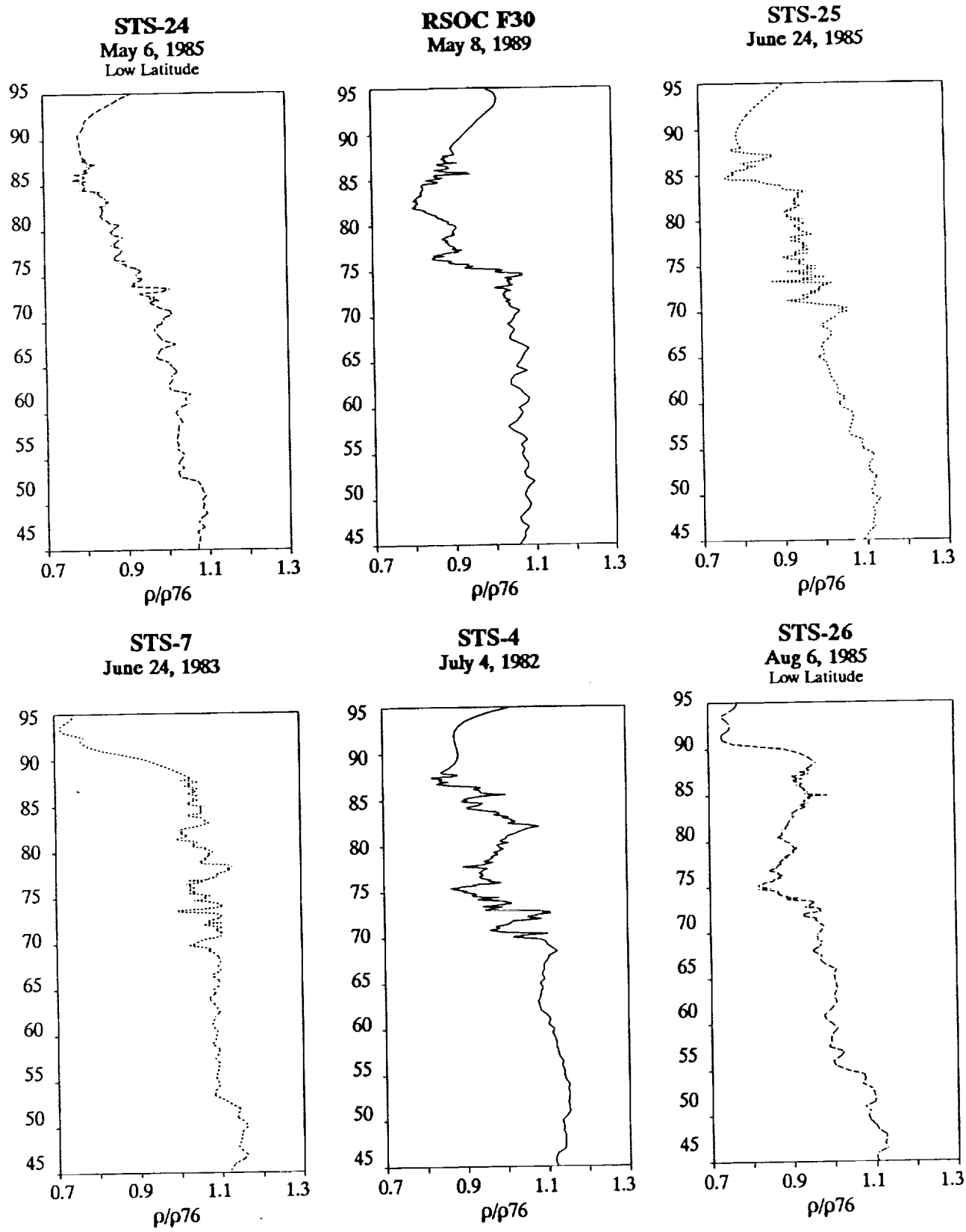

Figure 17. (continued)

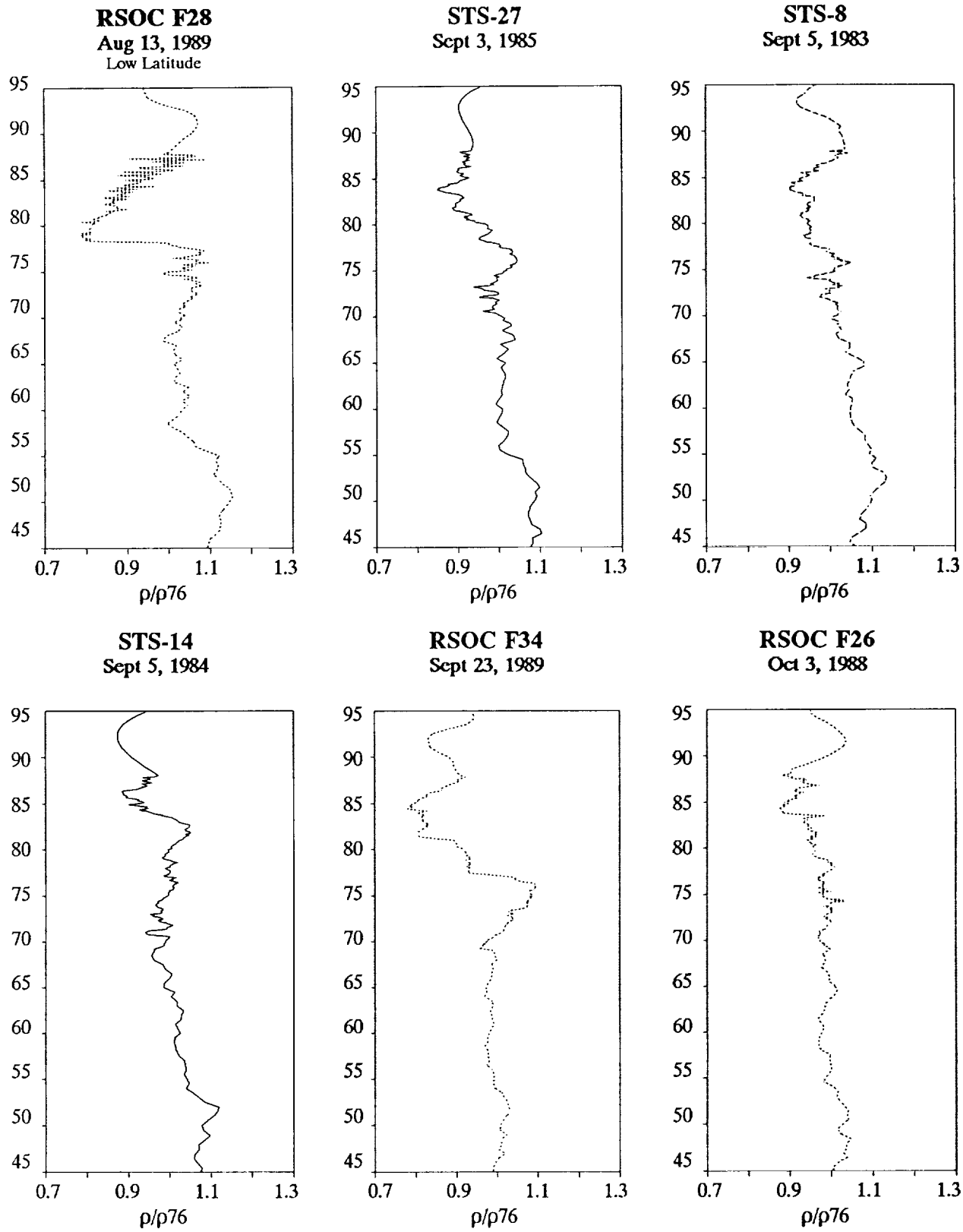

Figure 17. (continued)

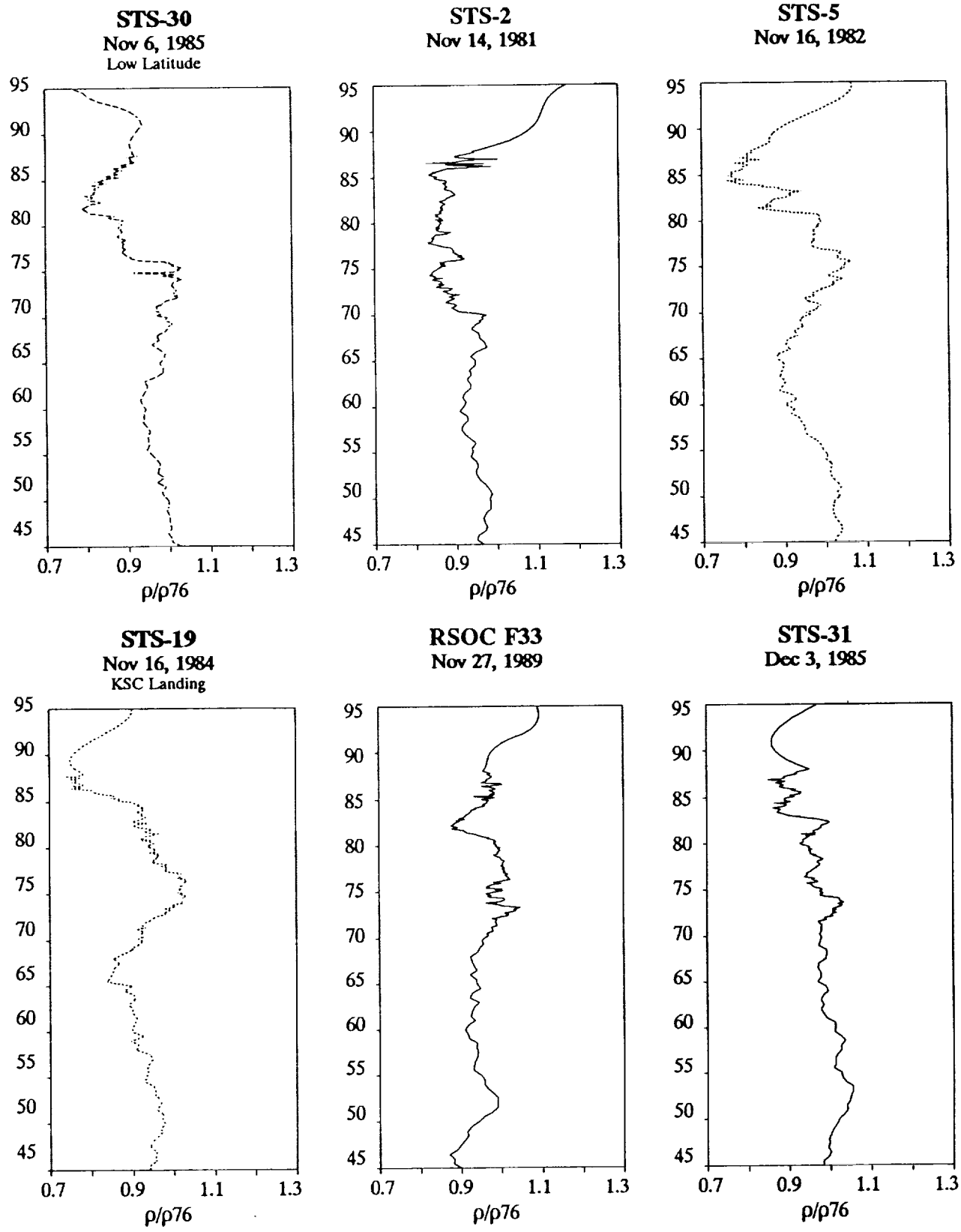

Figure 17. (continued)

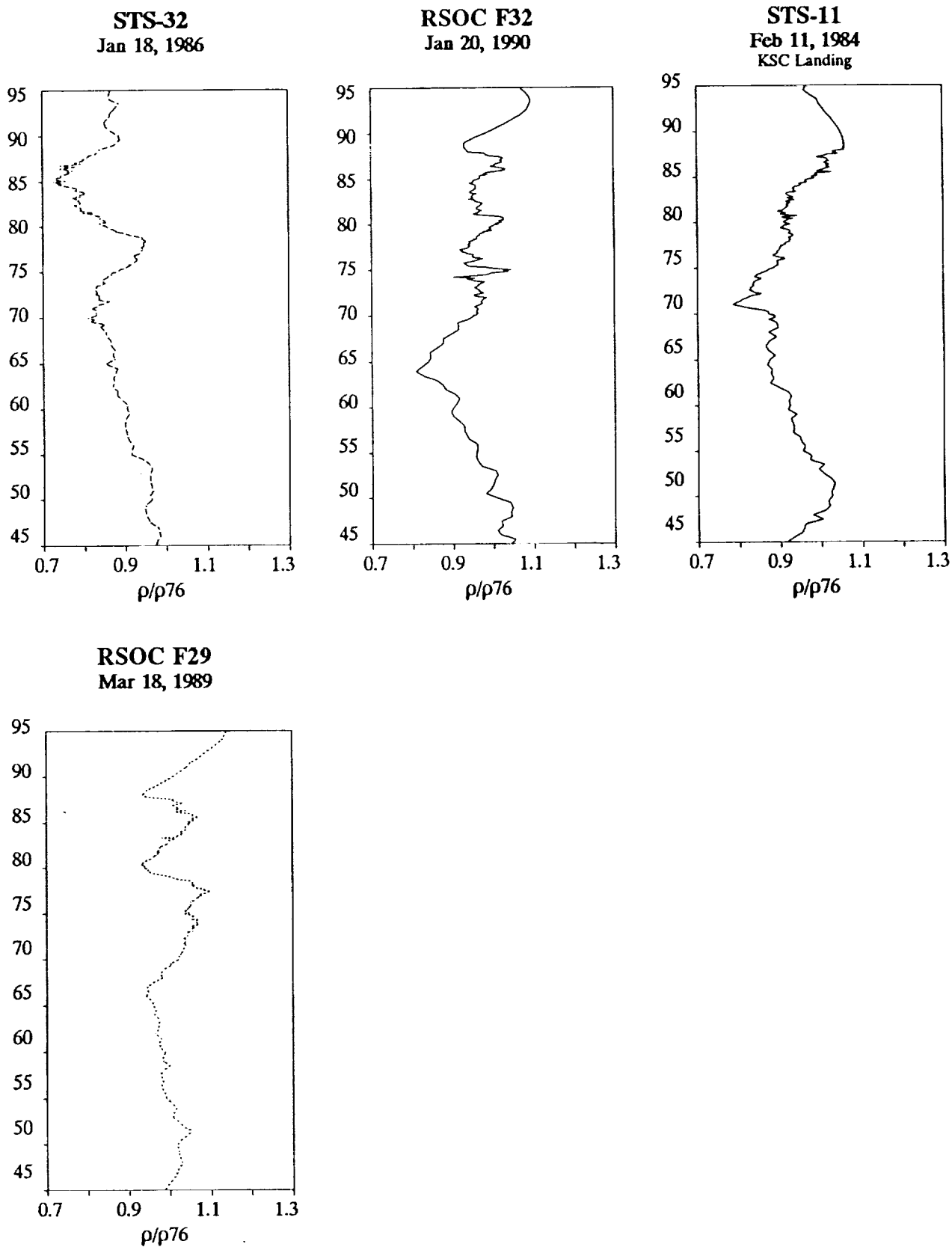

Figure 17. (concluded)

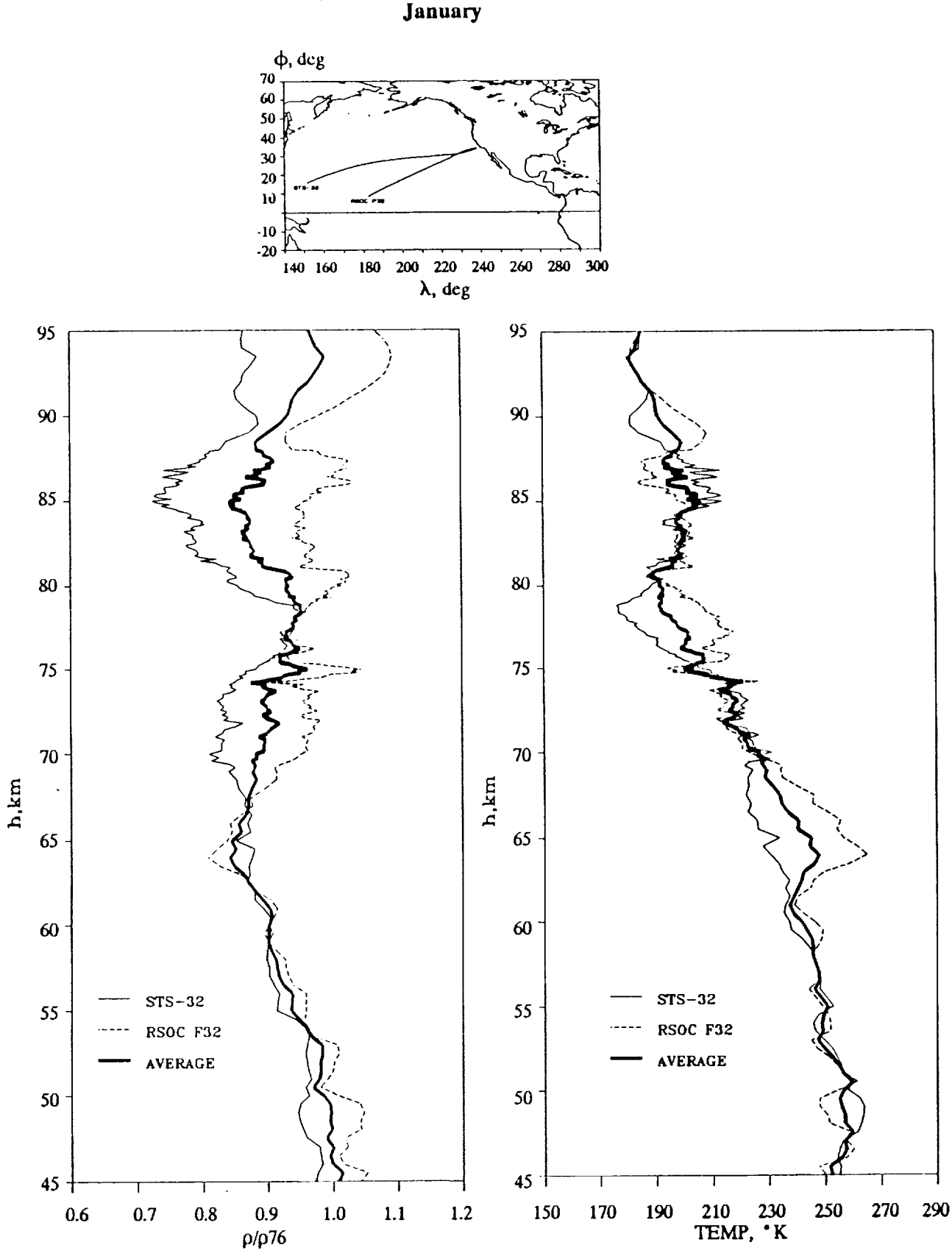

Figure 18. January density and temperature profiles.

March

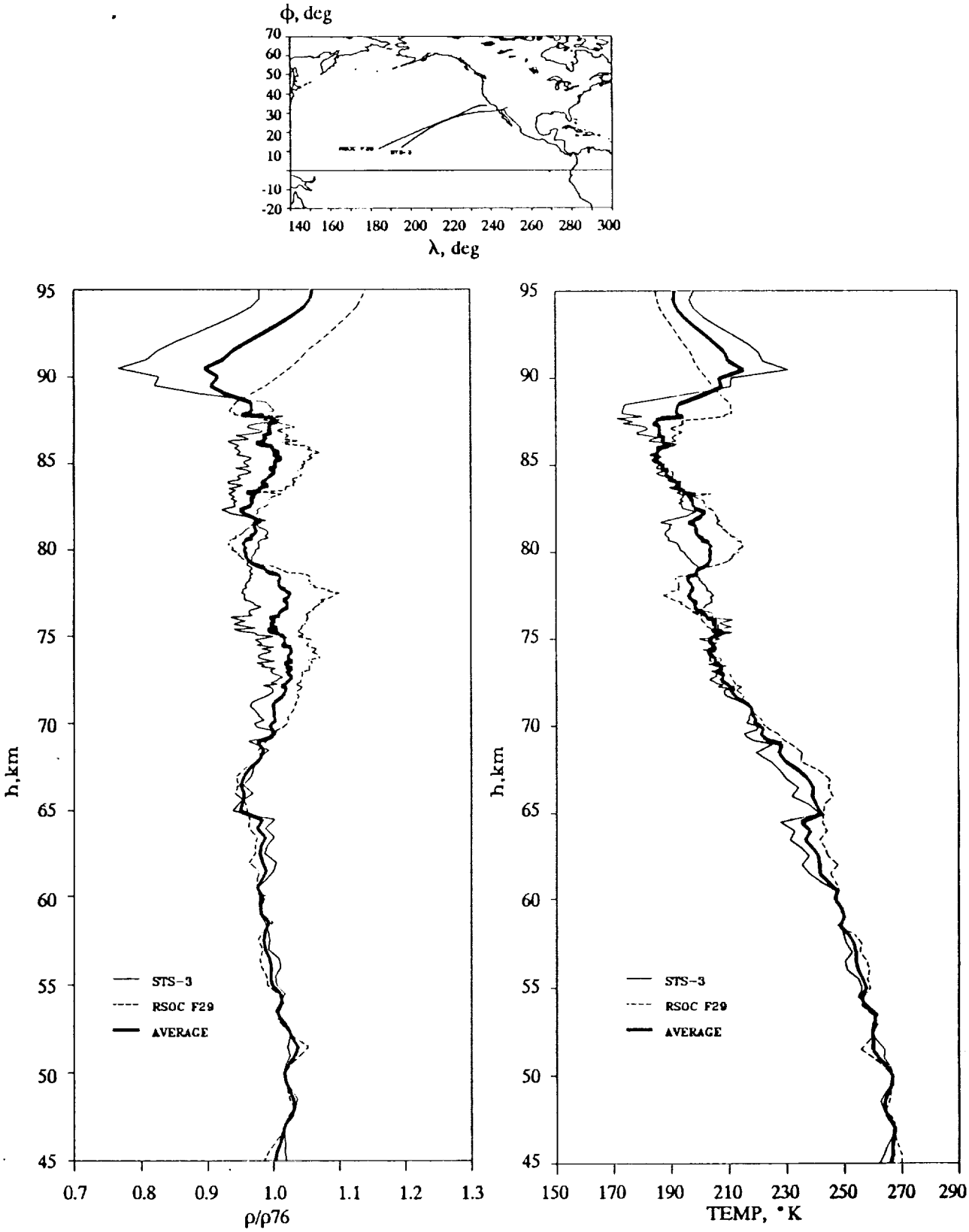

Figure 19. March density and temperature profiles.

April

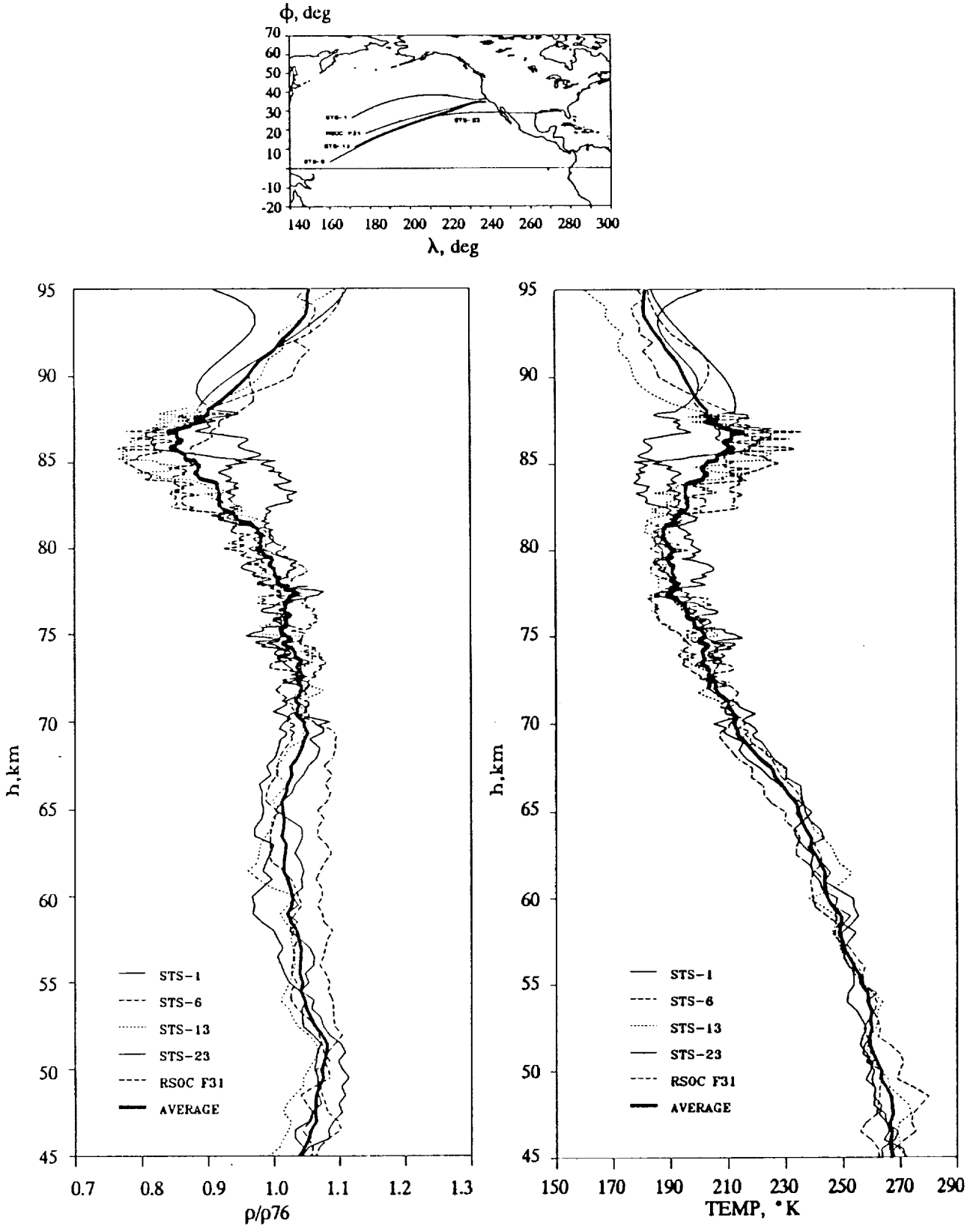

Figure 20. April density and temperature profiles.

May

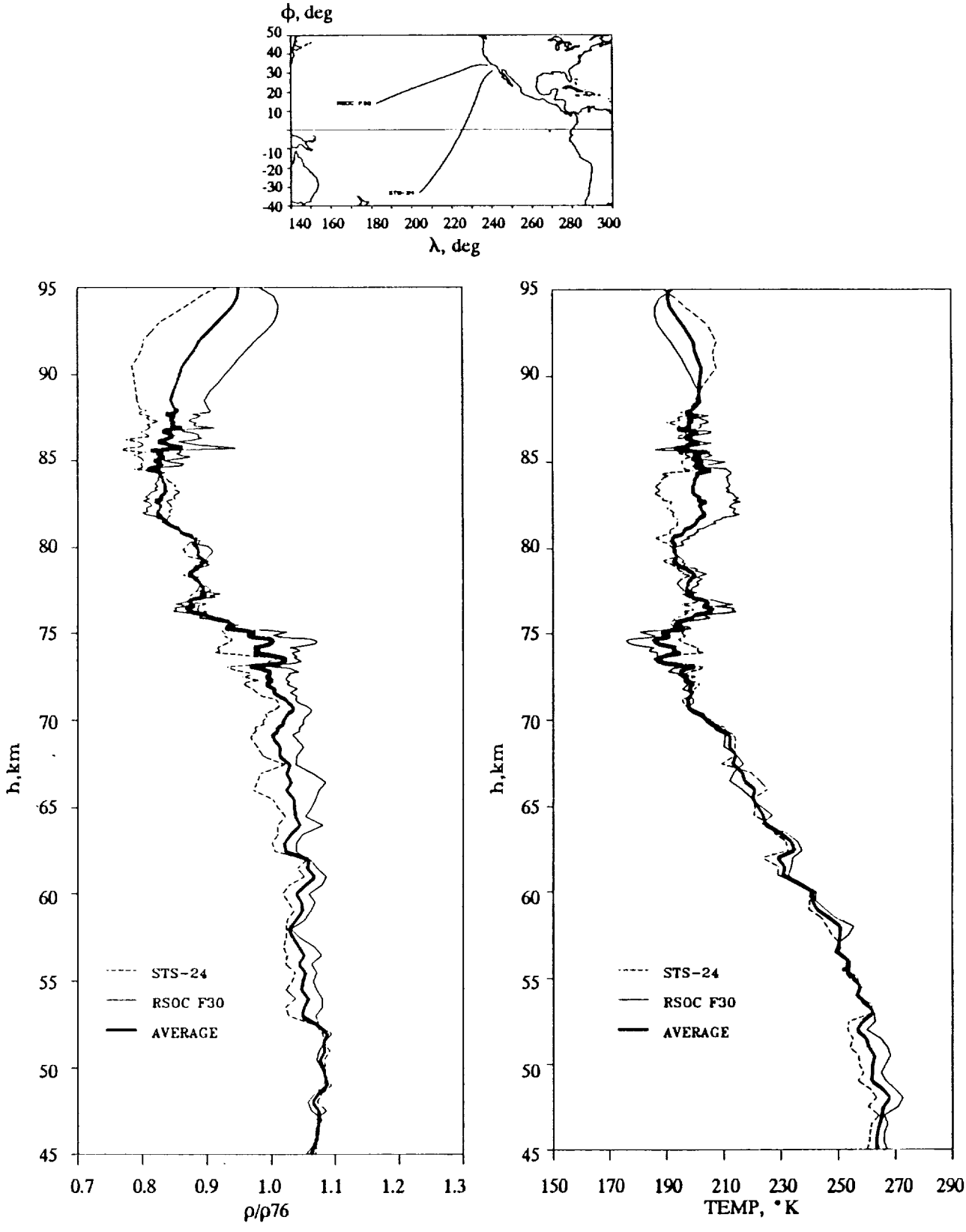

Figure 21. May density and temperature profiles.

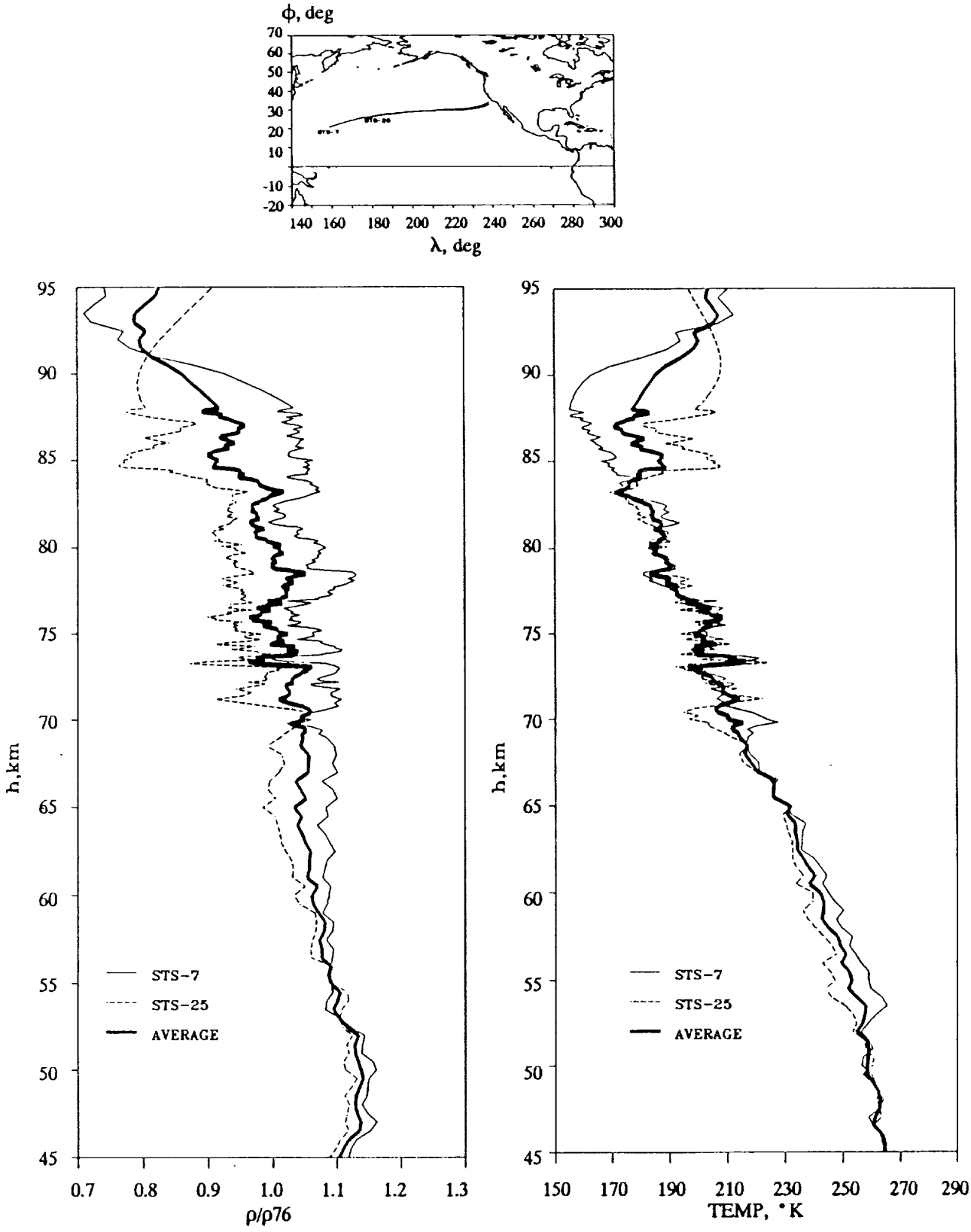

Figure 22. June density and temperature profiles.

August

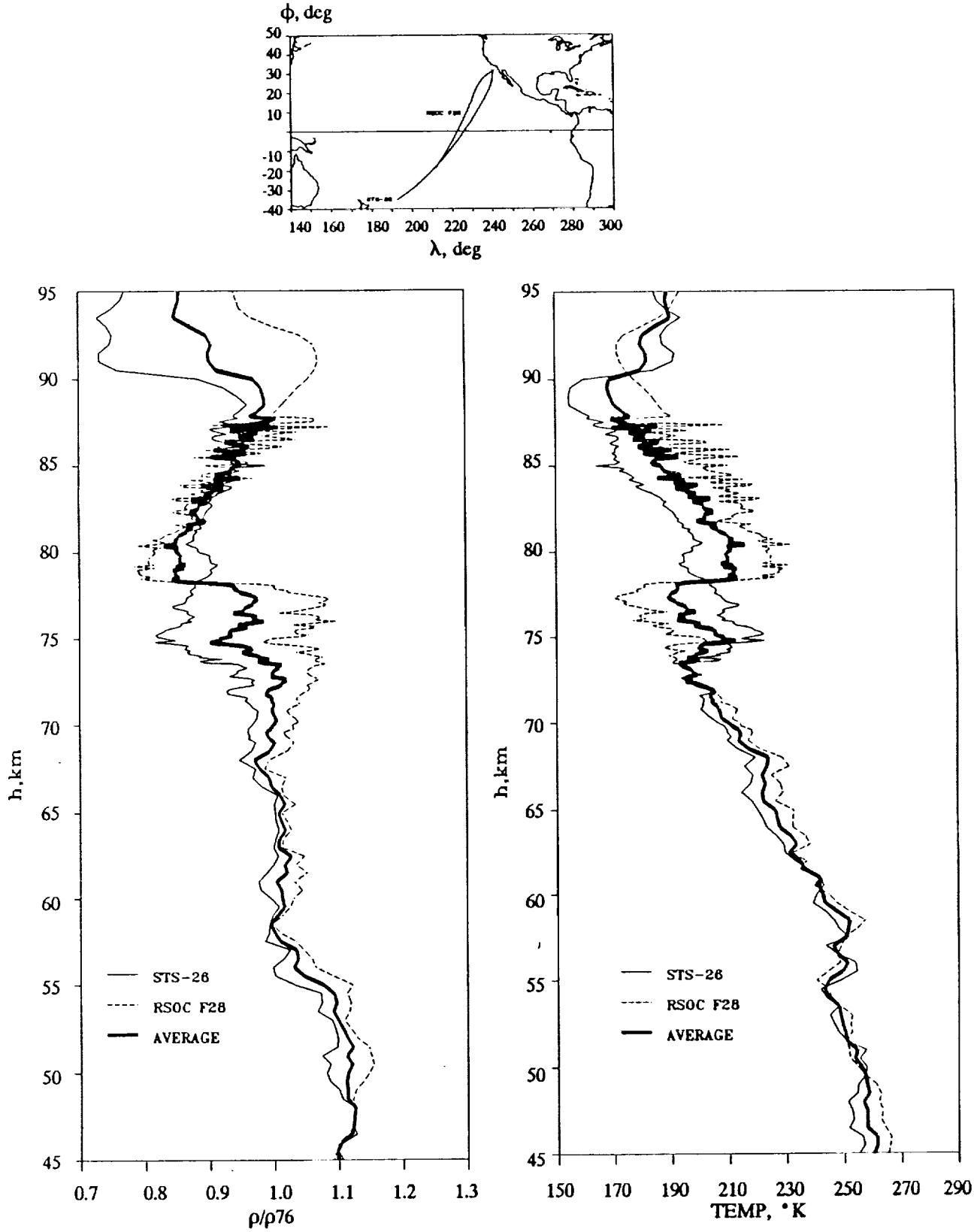

Figure 23. August density and temperature profiles.

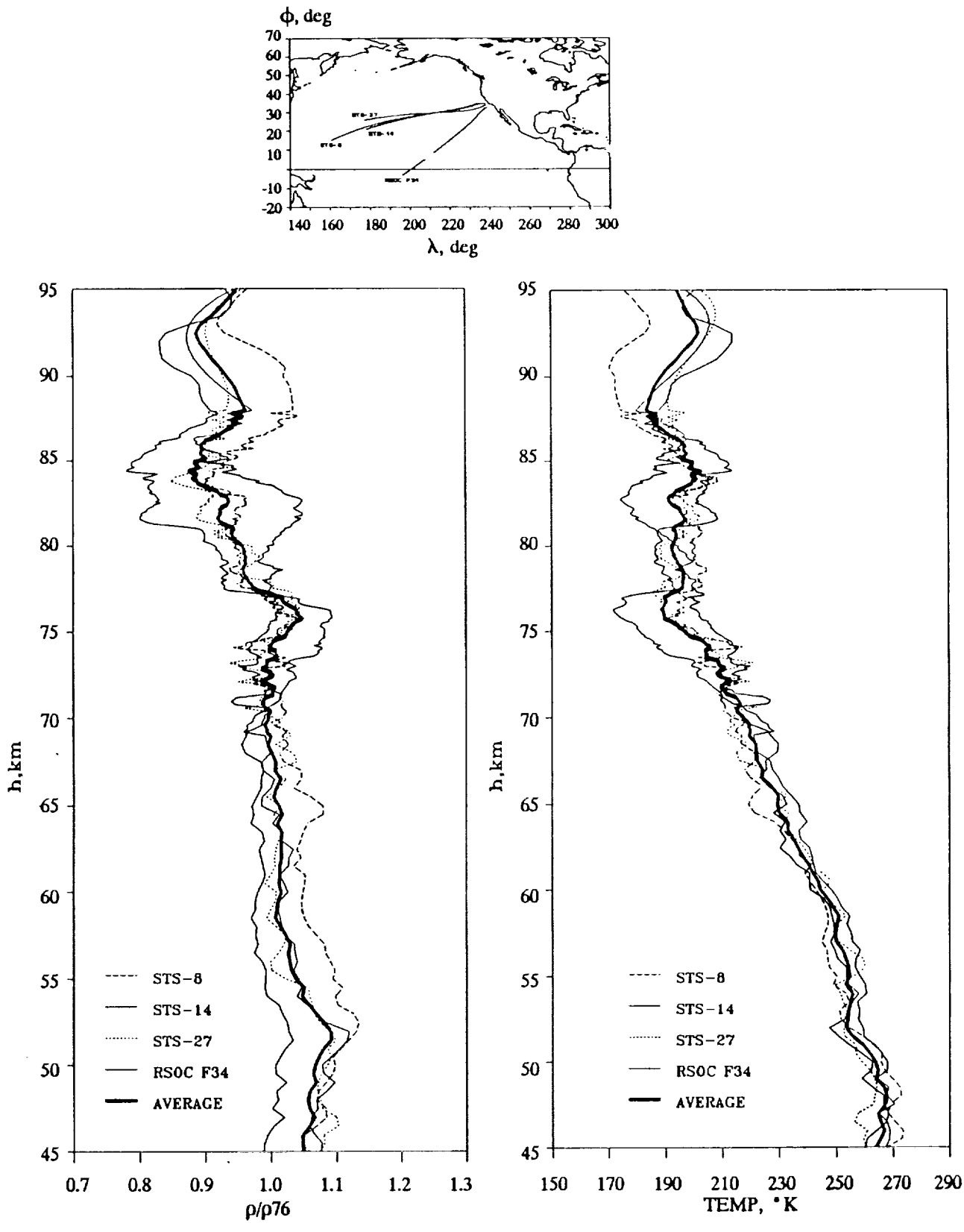

Figure 24. September density and temperature profiles.

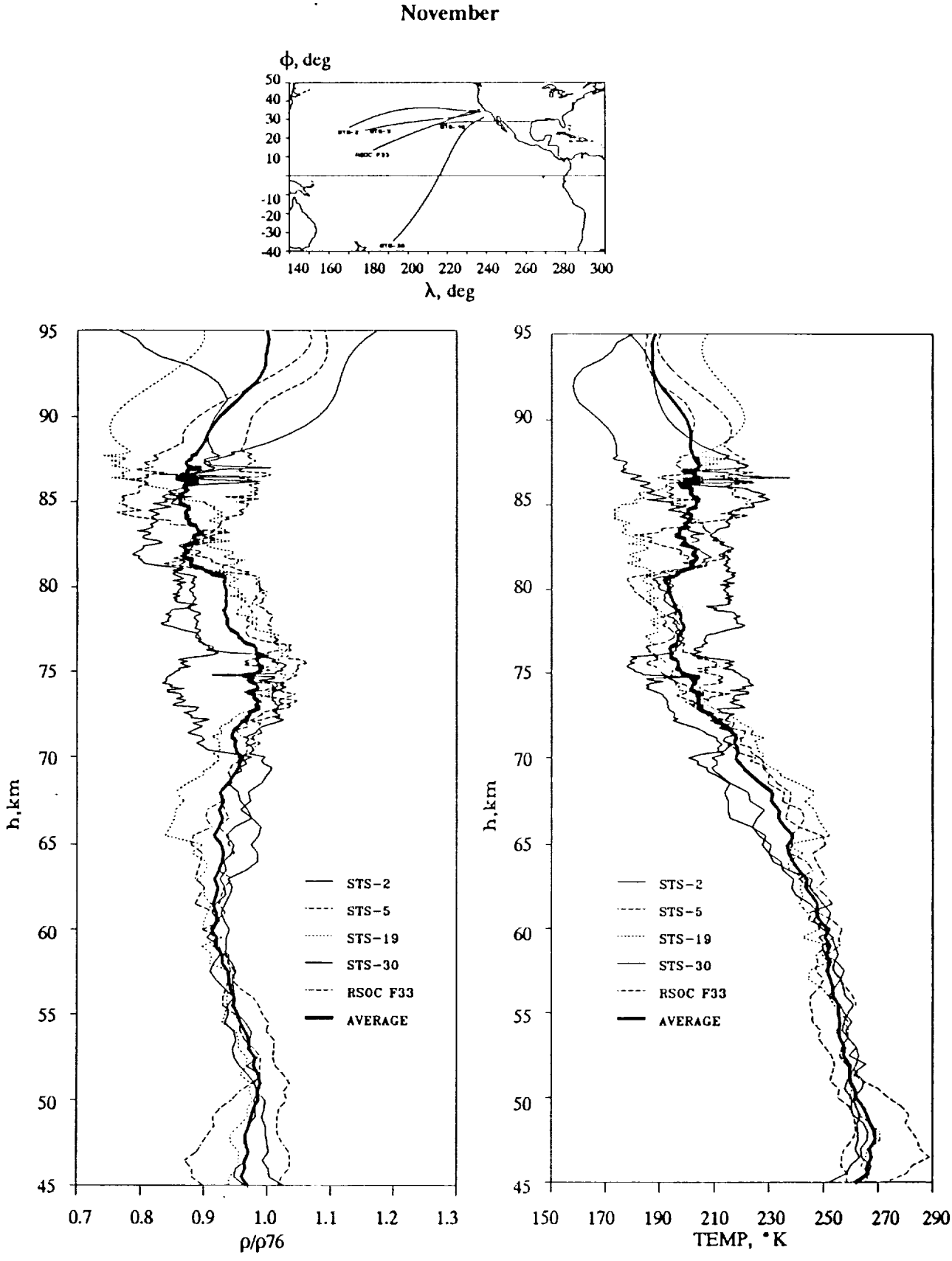

Figure 25. November density and temperature profiles.

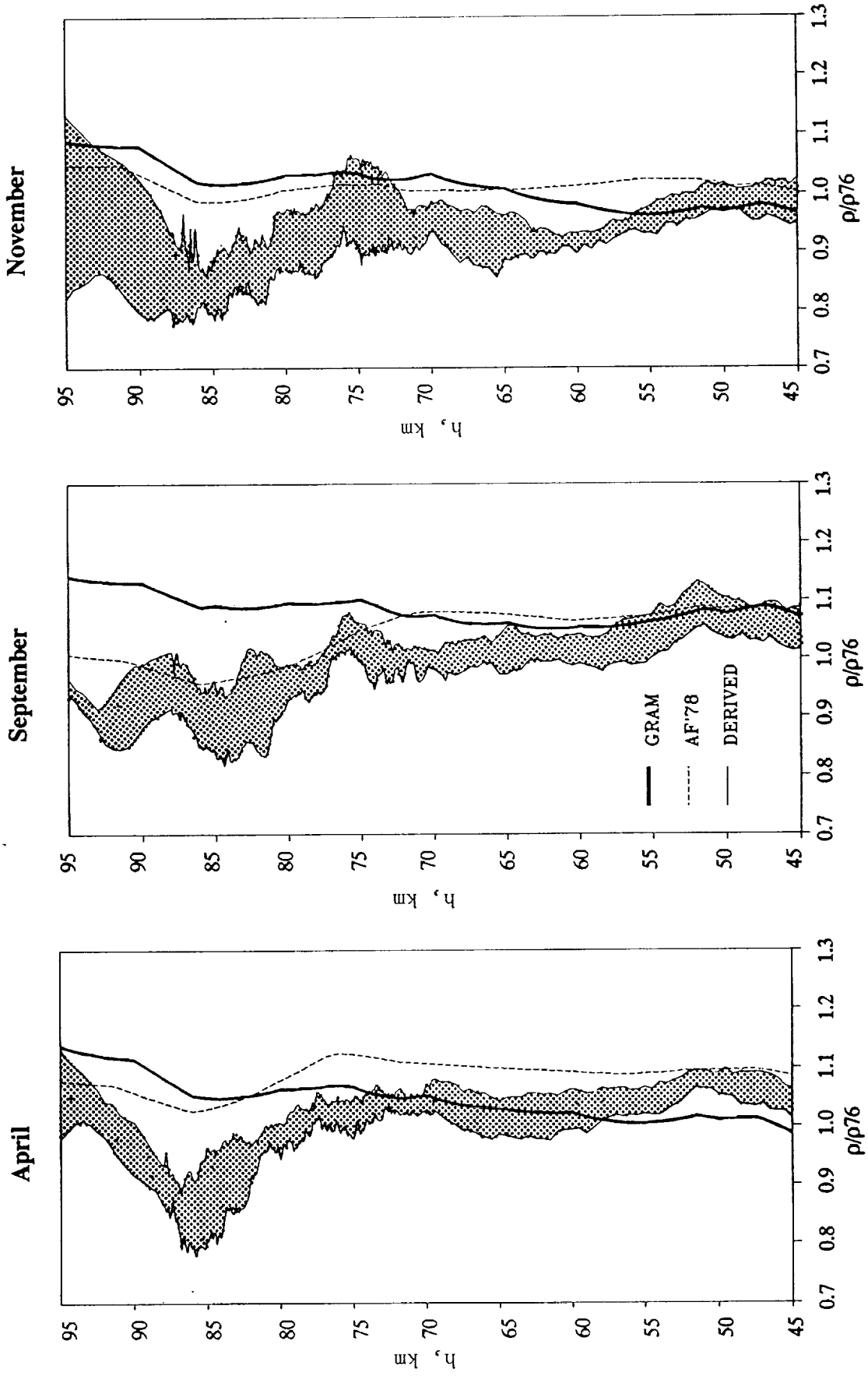

Figure 26 Comparisons between monthly derived and model densities.

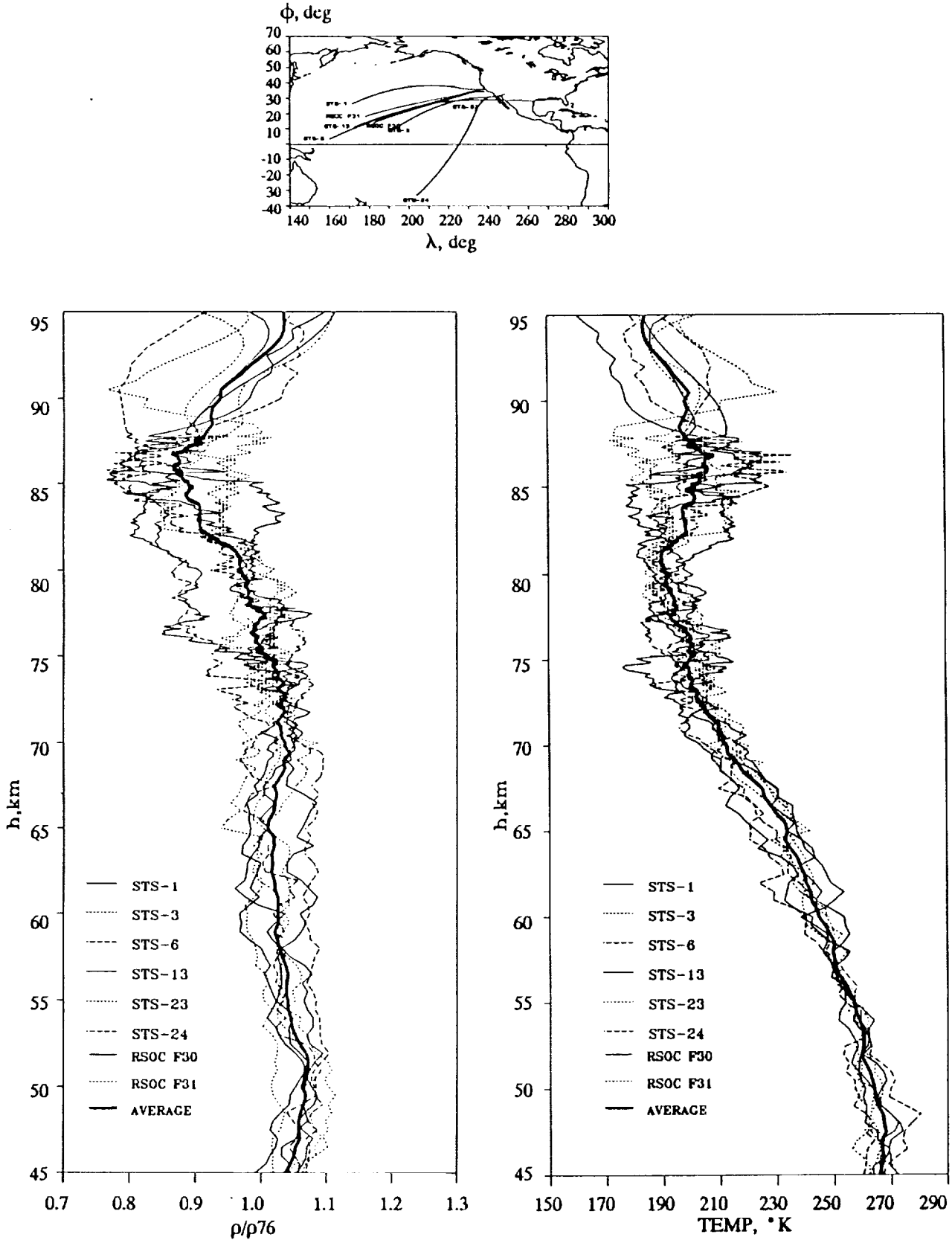

Figure 27. Spring density and temperature profiles.

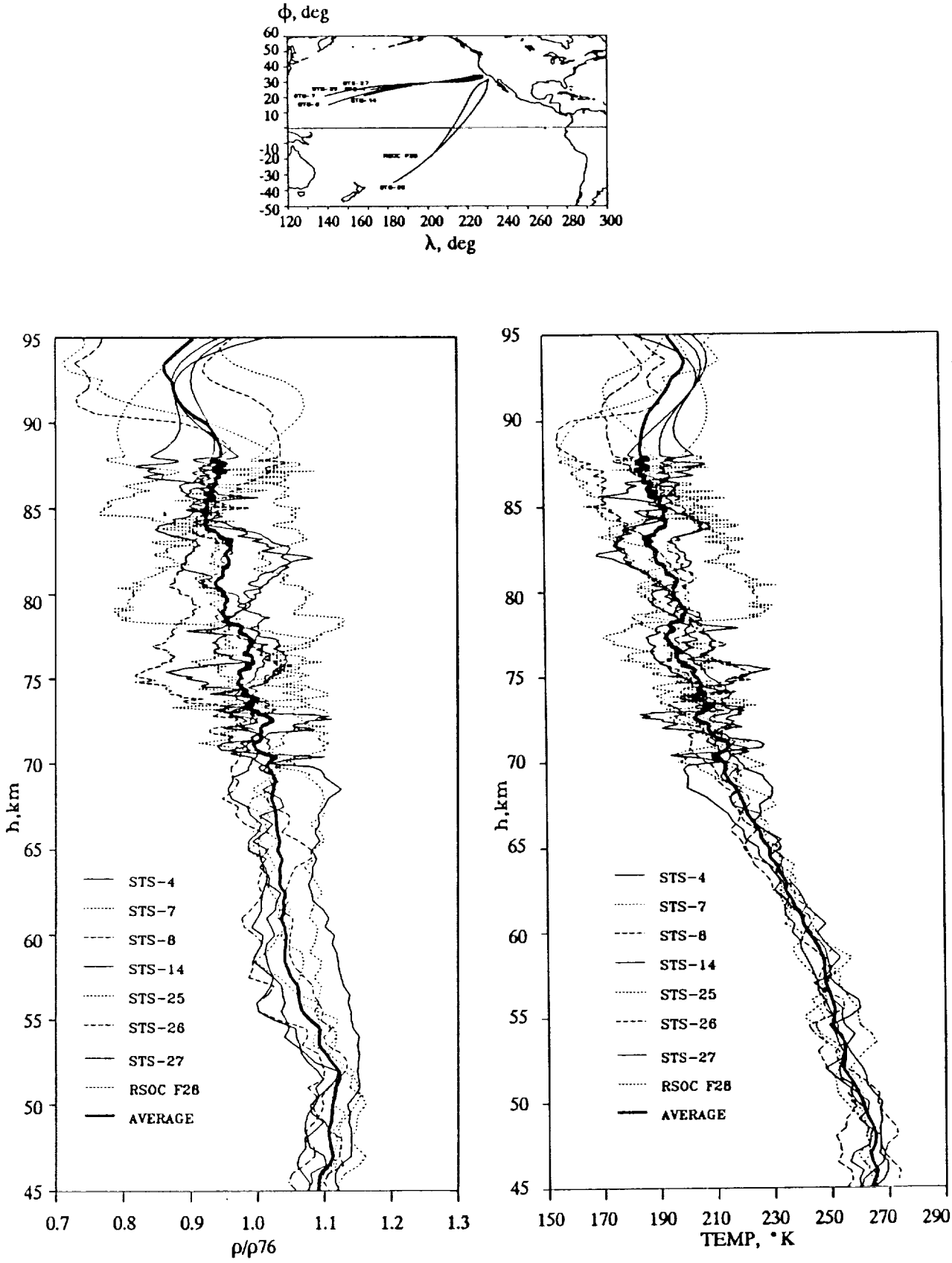

Figure 28. Summer density and temperature profiles.

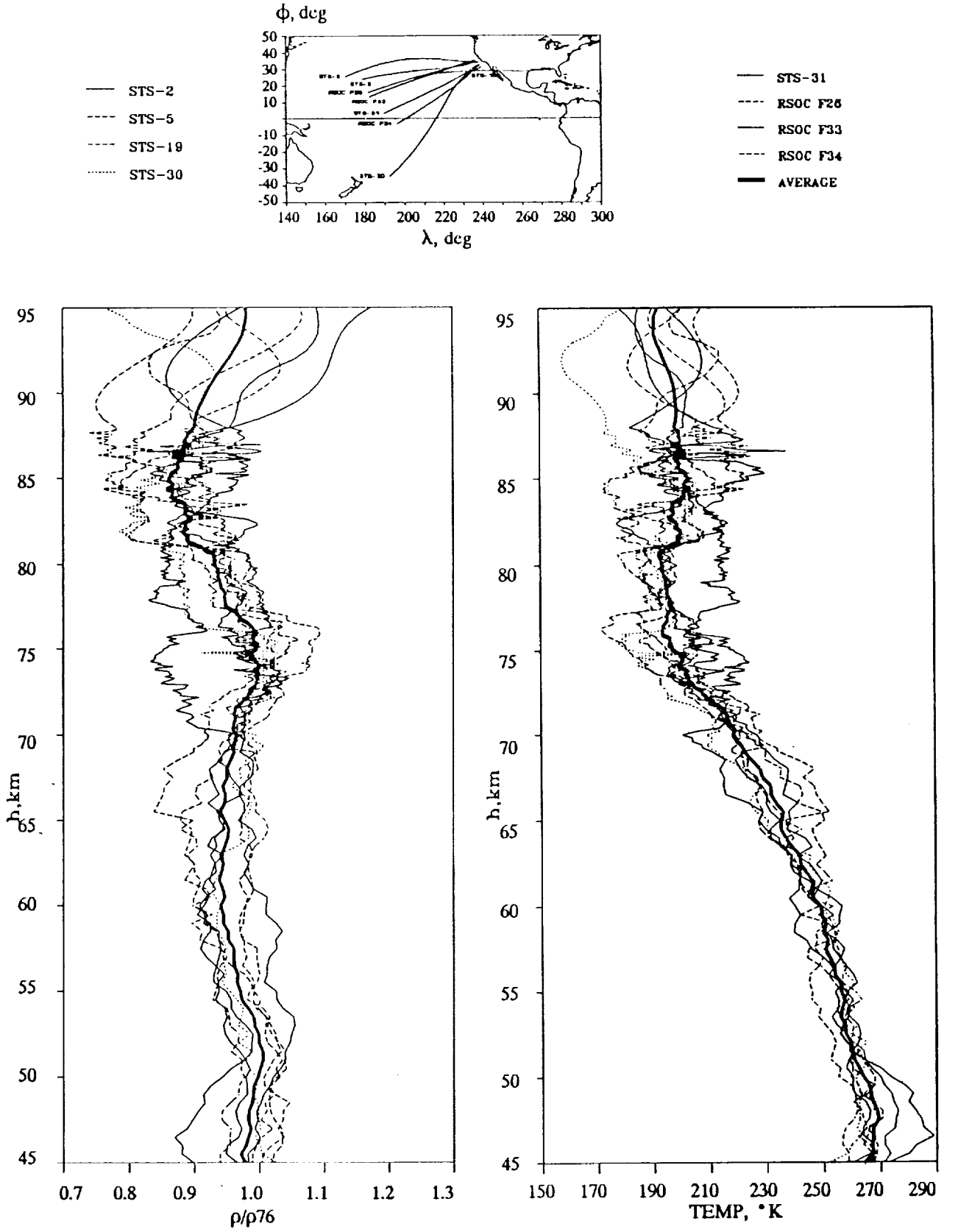

Figure 29. Fall density and temperature profiles.

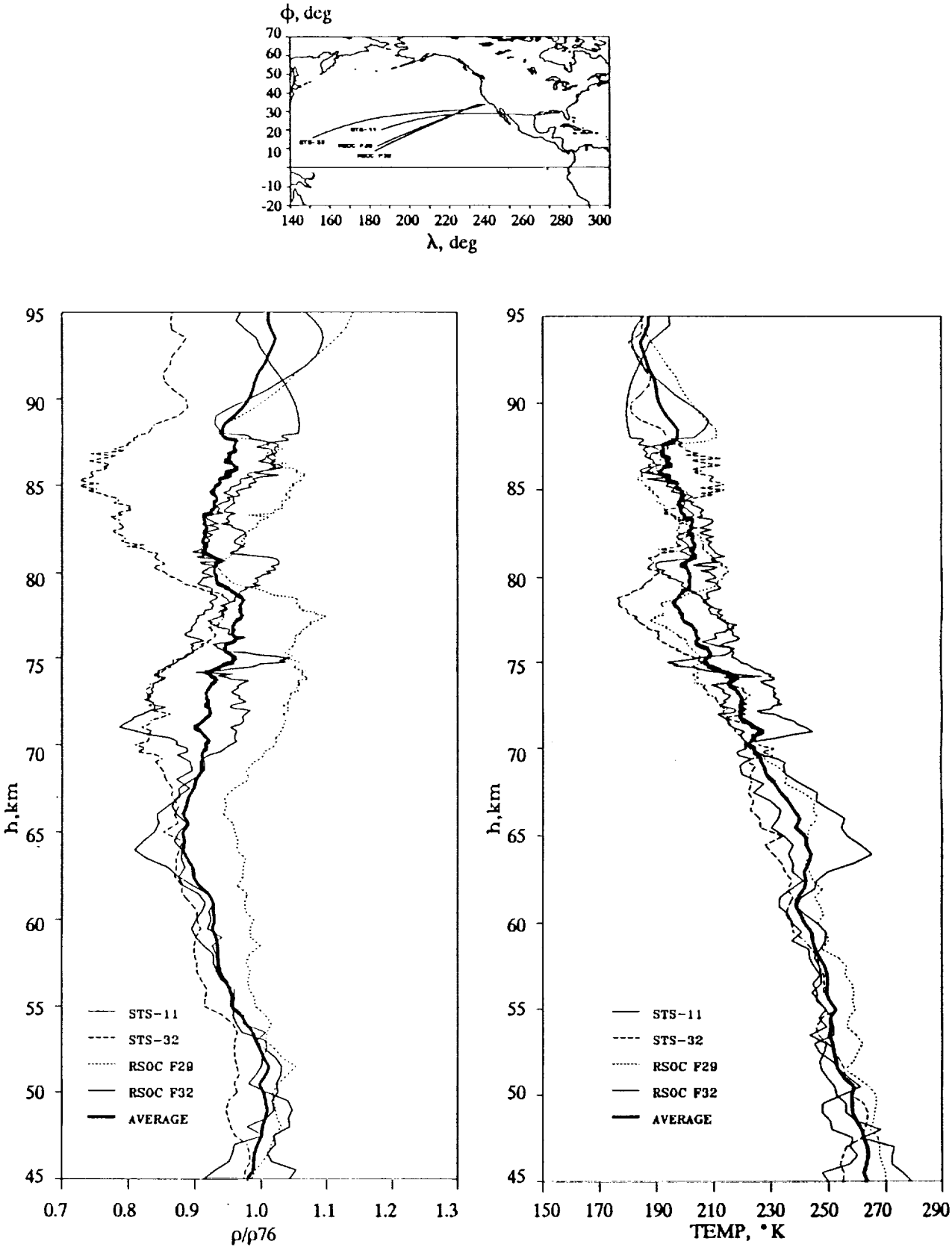

Figure 30. Winter density and temperature profiles.

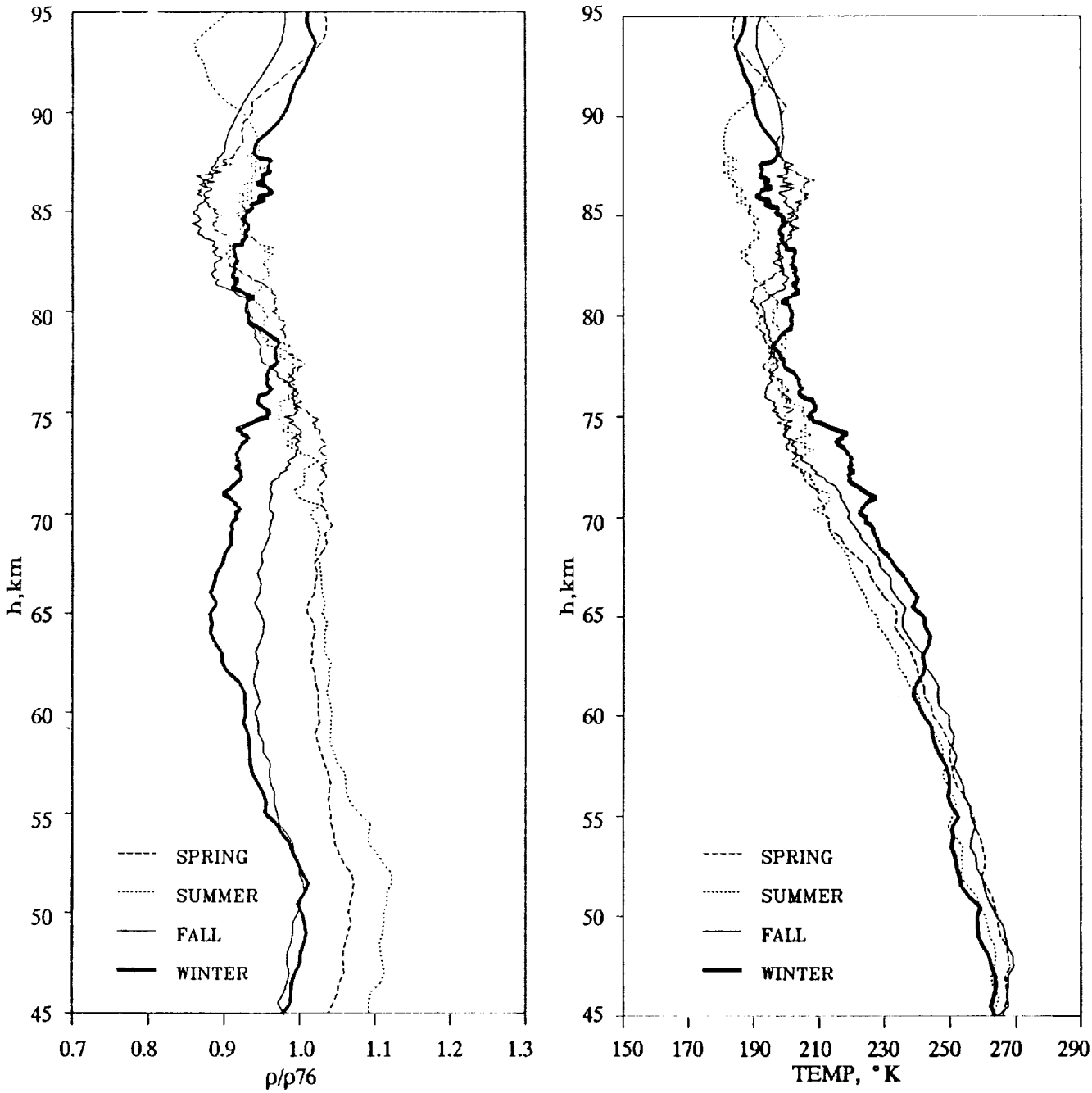

Figure 31. Average density and temperature variations with seasons.

CONCLUSIONS

A final atmospheric database based on 32 Shuttle descent flights is presented. Accurate density profiles are determined based on in situ inertial quality acceleration measurements and flight-substantiated aerodynamic performance predictions. Shuttle-derived density profiles yield structure with unprecedented vertical resolution. Density shears and offsets are common occurrences which support internal gravity wave arguments and suggest regions of atmospheric instabilities for atmospheric science investigations. The results consistently exhibit low density over the more northerly latitudes which can lead toward model improvements. Similarly, monthly trends for April, September and November can be used for model evaluations and upgrades as appropriate. However, additional missions would be required to increase the ensemble of flights to establish similar data for other months and enable one to better ascertain seasonal effects.

REFERENCES

(1) *Findlay, J. T., et al ;*
"Reconstruction of the 1st Space Shuttle (STS-1) Entry Trajectory," NASA CR 3561, June 1982.

(2) *Schlosser, D. C. and Bornemann, W. E. (approved by) ;*
"Pre-Operational Aerodynamic Design Data Book, Volume I, Orbiter Vehicle," Rockwell International Report SD72-SH-0060-1L-7, April 1982.

(3) *Romere, P. O. (prepared by) ;*
"Flight Assessment Package, Orbiter Aerodynamics, FAD26," JSC-22078, April 1986.

(4) *Findlay, J. T., et al ;*
"Shuttle 'Challenger' Aerodynamic Performance from Flight Data - Comparisons with Predicted Values and 'Columbia' Experience," AIAA Paper No. 84-0485, January 1984.

(5) *Siemers, P. M., et al ;*
"Shuttle Entry Air Data System Concepts Applied to Space Shuttle Orbiter Flight Pressure Data to Determine Air Data - STS 1-4," AIAA Paper No. 83-0118, January 1983.

(6) *Findlay, J. T., et al ;*
"Shuttle-Derived Density Profiles in the Middle Atmosphere," NASA CR 4109, February 1988.

(7) *Blanchard, R. C., and Larman, K. T. ;*
"Rarefied Aerodynamics and Upper Atmospheric Flight Results from the Orbiter High Resolution Accelerometer Package Experiment," AIAA Paper No. 87-2366, August 1987.

(8) *Findlay, J. T. ;*
"Analysis and Development of Extended Shuttle-derived Atmospheric Database to Include Thermospheric Altitudes," NASA CR 172043, December 1987.

(9) *Gamble, J. D., and Findlay, J. T. ;*
"Shuttle-Derived Densities in the Middle Atmosphere," AIAA Paper No. 88-4352, August 1988.

(10) *Justus, C. G., et al ;*
"The NASA/MSFC Global Reference Atmospheres - Mod 3 (With Spherical Harmonic Wind Model)," NASA CR-3256, March 1980.

(11) *Cole, A. E., and Kantor, A. J. ;*
"Air Force Reference Atmospheres," AFGL-TR-78-0051, Air Force Surveys in Geophysics, No. 382, February 1978.

(12) *Price, J. M. ;*
"Atmospheric Definition for Shuttle Aerothermodynamic Investigations," Journal of Spacecraft and Rockets, Vol. 20, pp. 133-140, March-April 1983.

(13) *Philbrick, C. R., et al ;*
"Density and Temperature Structure over Northern Europe," Journal of Atmospheric and Terrestial Physics, Vol. 47, No. 1-3, pp. 159-172, 1985.

APPENDIX A - RESULTS OF PREVIOUS 22 FLIGHTS

A series of 22 charts are included herein which show the individual comparisons of density and temperature for the first 22 Shuttle missions. [6, 8, 9] Included are the Shuttle-derived results, data from both the GRAM and AF'78 models, and the measured (translated) meteorology data for each mission. Ground tracks are also provided with approximate altitude benchmarks as noted. For the most part, these indicators are every 10 km between 95 km and 45 km. As previously noted, data from some of the flights are available at higher altitudes.

As part of this task, data from these flights have been reloaded to the common schema adopted for the final database, FINLATM. The GRAM data have been reworked to correct some of the SCIDAT data per the recent ('88) model update as well as eliminate a subtle (2 to 3 percent) fairing problem at 90 km pursuant to the '86 GRAM update. As reported previously, DFI results were utilized in lieu of the remote data over a limited altitude region for both STS-3 and STS-5. This should be evident by inspection of the respective curves presented. All density profiles are normalized against the 1976 Standard Atmosphere. Derived temperature data are provided based on the two optional initialization processes discussed in the text. Shading between the two determinations exemplifies the associated differences which, as can be seen, are more significant in the thermosphere as discussed in Reference 8.

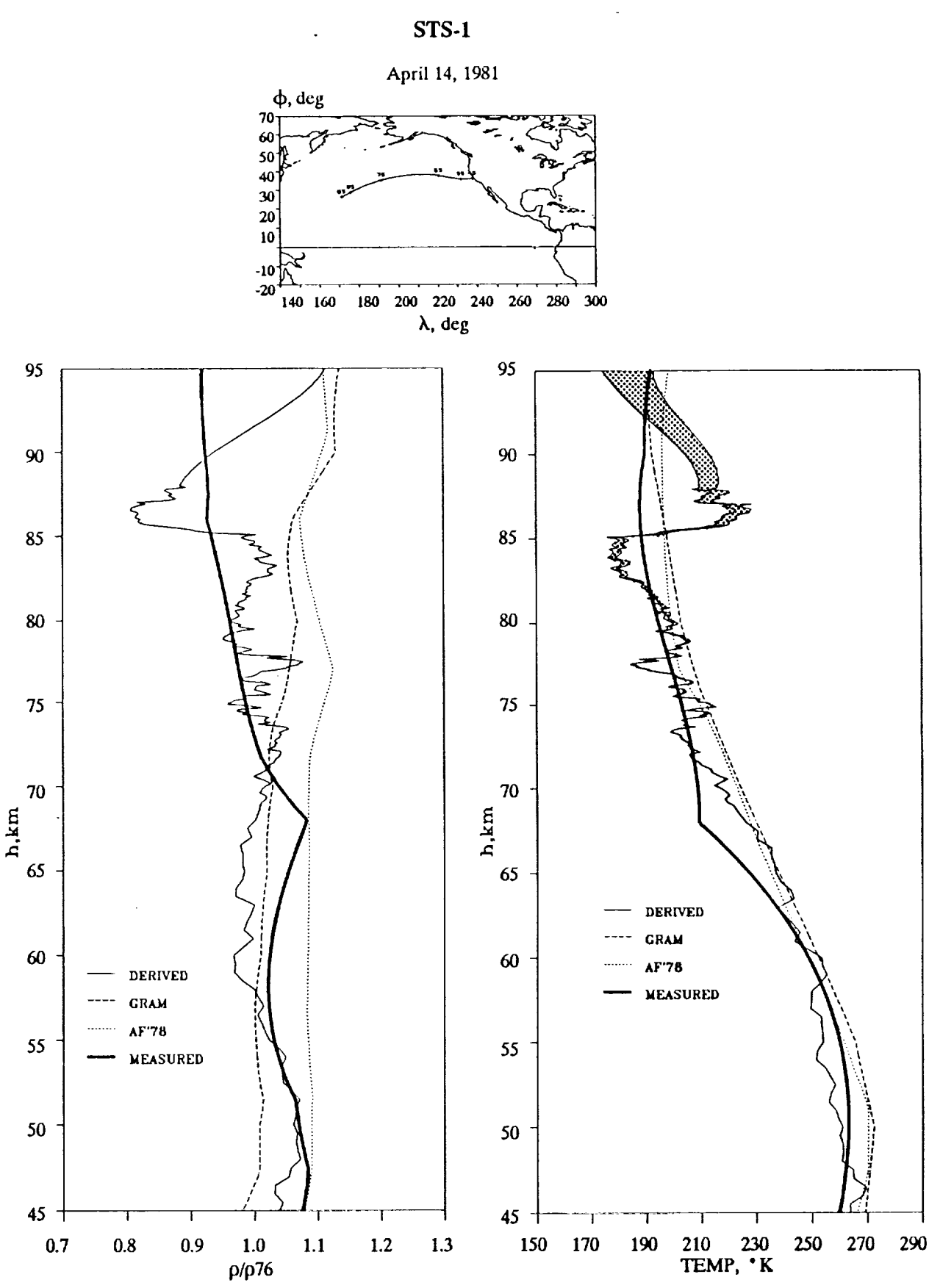

Figure A-1. STS-1 density and temperature profile comparisons.

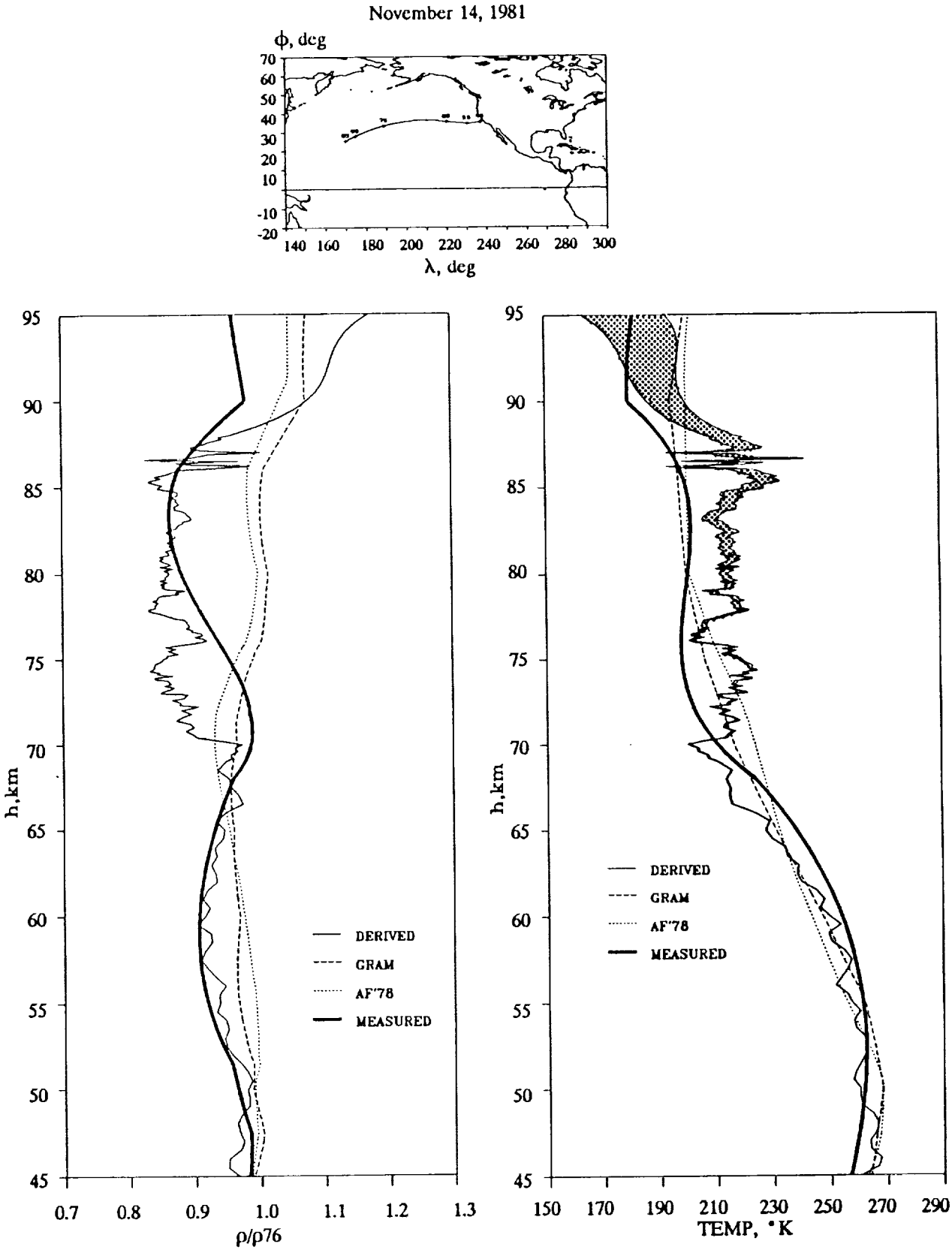

Figure A-2. STS-2 density and temperature profile comparisons.

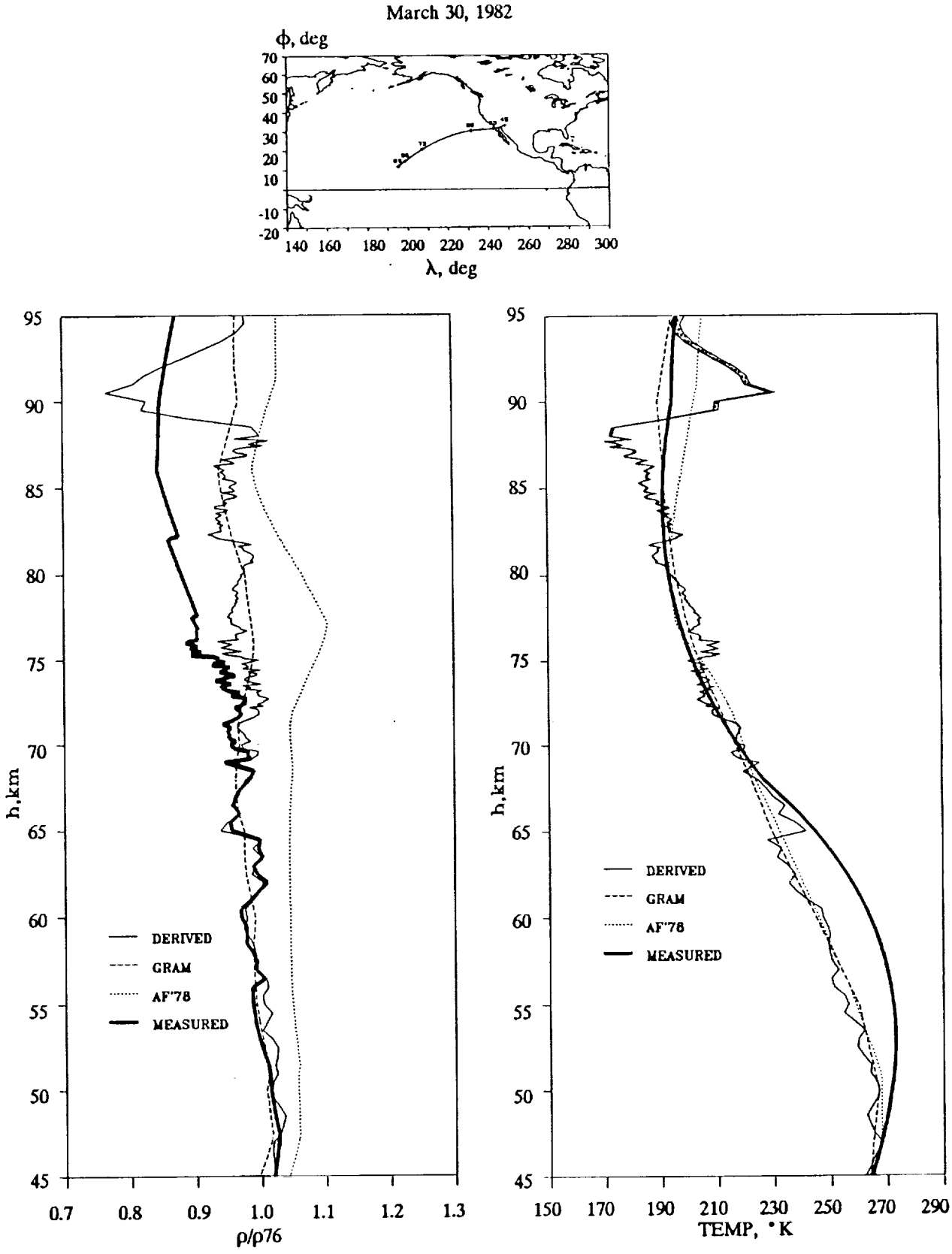

Figure A-3. STS-3 density and temperature profile comparisons.

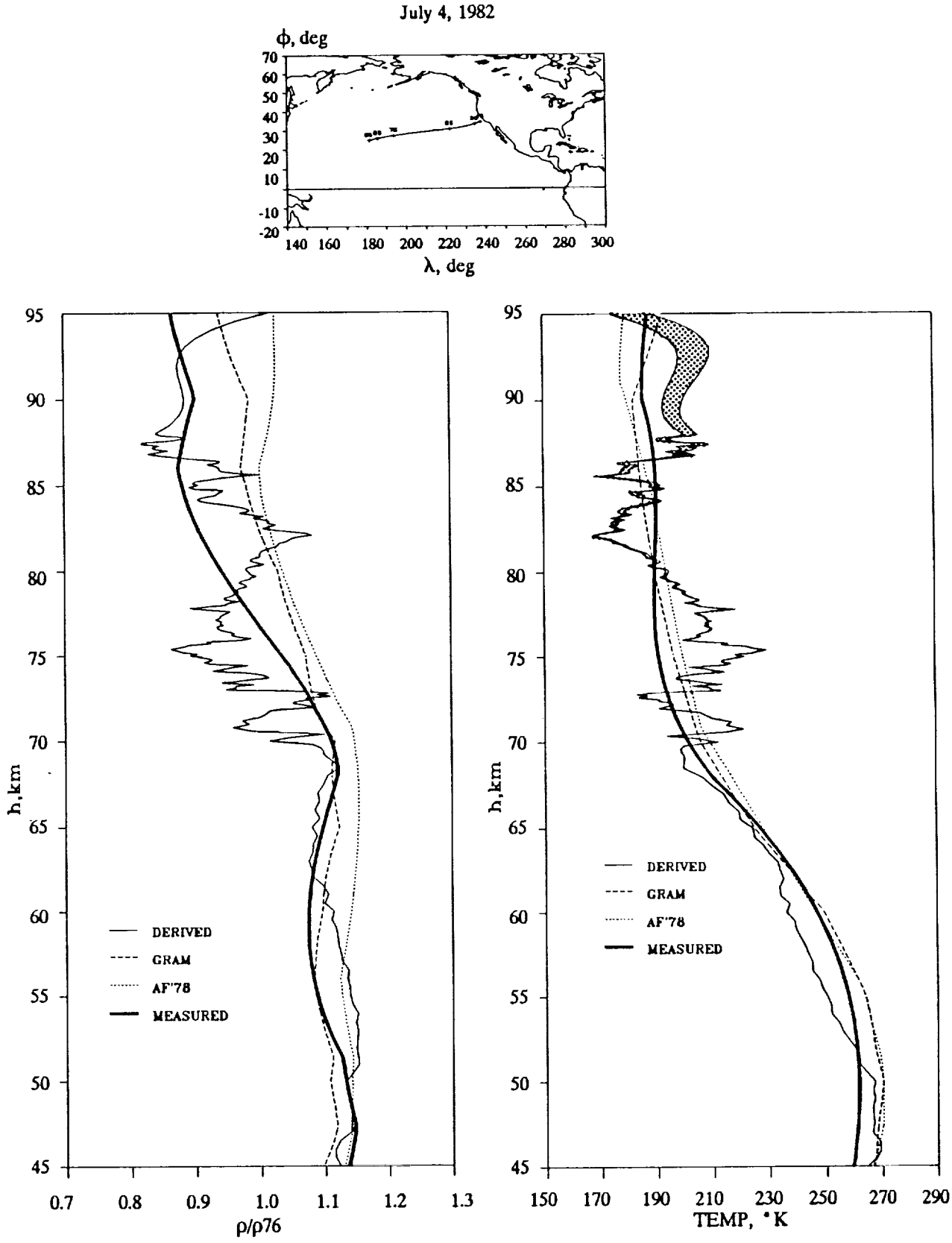

Figure A-4. STS-4 density and temperature profile comparisons.

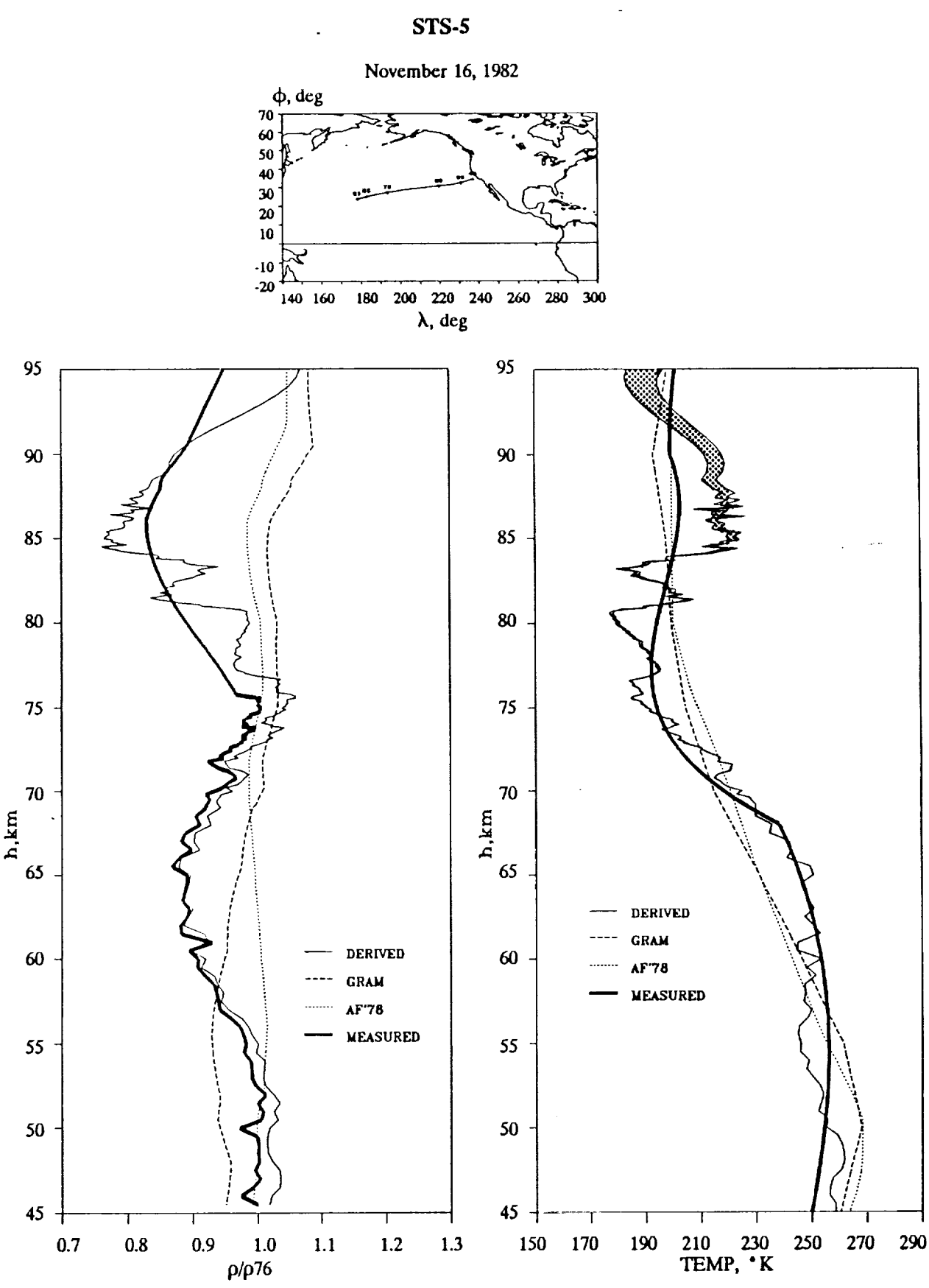

Figure A-5. STS-5 density and temperature profile comparisons.

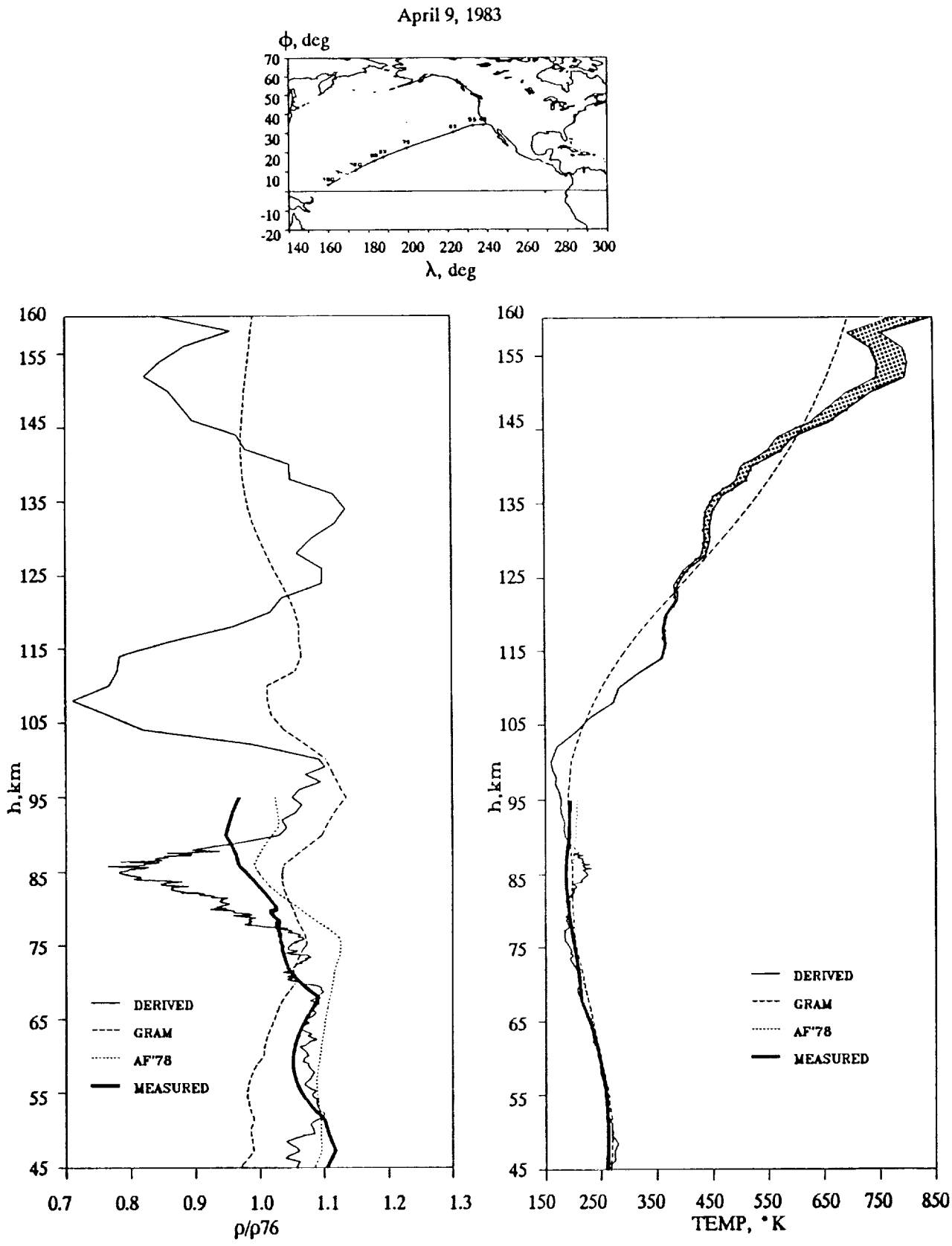

Figure A-6. STS-6 density and temperature profile comparisons.

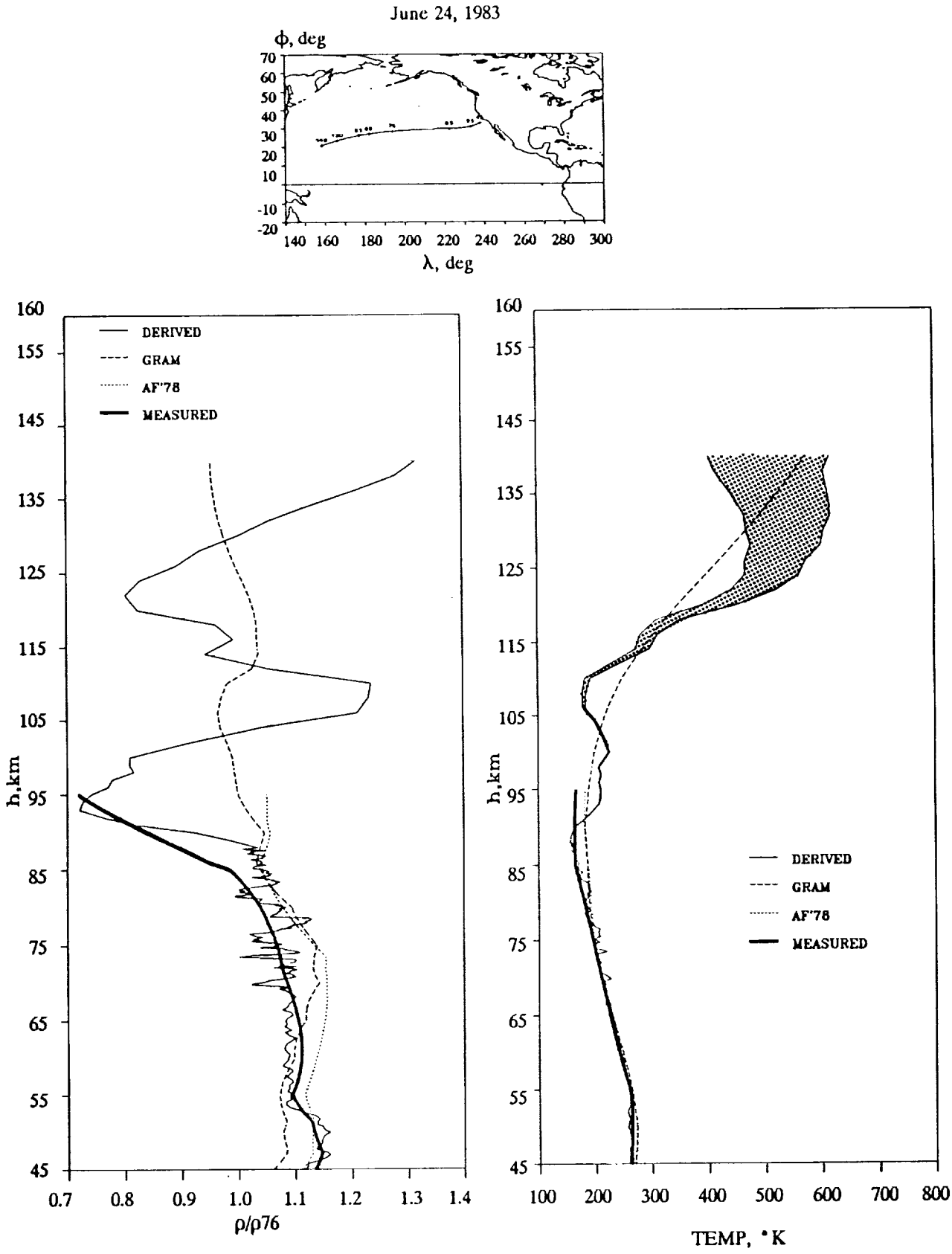

Figure A-7. STS-7 density and temperature profile comparisons.

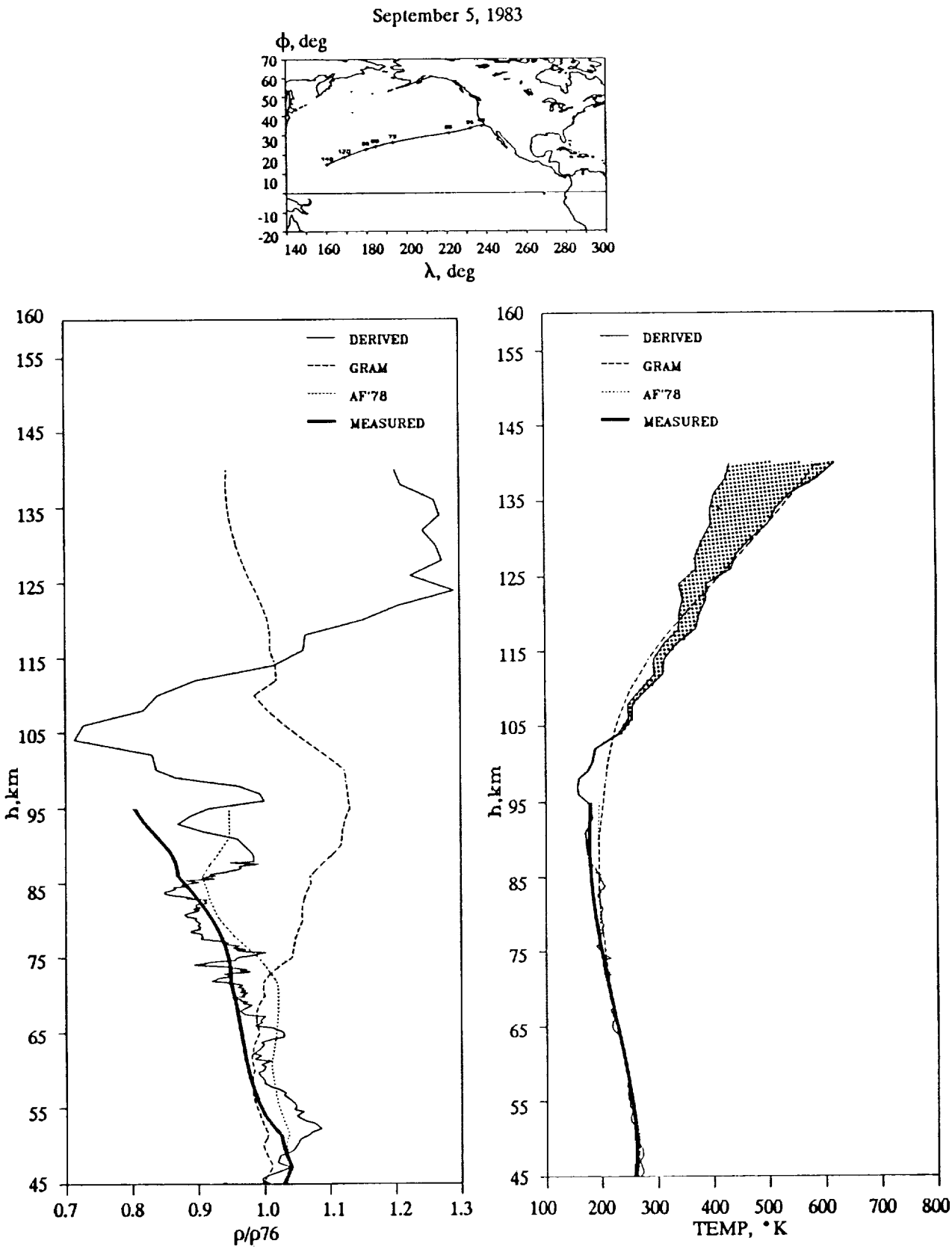

Figure A-8. STS-8 density and temperature profile comparisons.

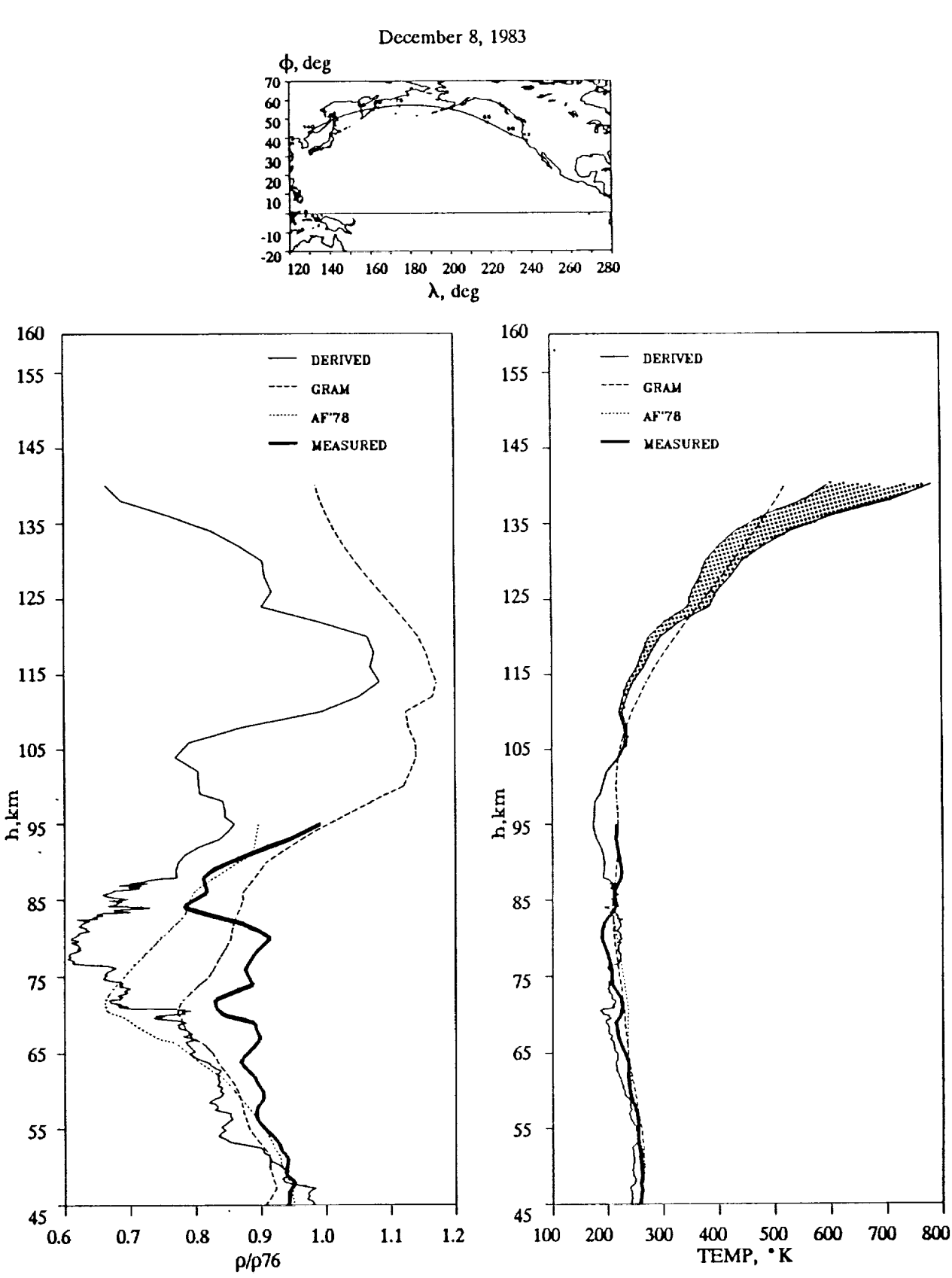

Figure A-9. STS-9 density and temperature profile comparisons.

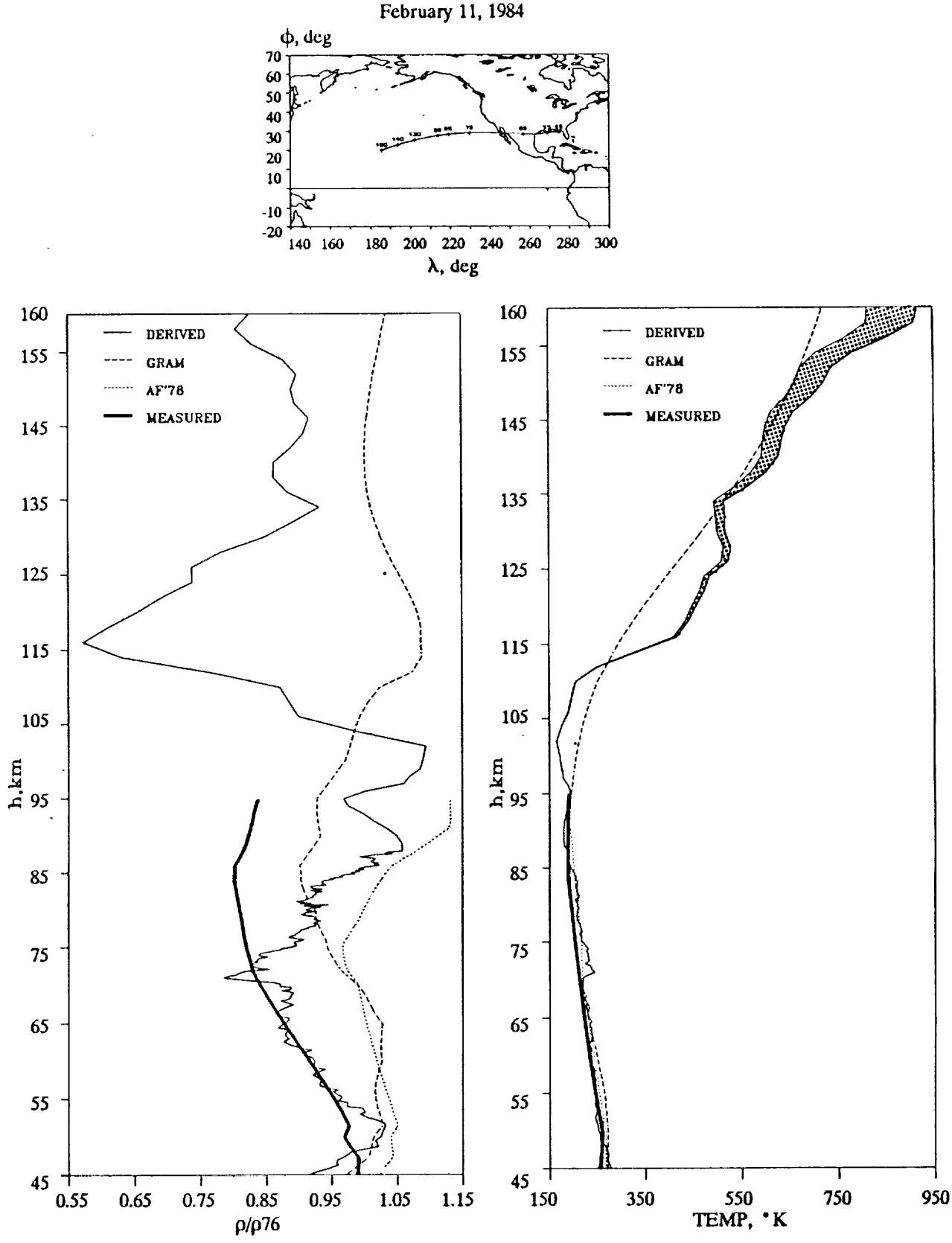

Figure A-10. STS-11 (41-B) density and temperature profile comparisons.

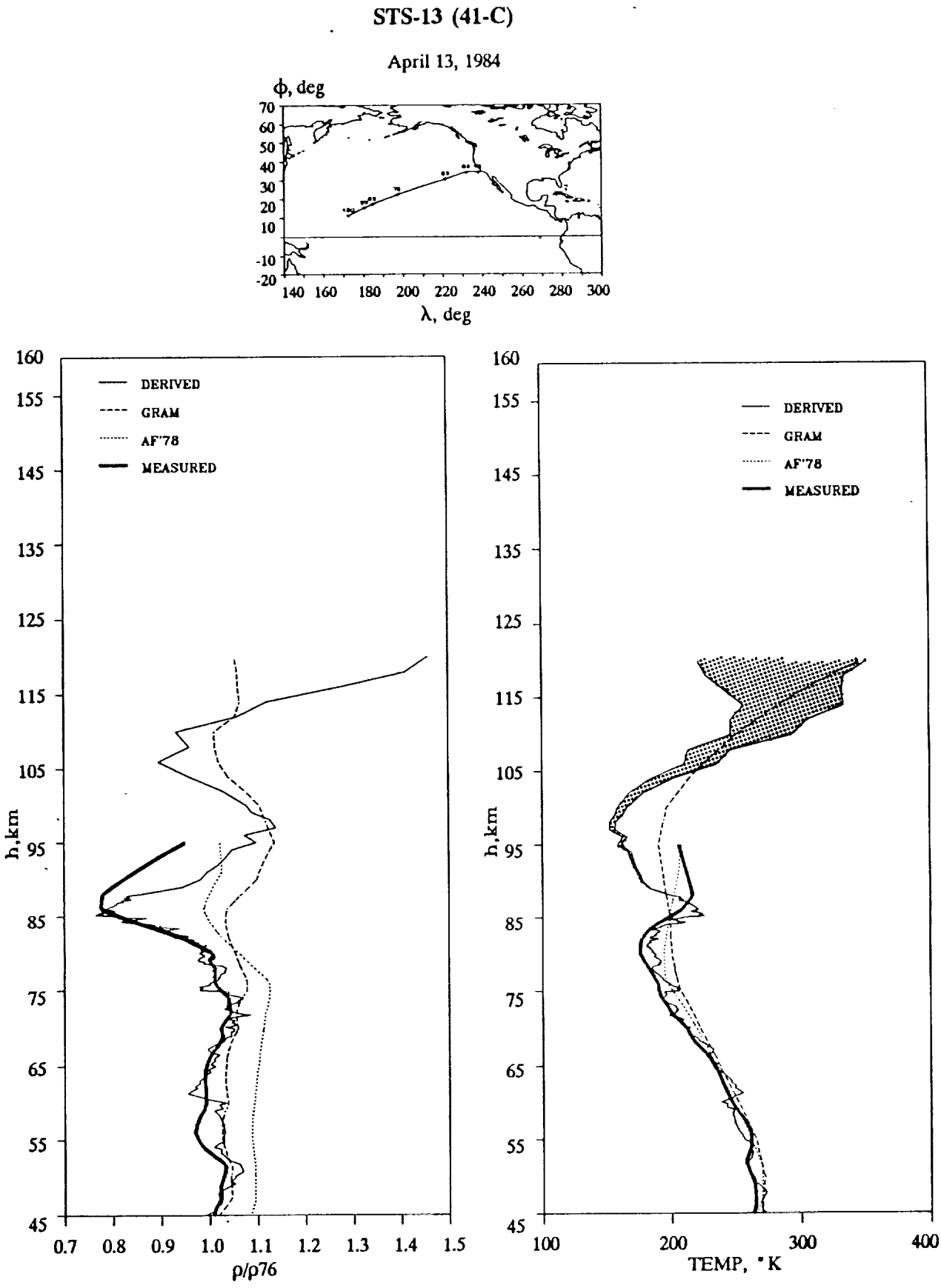

Figure A-11. STS-13 (41-C) density and temperature profile comparisons.

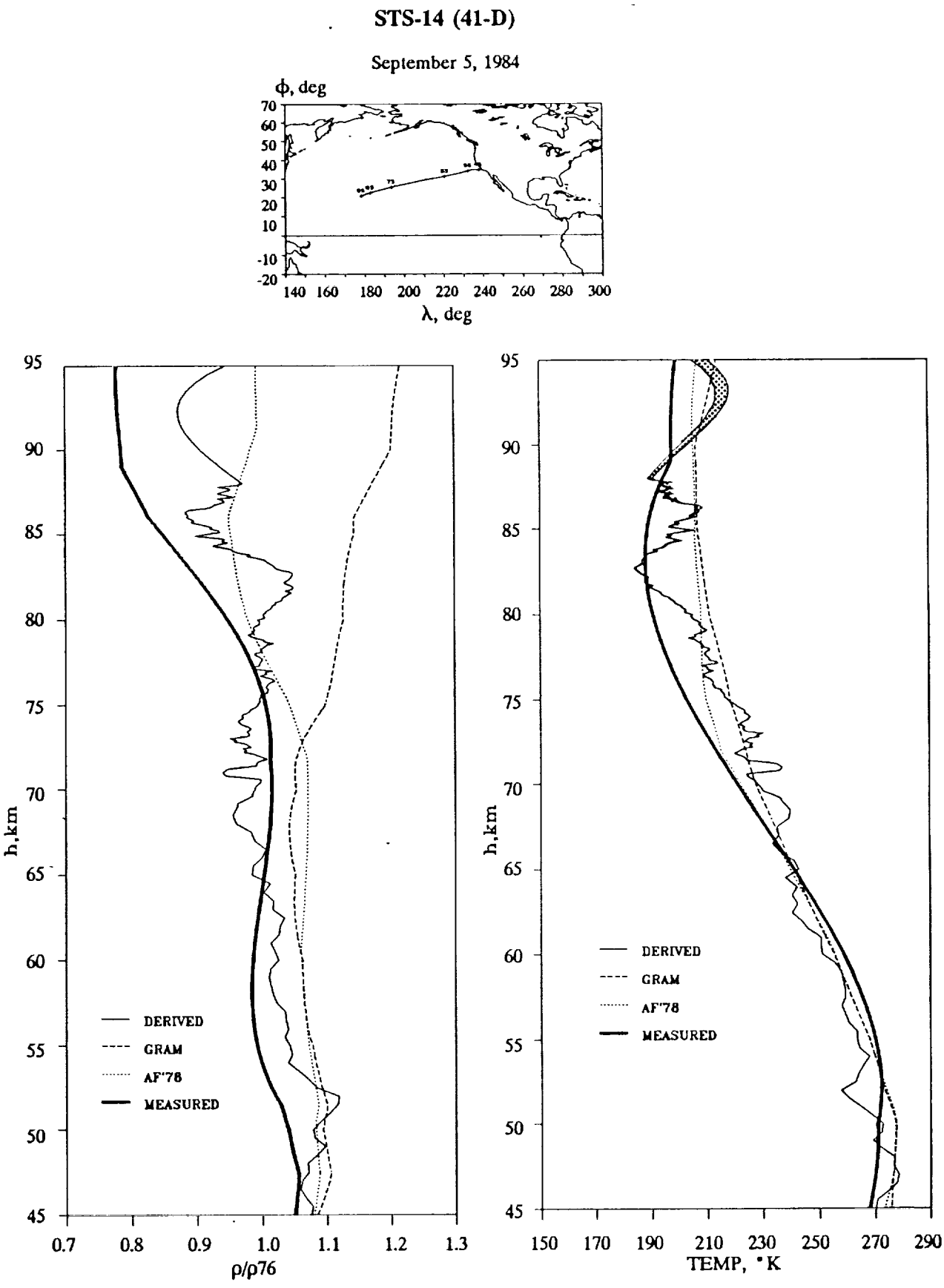

Figure A-12. STS-14 (41-D) density and temperature profile comparisons.

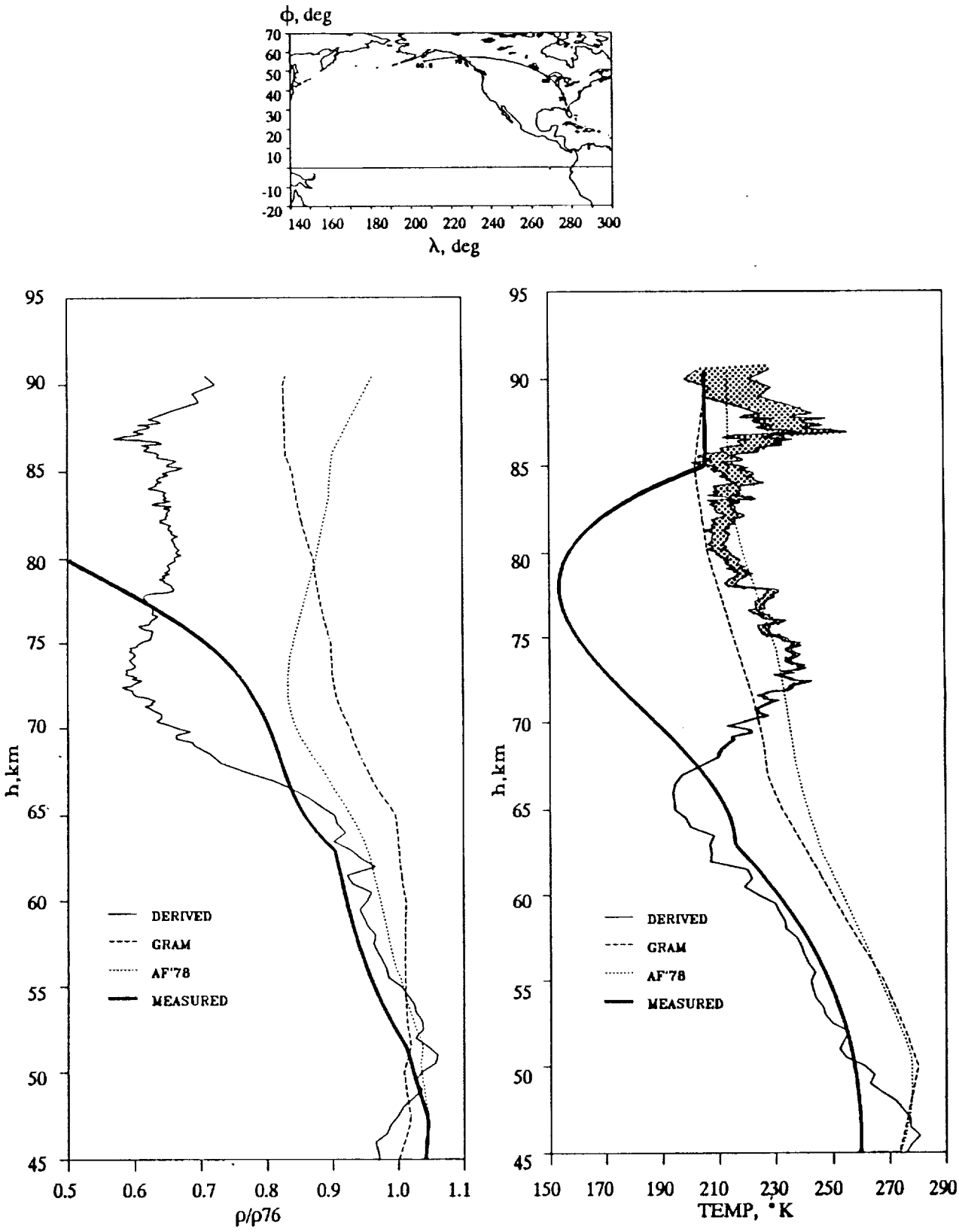

Figure A-13. STS-17 (41-G) density and temperature profile comparisons.

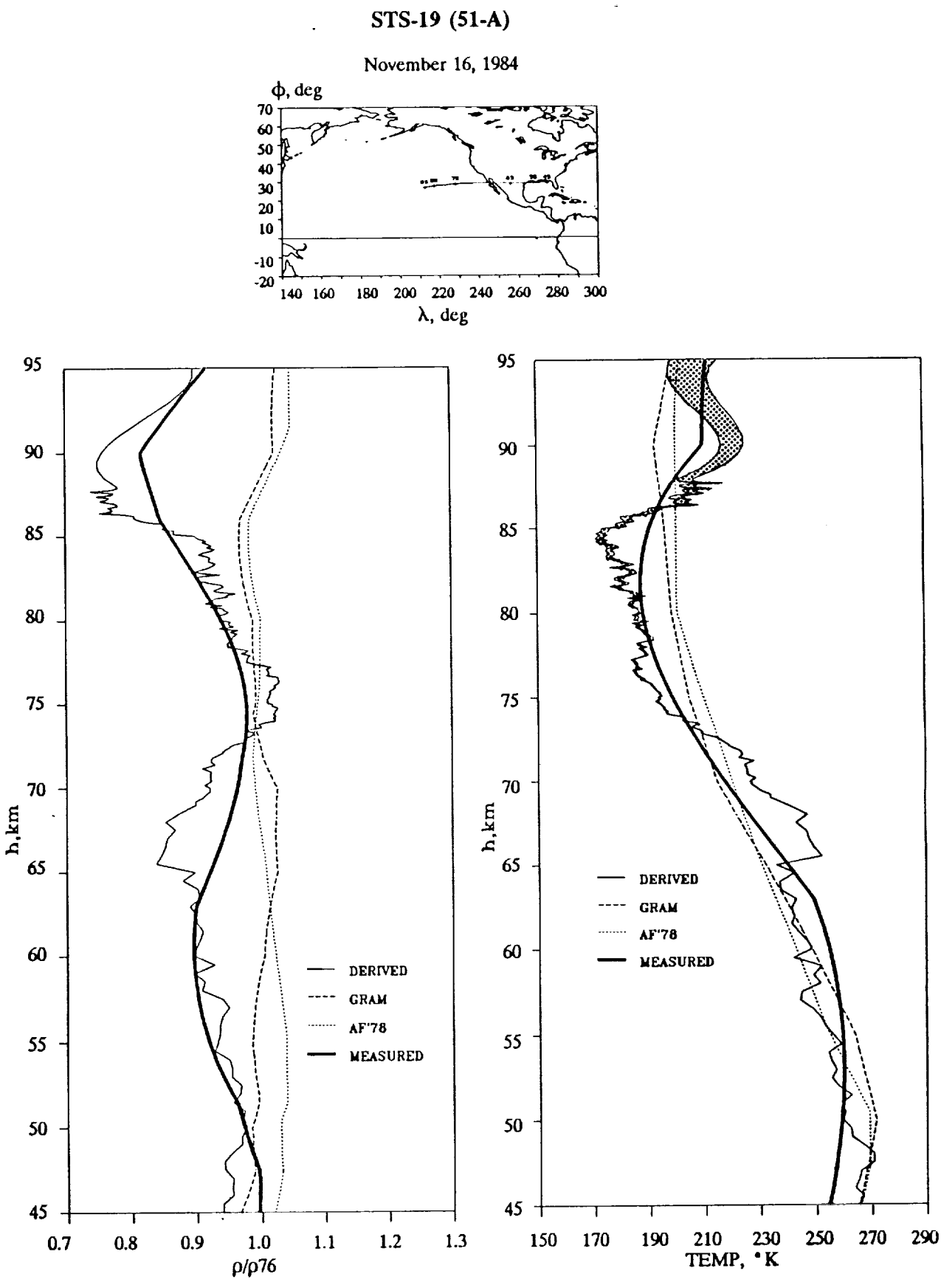

Figure A-14. STS-19 (51-A) density and temperature profile comparisons.

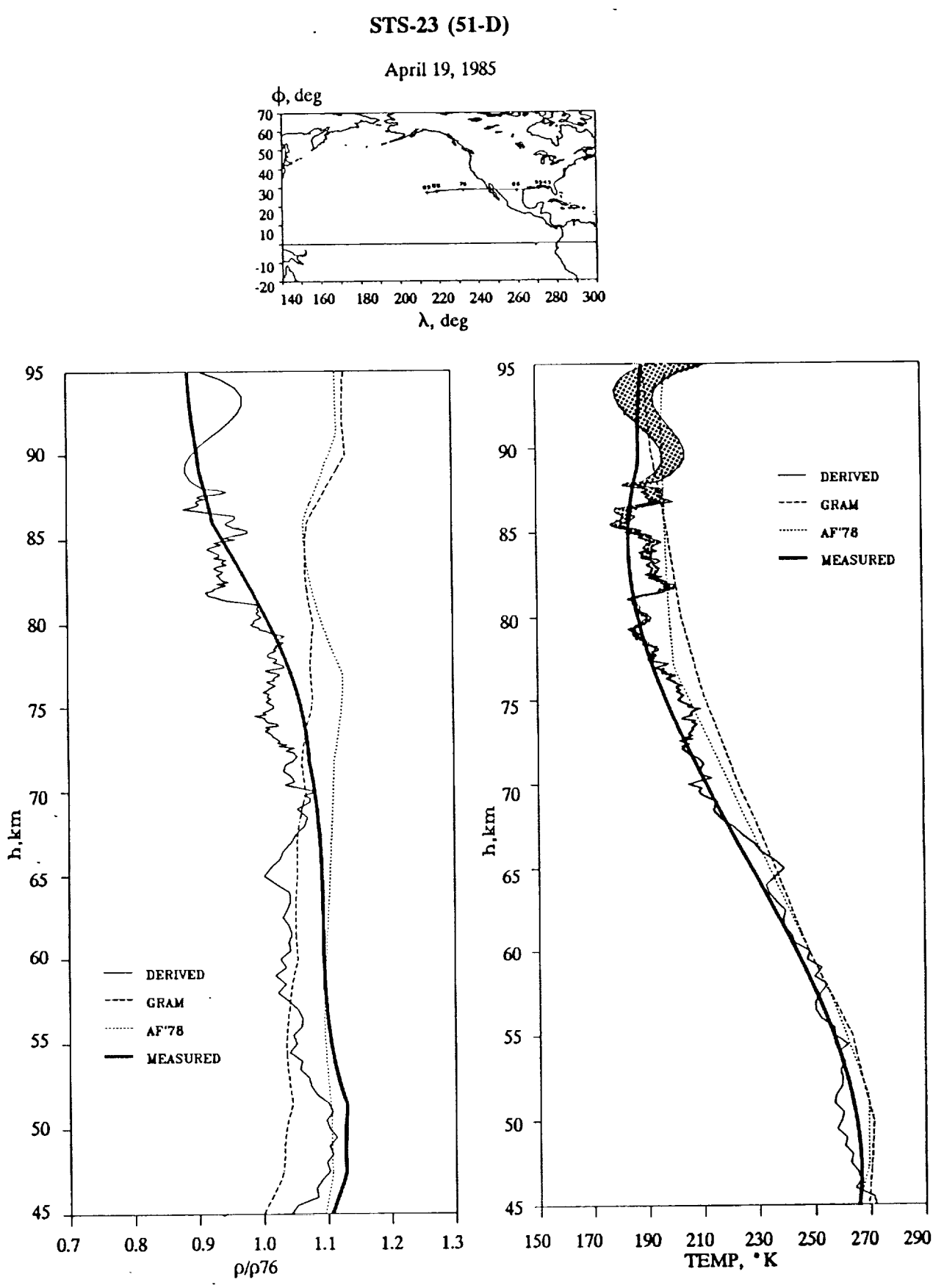

Figure A-15. STS-23 (51-D) density and temperature profile comparisons.

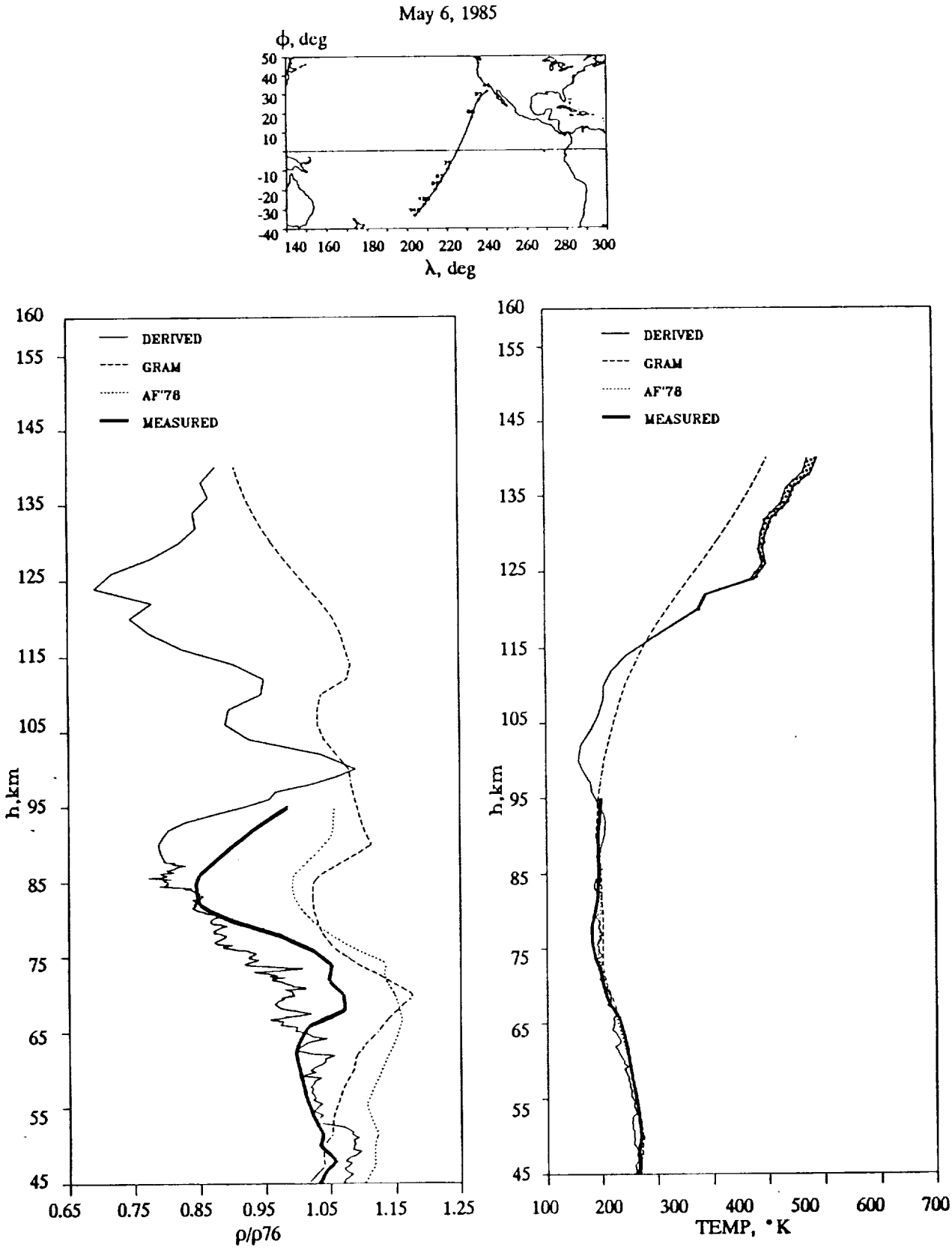

Figure A-16. STS-24 (51-B) density and temperature profile comparisons.

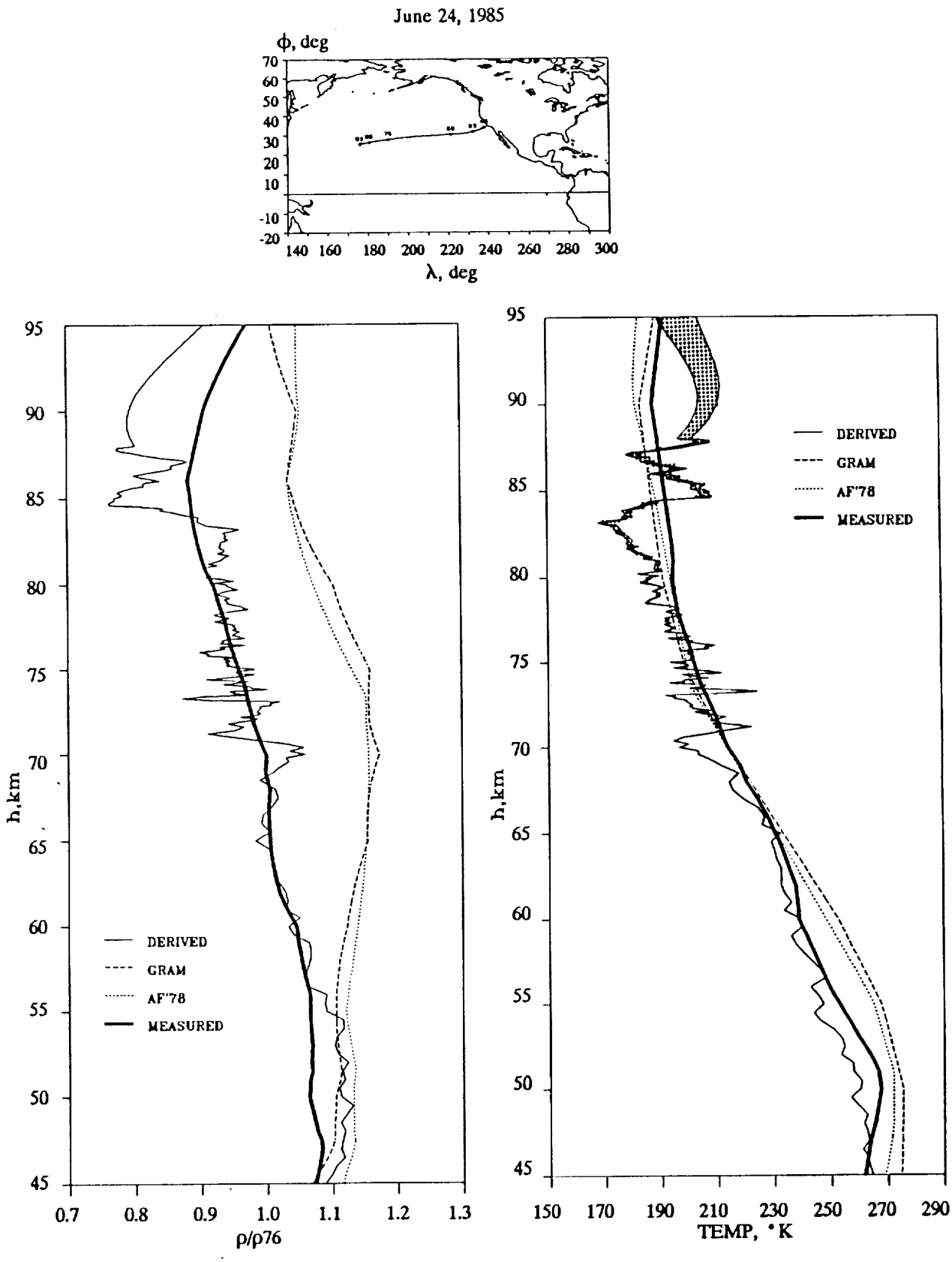

Figure A-17. STS-25 (51-G) density and temperature profile comparisons.

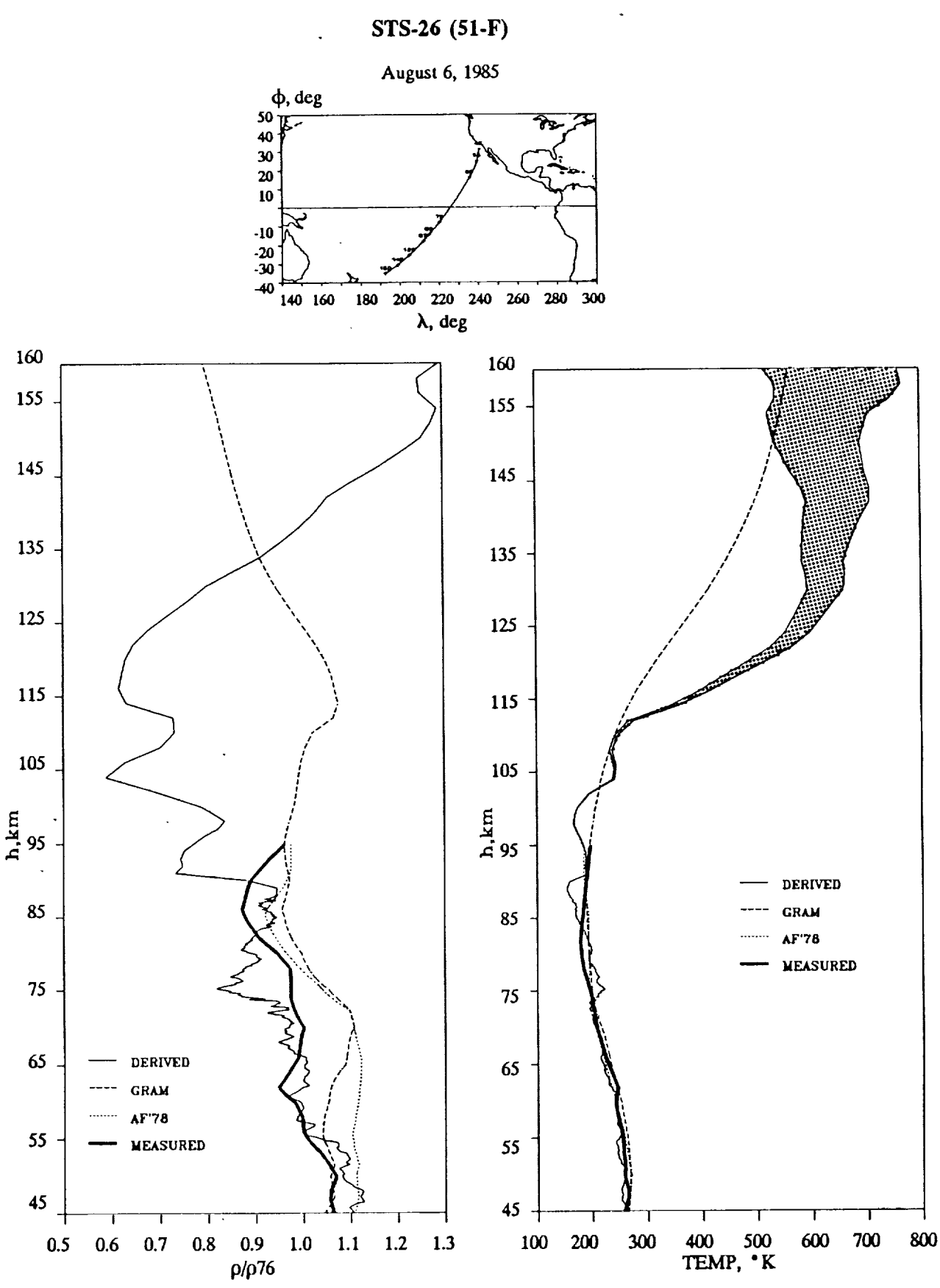

Figure A-18. STS-26 (51-F) density and temperature profile comparisons.

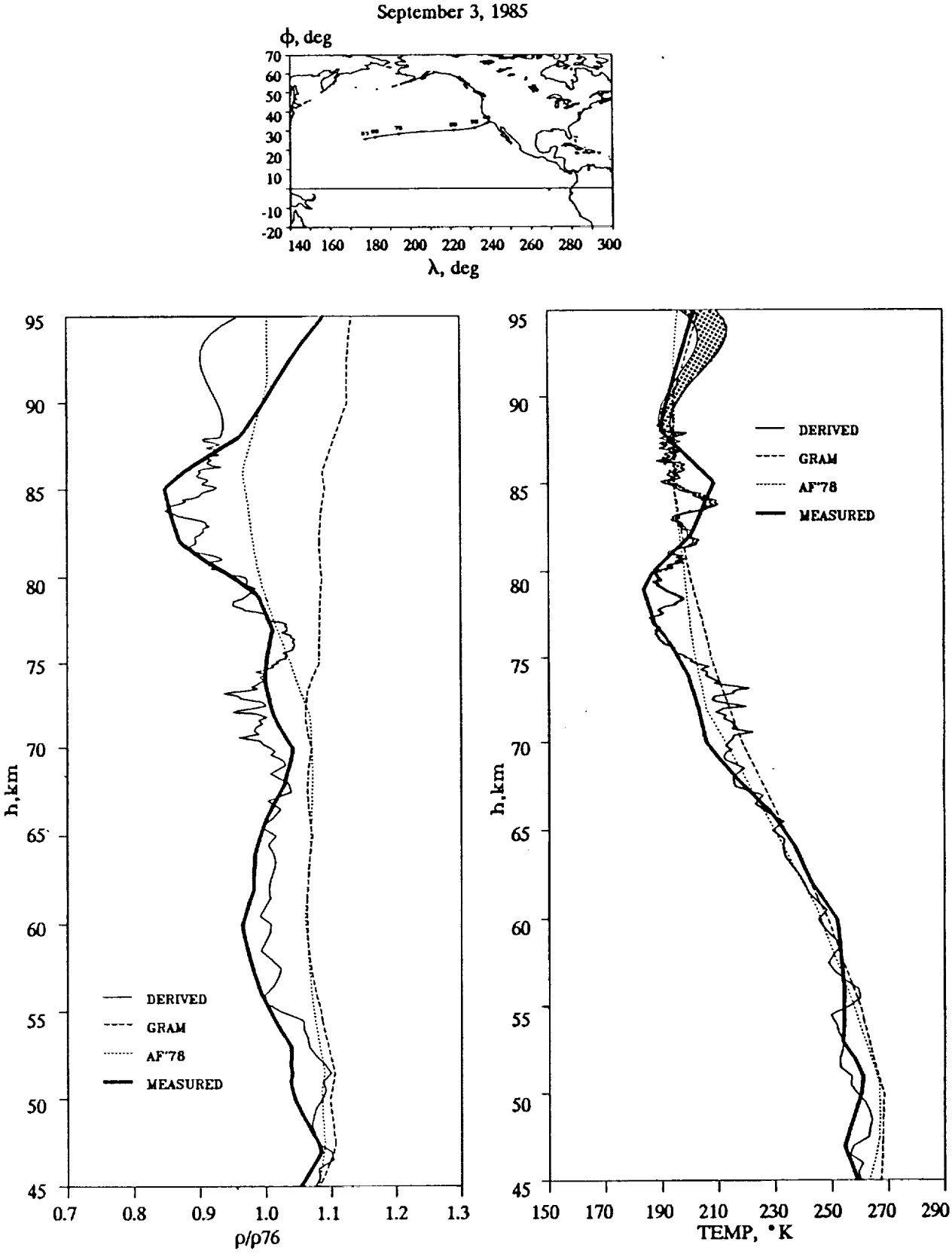

Figure A-19. STS-27 (51-I) density and temperature profile comparisons.

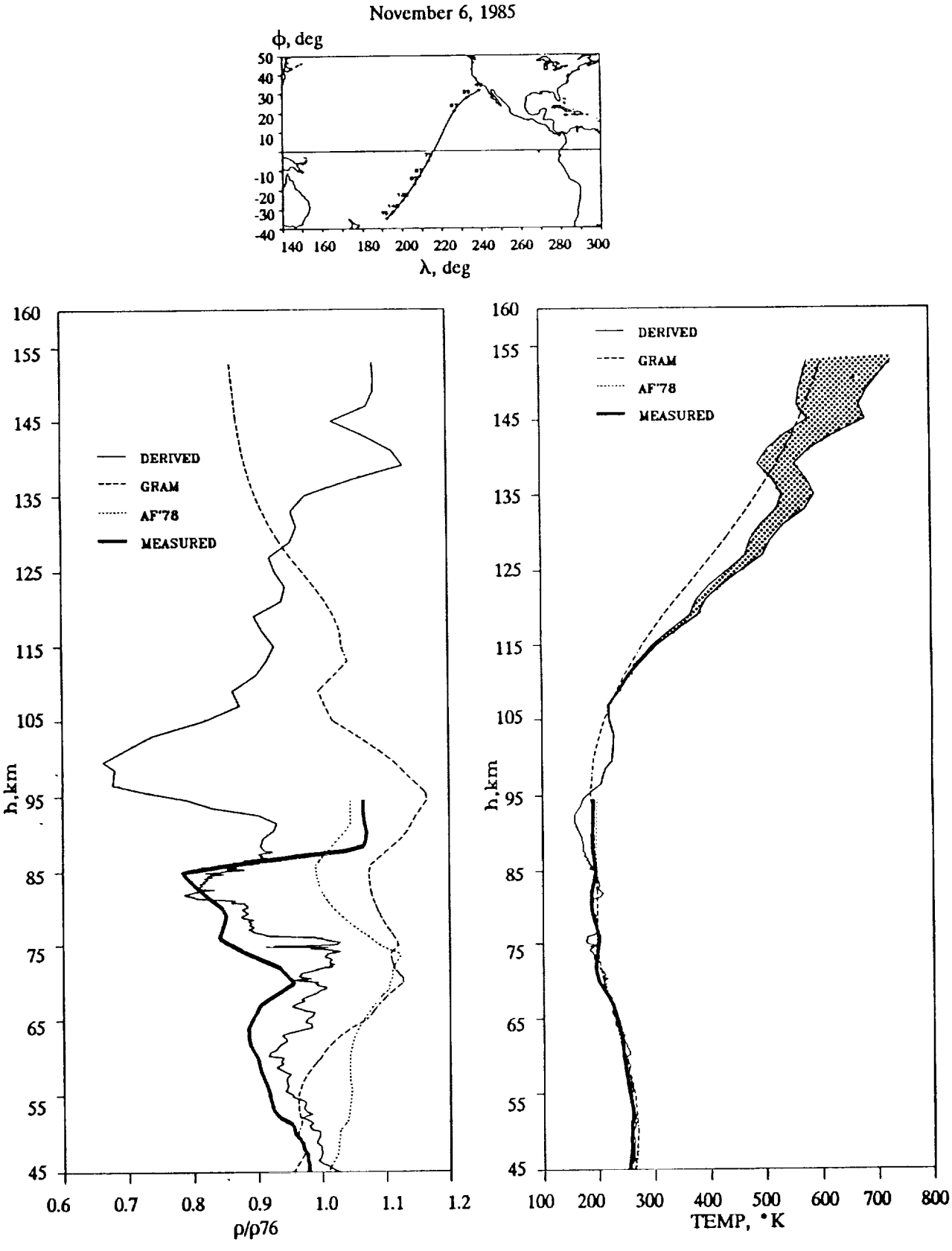

Figure A-20. STS-30 (61-A) density and temperature profile comparisons.

STS-31 (61-B)

December 3, 1985

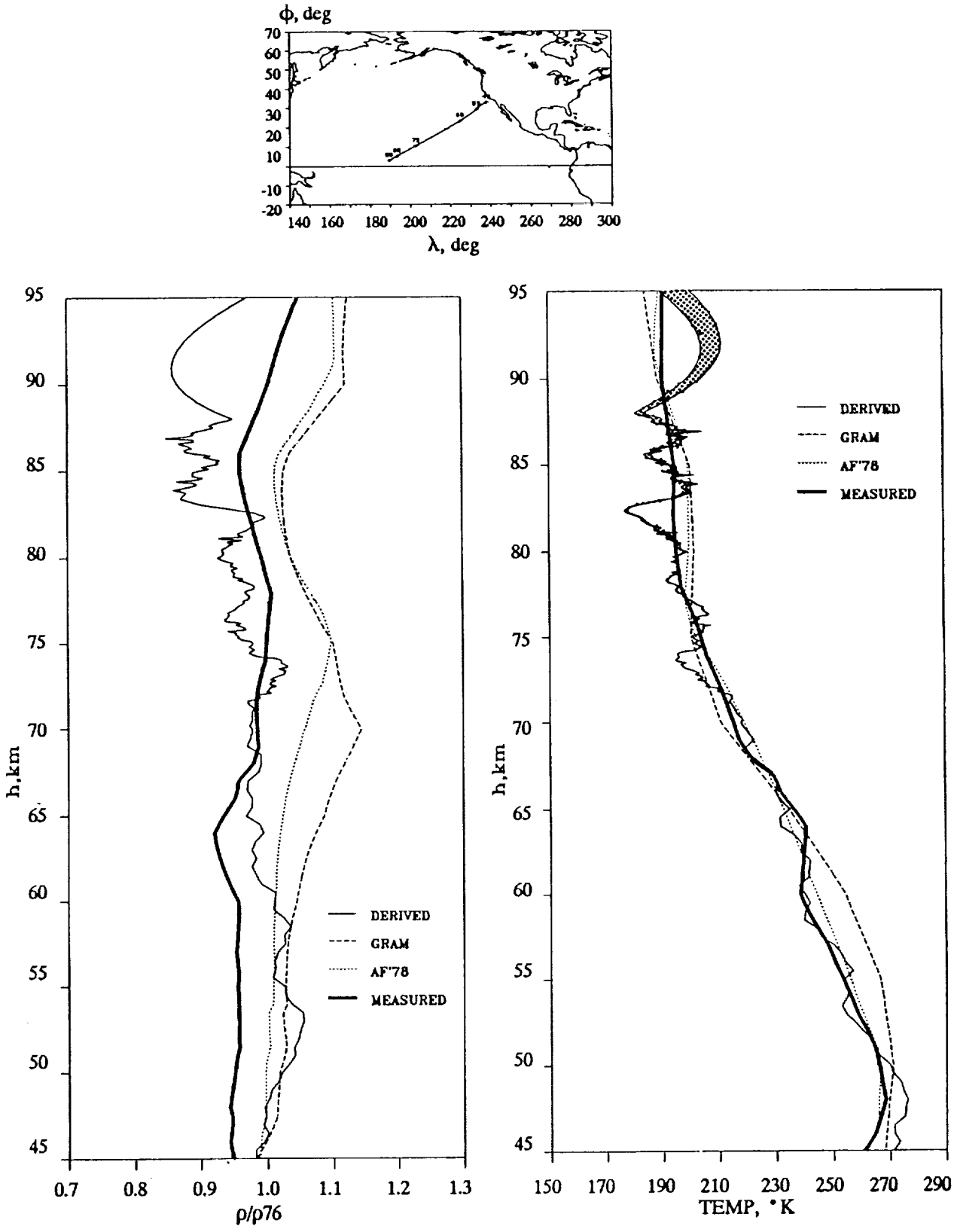

Figure A-21. STS-31 (61-B) density and temperature profile comparisons.

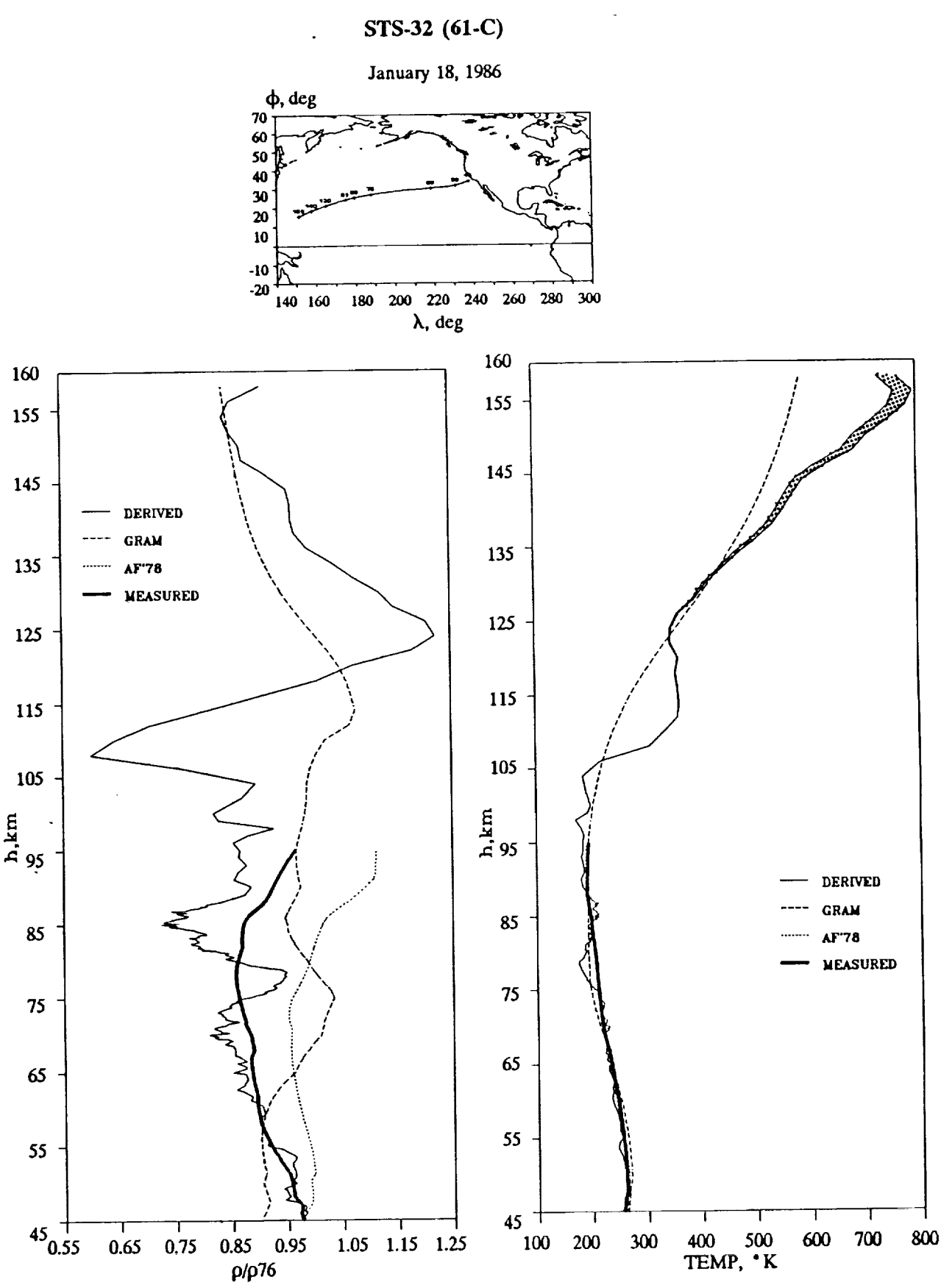

Figure A-22. STS-32 (61-C) density and temperature profile comparisons.

U.S. Gov't

1. Report No.	2. Government Accession No.	3. Recipient's Catalog No.
NASA CR		

4. Title and Subtitle	5. Report Date
Final Shuttle-derived Atmospheric Database: Development and Results from Thirty-two Flights	July 1990
	6. Performing Organization Code

7. Author(s)	8. Performing Organization Report No.
John T. Findlay Rachel A. Jasinski	
	10. Work Unit No.

9. Performing Organization Name and Address	11. Contract or Grant No.
Flight Mechanics & Control, Inc. 47 East Queen's Way Hampton, VA 23669	NAS9-17394
	13. Type of Report and Period Covered
	Contractor Report

12. Sponsoring Agency Name and Address	14. Sponsoring Agency Code
National Aeronautics and Space Administration Lyndon B. Johnson Space Center Houston, TX 77058	

15. Supplementary Notes

NASA Johnson Technical Monitor: Joe D. Gamble
Final Report

16. Abstract The final Shuttle-derived atmospheric database developed for the National Aeronautics and Space Administration under NASA Contract NAS9-17394 to the Lyndon B. Johnson Space Center is presented herein. The relational database is comprised of data from thirty-two (32) Space Transportation System (STS) descent flights, to include the available meteorology data taken in support of each flight as well as model data based on the United States Standard 1976 and 1962 atmospheres, the NASA Marshall Space Flight Center (MSFC) Global Reference Atmospheric Model (GRAM), and the United States Air Force 1978 Reference Atmospheres (AF'78). For the most part, the available data are restricted to the middle atmosphere. In situ accelerations, sensed by the tri-redundant Inertial Measurement Unit (IMU) to an accuracy better than one milli-g, are combined with post-flight Best Estimate Trajectory (BET) information and predicted, flight-substantiated Orbiter aerodynamics to provide determinations up to altitudes of 95 km. In some instances, alternate accelerometry data with micro-g resolution were utilized to extend the database well into the thermosphere. Though somewhat limited, the ensemble of flights permit a reasonable sampling of monthly, seasonal and latitudinal variations which can be utilized for atmospheric science investigations and model evaluations and upgrades as appropriate. More significantly, the unparalleled vertical resolution in the Shuttle-derived results indicate density shears normally associated with internal gravity waves or local atmospheric instabilities. Consequently, these atmospheres can also be used as stress-atmospheres for Guidance, Navigation and Control (GN&C) system development and analysis as part of any advanced space vehicle design activities.

17. Key Words (Suggested by Author(s))	18. Distribution Statement
Shuttle-derived atmospheres, mesosphere thermosphere, Global Reference Atmospheric Model, Air Force 1978 Reference Atmospheres, remote measurements, density structure, model comparisons	

19. Security Classif. (of this report)	20. Security Classif. (of this page)	21. No. of Pages	22. Price
Unclassified	Unclassified	84	